Measurements of inclusive and differential cross-sections of combined $t\bar{t}\gamma$ and $tW\gamma$ production in the $e\mu$ channel at 13 TeV with the ATLAS detector

Article *in* Journal of High Energy Physics · September 2020

DOI: 10.1007/jhep09(2020)049

CITATION
1

READS
44

2929 authors, including:

Adam Abed Abud
University of Liverpool
135 PUBLICATIONS **1,593** CITATIONS
SEE PROFILE

Nicola Abraham
Helmholtz-Zentrum Hereon
563 PUBLICATIONS **15,933** CITATIONS
SEE PROFILE

Baida Achkar
Georg-August-Universität Göttingen
130 PUBLICATIONS **2,246** CITATIONS
SEE PROFILE

Lutfi Adam
Bogor Agricultural University
187 PUBLICATIONS **2,909** CITATIONS
SEE PROFILE

Published for SISSA by Springer

Received: *July 15, 2020*
Accepted: *July 28, 2020*
Published: *September 7, 2020*

Measurements of inclusive and differential cross-sections of combined $t\bar{t}\gamma$ and $tW\gamma$ production in the $e\mu$ channel at 13 TeV with the ATLAS detector

The ATLAS collaboration

E-mail: atlas.publications@cern.ch

Abstract: Inclusive and differential cross-sections for the production of top quarks in association with a photon are measured with proton-proton collision data corresponding to an integrated luminosity of 139 fb^{-1}. The data were collected by the ATLAS detector at the LHC during Run 2 between 2015 and 2018 at a centre-of-mass energy of 13 TeV. The measurements are performed in a fiducial volume defined at parton level. Events with exactly one photon, one electron and one muon of opposite sign, and at least two jets, of which at least one is b-tagged, are selected. The fiducial cross-section is measured to be $39.6\,^{+2.7}_{-2.3}$ fb. Differential cross-sections as functions of several observables are compared with state-of-the-art Monte Carlo simulations and next-to-leading-order theoretical calculations. These include cross-sections as functions of photon kinematic variables, angular variables related to the photon and the leptons, and angular separations between the two leptons in the event. All measurements are in agreement with the predictions from the Standard Model.

Keywords: Hadron-Hadron scattering (experiments), Top physics

ArXiv ePrint: 2007.06946

https://doi.org/10.1007/JHEP09(2020)049

JHEP09(2020)049

Contents

JHEP09(2020)049

1 Introduction

Precise measurements of top-quark production and decay properties provide crucial information for testing the predictions of the Standard Model (SM) and its possible extensions. In particular, the study of the associated production of a top-quark pair ($t\bar{t}$) with a high-energy photon probes the $t\gamma$ electroweak coupling. Furthermore, measurements of the inclusive and differential cross-sections of this process are of particular interest because these topologies are sensitive, for instance, to new physics through anomalous dipole moments of the top quark [1–3] and in the context of effective field theories [4].

First evidence for the production of $t\bar{t}$ in association with a photon ($t\bar{t}\gamma$) was reported by the CDF Collaboration [5], while the observation of the $t\bar{t}\gamma$ process was established by the ATLAS Collaboration in proton-proton (pp) collisions at $\sqrt{s} = 7$ TeV [6]. Both the ATLAS and CMS Collaborations measured the $t\bar{t}\gamma$ cross-section at $\sqrt{s} = 8$ TeV [7, 8].

First measurements of the inclusive and differential cross-sections at $\sqrt{s} = 13$ TeV were performed by the ATLAS Collaboration [9].

This paper presents a measurement of the fiducial inclusive and differential combined $t\bar{t}\gamma + tW\gamma$ production cross-sections in the final state with one electron and one muon, referred to as the $e\mu$ channel. Events where the electrons and muons arise from the leptonic decays of τ-leptons are considered as background. The measurement is performed using the full data set recorded at the LHC between 2015 and 2018 at a centre-of-mass energy of $\sqrt{s} =$ 13 TeV and corresponding to an integrated luminosity of 139 fb^{-1}. The fiducial inclusive cross-section is measured using a profile likelihood fit to the distribution of S_{T}, defined as the scalar sum of all transverse momenta in the event, including leptons, photons, jets and missing transverse momentum. The differential cross-sections, absolute and normalised to unity, are measured in the same fiducial region as the inclusive cross-section, as functions of photon kinematic variables, angular variables related to the photon and the leptons, and angular separations between the two leptons in the event.

Compared to the previous $t\bar{t}\gamma$ ATLAS analysis with 13 TeV data [9], only the $e\mu$ channel is considered since it provides a clean final state with a small background contribution and, thus, no multivariate analysis techniques are needed to separate signal and background processes. Additionally, the cross-sections are measured at parton level rather than at particle level to allow comparison with the theory calculation in refs. [10, 11]. The calculation constitutes the first full computation for $t\bar{t}$ production with a hard final-state photon in hadronic collisions at next-to-leading order (NLO) in quantum chromodynamics (QCD), $pp \to bWbW\gamma$, including all resonant and non-resonant diagrams, interferences, and off-shell effects of the top quarks and the W bosons. Therefore, in this paper the combined cross-section of resonant $t\bar{t}\gamma$ and non-resonant $tW\gamma$ production is measured, referred to as signal in the following. Example Feynman diagrams at leading order in QCD for $t\bar{t}\gamma$ and $tW\gamma$ production are shown in figure 1.

The paper is organised as follows. The ATLAS detector is briefly introduced in section 2. Details of the event-simulation generators and their theoretical predictions are given in section 3. The event selection and the analysis strategy are presented in sections 4 and 5. The systematic uncertainties are described in section 6. The results for the fiducial inclusive and differential cross-sections are presented in sections 7 and 8, respectively. Finally, a summary is given in section 9.

2 ATLAS detector

ATLAS [12–14] is a multipurpose detector with a forward-backward symmetric cylindrical geometry with respect to the LHC beam axis.[1] The innermost layers consist of tracking detectors in the pseudorapidity range $|\eta| < 2.5$. This inner detector (ID) is surrounded

[1] ATLAS uses a right-handed coordinate system with its origin at the nominal interaction point (IP) in the centre of the detector and the z-axis along the beam pipe. The x-axis points from the IP to the centre of the LHC ring, and the y-axis points upwards. Cylindrical coordinates (r, ϕ) are used in the transverse plane, ϕ being the azimuthal angle around the z-axis. The pseudorapidity is defined in terms of the polar angle θ as $\eta = -\ln\tan(\theta/2)$. Angular distance is measured in units of $\Delta R \equiv \sqrt{(\Delta\eta)^2 + (\Delta\phi)^2}$.

JHEP09(2020)049

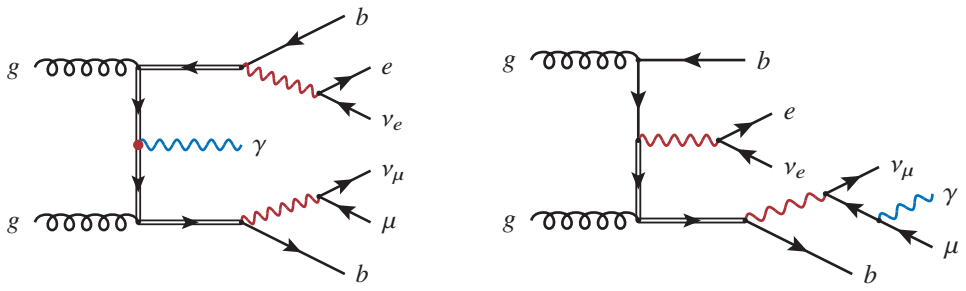

Figure 1. Example Feynman diagrams at leading order for $t\bar{t}\gamma$ (left) and $tW\gamma$ production (right) in the $e\mu$ channel. The top-quark mass resonances are marked with double-lined arrows, while W bosons are marked in red.

by a thin superconducting solenoid that provides a 2 T axial magnetic field. It is enclosed by the electromagnetic and hadronic calorimeters, which cover $|\eta| < 4.9$. The outermost layers of ATLAS consist of an external muon spectrometer within $|\eta| < 2.7$, incorporating three large toroidal magnetic assemblies with eight coils each. The field integral of the toroids ranges between 2.0 and 6.0 Tm for most of the acceptance. The muon spectrometer includes precision tracking chambers and fast detectors for triggering. A two-level trigger system [15] reduces the recorded event rate to an average of 1 kHz.

3 Signal and background modelling

The estimation of signal and background contributions relies on the modelling of these processes with simulated events produced with Monte Carlo (MC) event generators. The response of the ATLAS detector was simulated [16] with GEANT4 [17]. For some of the estimates of modelling uncertainties, the fast-simulation package ATLFAST-II was used instead of the full detector simulation. Additional pp interactions (pile-up) were generated with PYTHIA 8 [18, 19] using a set of tuned parameters called the A3 tune [20] and the NNPDF2.3LO parton distribution function (PDF) set [21]. Corrections to the pile-up profile, selection efficiencies, energy scales and resolutions derived from dedicated data samples are applied to the MC simulation to improve agreement with data.

This analysis uses both *inclusive* samples, in which processes were generated at matrix-element (ME) level without explicitly including a photon in the final state, and *dedicated* samples for certain processes, where photons were included in the ME-level generation step. Dedicated samples with a photon in the ME were generated for the $t\bar{t}\gamma$ and $tW\gamma$ final states, as well as for $V\gamma$ processes with additional jets. Here, V denotes either a W or a Z boson. Although no photons were generated at ME level in the inclusive samples, initial- and final-state radiation of photons is accounted for by the showering algorithm. Combining inclusive and dedicated samples for the modelling of processes might result in double-counting photon radiation in certain phase-space regions. As a consequence, a procedure to remove overlaps between the inclusive and dedicated samples was performed. Photon radiation simulated at ME level in dedicated samples achieves higher accuracy than the photon radiation in the showering algorithm. On the other hand, kinematic

JHEP09(2020)049

requirements are applied to the kinematic properties of the photons at ME level in the dedicated samples. In the overlap-removal procedure, all events from the dedicated samples are kept while events from the inclusive samples are discarded if they contain a parton-level photon that fulfils the dedicated samples' kinematic requirements of $p_{\mathrm{T}}(\gamma) > 15\,\mathrm{GeV}$ and $\Delta R(\gamma, \ell) > 0.2$, where $p_{\mathrm{T}}(\gamma)$ is the photon's transverse momentum and $\Delta R(\gamma, \ell)$ is the angular distance between the photon and any charged lepton.

The dedicated sample for the $t\bar{t}\gamma$ signal process was simulated using the MadGraph5_aMC@NLO generator (v2.3.3) [22] and the NNPDF2.3LO PDF set at leading order (LO) in QCD. The events were generated as a doubly resonant $2 \to 7$ process, e.g. as $pp \to b\ell\nu b\ell\nu\gamma$, thus, diagrams where the photon is radiated from the initial state (in the case of quark-antiquark annihilation), intermediate top quarks, the b-quarks, and the intermediate W bosons, as well as the decay products of the W bosons, are included. To prevent divergences, the photon was required to have $p_{\mathrm{T}} > 15$ GeV and $|\eta| < 5.0$ and the leptons to satisfy $|\eta| < 5.0$. The ΔR between the photon and any of the charged particles among the seven final-state particles were required to be greater than 0.2. The top-quark mass in this and all other samples was set to 172.5 GeV. The renormalisation and the factorisation scales were set to $0.5\times \sum_i \sqrt{m_i^2 + p_{\mathrm{T},i}^2}$, where the sum runs over all the particles generated from the ME calculation. The event generation was interfaced to Pythia 8 (v8.212) using the A14 tune [23] to model parton showers, hadronisation, fragmentation and the underlying event. Heavy-flavour hadron decays were modelled with EvtGen [24]; this program was used for all samples, except for those generated using the Sherpa MC program [25, 26]. In the latter case, heavy-flavour decays were modelled directly with Sherpa.

Two dedicated samples for the $tW\gamma$ process were generated with the MadGraph5_aMC@NLO generator as well. The first one was produced at LO in the five-flavour scheme for the $2 \to 3$ process (e.g. $pp \to tW\gamma$) assuming a stable top quark. The second set of events was generated at LO as a $2 \to 6$ process (e.g. $pp \to b\ell\nu\ell\nu\gamma$) in the five-flavour scheme, where the photon is radiated from any other charged final-state particle. In the five-flavour scheme, the b-quarks are treated as massless and the LO representation of the process includes a b-quark in the initial state. The two sets of events are complementary and, once combined, provide a full simulation of the $tW\gamma$ process. Both samples make use of the NNPDF2.3LO PDF set and were interfaced to Pythia 8 (v8.212) for parton showering using the A14 tune. The photon was also required to have $p_{\mathrm{T}} > 15$ GeV and $|\eta| < 5.0$ and to be separated by $\Delta R > 0.2$ from any parton. Although possible interference effects between $t\bar{t}\gamma$ and $tW\gamma$ are still missing in the simulated LO samples, the $tW\gamma$ process is treated as part of the signal in this analysis.

Events with $W\gamma$ and $Z\gamma$ final states (with additional jets) were simulated as dedicated samples. The $W\gamma$ processes were simulated with Sherpa 2.2.2 at NLO accuracy in QCD using the NNPDF3.0NNLO PDF set, whereas $Z\gamma$ events were generated with Sherpa 2.2.4 at LO in QCD with the same PDF set. The samples are normalised to the cross-sections given by the corresponding MC simulation. The Sherpa generator performs all steps of the event generation, from the hard process to the observable particles. All samples were

JHEP09(2020)049

matched and merged by the Sherpa-internal parton showering based on Catani-Seymour dipoles [27, 28] using the MEPS@NLO prescription [29–31]. Virtual corrections for the NLO accuracy in QCD in the matrix element were provided by the OpenLoops library [32, 33].

Inclusive $t\bar{t}$ production processes were simulated at matrix-element level at NLO accuracy in QCD using Powheg-Box v2 [34–36]. The calculation used the NNPDF3.0NLO PDF set [37]. The parton shower was generated with Pythia 8 (v8.230), for which the A14 tune [38] was used. The $t\bar{t}$ events are normalised to a cross-section value calculated with the Top++2.0 program at next-to-next-to-leading order (NNLO) in perturbative QCD, including soft-gluon resummation to next-to-next-to-leading-logarithm order (see ref. [39] and references therein).

Events with inclusive W- and Z-boson production in association with additional jets were simulated with Sherpa 2.2.1 [25, 26] at NLO in QCD. The NNPDF3.0NLO PDF set was used in conjunction with a dedicated tune provided by the Sherpa authors. The samples are normalised to the NNLO cross-section in QCD [40].

Events with two directly produced vector bosons, i.e. WW, WZ and ZZ, were generated with Sherpa versions 2.2.2 (purely leptonic decays) and 2.2.1 (all others) at LO in QCD. The NNPDF3.0NNLO PDF set was used in conjunction with a dedicated tune provided by the Sherpa authors. The samples are normalised to NLO accuracy cross-sections in QCD [41].

Events with a $t\bar{t}$ pair and an associated W or Z boson ($t\bar{t}V$) were simulated at NLO at the ME level with MadGraph5_aMC@NLO using the NNPDF3.0NLO PDF set. The ME generator was interfaced to Pythia 8 (v8.210), for which the A14 tune was used in conjunction with the NNPDF2.3LO PDF set. The samples are normalised to NLO in QCD and electroweak theory [42].

The background processes are sorted into three categories based on the origin of the reconstructed photon required in the event selection. The three are estimated from MC simulation by categorising events from all considered samples that are not classified as signal events. The MC simulations for all categories include processes without prompt photons such as $t\bar{t}$, W+jets, Z+jets, diboson and $t\bar{t}V$ production, as well as background processes with an additional prompt photon. The first category is labelled *h-fake* and contains any type of hadronic fakes that mimic a photon signature in the detector. This category includes not only photon signatures faked by hadronic energy depositions in the electromagnetic calorimeter, but also hadron decays involving photons, for example $\pi^0 \to \gamma\gamma$ decays. It also includes processes with a prompt photon, where the prompt photon is not reconstructed in the detector or does not pass the selection requirements, but a h-fake photon does. Studies performed with data-driven techniques following the approach described in ref. [9] show that possible data-driven corrections have a negligible effect on the distribution shapes of relevant observables. Possible differences in the total expected number of events are covered by a normalisation uncertainty as described in section 6. The second category is labelled *e-fake* and contains processes with an electron mimicking a photon signature in the calorimeter. Similarly to the h-fake category, this category includes contributions from processes without a prompt photon but with an e-fake photon, as well as processes with a prompt photon in the simulation but an e-fake photon in the reconstruction. This

JHEP09(2020)049

category represents a minor background contribution. The third category is called *prompt γ background* and contains any type of background process with a prompt photon. The background contribution from $t\bar{t}$ production with a photon produced in an additional pp interaction in the same bunch crossing was found to be negligible. This was estimated by comparing the significance of the distance in z between the photon's origin and the primary vertex in data and simulation.

The $t\bar{t}\gamma$ and $tW\gamma$ events where one or both W bosons decay into τ-leptons, which then subsequently decay into e or μ, are categorised as *Other* $t\bar{t}\gamma/tW\gamma$, and not as $e\mu$ signal, following the definition of signal events in the theory calculation in refs. [10, 11]. Single-lepton events, where a second lepton is faked by hadronic energy depositions, are also included in the category *Other* $t\bar{t}\gamma/tW\gamma$. The contribution of $t\bar{t}\gamma$ single-lepton events was found to be negligible in the $e\mu$ final state in the previous measurement [9] and it is therefore estimated from the MC simulation.

4 Event selection

The data set used in this analysis corresponds to the 139 fb^{-1} of integrated luminosity collected with the ATLAS detector during the Run 2 period. Each event in data and simulation is required to have at least one reconstructed primary vertex with at least two associated reconstructed tracks. Furthermore, only events where at least one of the single-electron [43] or single-muon [44] triggers was fired are selected.

The main physics objects considered in this analysis are electrons, muons, photons, jets, b-jets and missing transverse momentum. Electrons are reconstructed from energy deposits in the electromagnetic calorimeter associated with reconstructed tracks in the ID system. They are identified with a combined likelihood technique [45] using a 'tight' working point, and are required to be isolated based on calorimeter and tracking quantities. The p_{T}- and η-dependent isolation criteria yield an efficiency of 90% for electrons with $p_{\mathrm{T}} = 25\,\mathrm{GeV}$ and 99% for those with $p_{\mathrm{T}} = 60\,\mathrm{GeV}$. The origin of the electron track has to be compatible with the primary vertex. Electrons are calibrated with the method described in ref. [45]. They are selected if they fulfil $p_{\mathrm{T}} > 25\,\mathrm{GeV}$ and $|\eta_{\mathrm{clus}}| < 2.47$, excluding the calorimeter barrel/endcap transition region $1.37 < |\eta_{\mathrm{clus}}| < 1.52$.[2]

Muons are reconstructed with an algorithm that combines the track segments in the various layers of the muon spectrometer and the tracks in the ID system. The reconstruction, identification and calibration methods are described in ref. [46]. Muons are required to be isolated according to track- and calorimeter-based criteria similar to those applied to electrons. Only muons with calibrated $p_{\mathrm{T}} > 25\,\mathrm{GeV}$ and $|\eta| < 2.5$ and passing 'medium' quality requirements are considered. The muon track is also required to originate from the primary collision vertex.

Photons are reconstructed from energy deposits in the central region of the electromagnetic calorimeters. If the cluster considered is not matched to any reconstructed track in the ID system, the photon candidate is classified as unconverted. If the cluster is matched with one or two reconstructed tracks that are consistent with originating from a photon

[2] η_{clus} denotes the pseudorapidity of the calorimeter cell cluster associated with the electron.

JHEP09(2020)049

conversion and if, in addition, a conversion vertex can be found, the photon candidate is classified as converted. Both kinds of photons are considered in this analysis. Photons are reconstructed and identified as described in ref. [47] and their energies are calibrated with the method described in ref. [48]. They are subject to a tight isolation requirement defined as $E_{\mathrm{T}}^{\mathrm{iso}}|_{\Delta R<0.4} < 0.022 \cdot E_{\mathrm{T}}(\gamma) + 2.45\,\mathrm{GeV}$ in conjunction with $p_{\mathrm{T}}^{\mathrm{iso}}|_{\Delta R<0.2} < 0.05 \cdot E_{\mathrm{T}}(\gamma)$, where $E_{\mathrm{T}}^{\mathrm{iso}}$ refers to the calorimeter isolation within $\Delta R < 0.4$ around the direction of the photon candidate and $p_{\mathrm{T}}^{\mathrm{iso}}$ is the track isolation within $\Delta R < 0.2$ [47]. Only photons with calibrated $E_{\mathrm{T}} > 20\,\mathrm{GeV}$ and $|\eta_{\mathrm{clus}}| < 2.37$, excluding the calorimeter transition region $1.37 < |\eta_{\mathrm{clus}}| < 1.52$, are considered.

Jets are reconstructed using the anti-k_t algorithm [49] in the FastJet implementation [50] with a distance parameter $R = 0.4$. They are reconstructed from topological clusters of cells in the calorimeter [51]. The jet energy scale and jet energy resolution are calibrated using information from both simulation and data [52]. The jets are required to have $p_{\mathrm{T}} > 25\,\mathrm{GeV}$ and $|\eta| < 2.5$. Jets with a large contribution from pile-up vertices are identified with the *Jet Vertex Tagger* [53] and rejected.

The b-tagging algorithm (MV2c10) applied to the selected jets to identify those from b-quark hadronisation [54] labelled as b-jets is based on a boosted decision tree combining information from other algorithms using track impact parameters and secondary vertices, and a multi-vertex reconstruction algorithm. A working point with a selection efficiency of 85% on simulated $t\bar{t}$ events is used, corresponding to rejection factors of 3.1 and 35 for jets initiated by charm quarks and light-flavour partons, respectively. The flavour-tagging efficiency for b-jets, as well as for c-jets and light-flavour jets, is calibrated as described in ref. [55].

The reconstructed missing transverse momentum $E_{\mathrm{T}}^{\mathrm{miss}}$ [56, 57] is computed as the negative vector sum over all reconstructed, fully calibrated physics objects, including photons, and the remaining unclustered energy, also called the *soft term*. The soft term is estimated from low-p_{T} tracks associated with the primary vertex but not with any reconstructed object.

An overlap-removal procedure is applied to avoid the reconstruction of the same energy clusters or tracks as different objects. First, electron candidates sharing their track with a muon candidate are removed and jets within a $\Delta R = 0.2$ cone around any remaining electron are excluded. Secondly, electrons within a $\Delta R = 0.4$ cone around any remaining jet are removed. If the distance between a jet and any muon candidate is $\Delta R < 0.4$, the muon candidate is discarded if the jet has more than two associated tracks, otherwise the jet is removed. Finally, photons within a $\Delta R = 0.4$ cone around any remaining electron or muon are removed and then jets within a $\Delta R = 0.4$ cone around any remaining photon are excluded.

The selected events must have exactly one electron and exactly one muon, each with $p_{\mathrm{T}} > 25\,\mathrm{GeV}$. At least one of these leptons has to be matched to a fired single-lepton trigger. Since the p_{T} threshold of the single-lepton triggers was increased over the different data-taking periods due to increased collisions rates, the offline p_{T} thresholds for these electrons and muons that are matched to a fired single-lepton trigger are chosen to be 25 GeV in 2015, 27 GeV in 2016, and 28 GeV in 2017 and 2018 in order to lie above the trigger thresholds. Electrons and muons must have opposite-sign charges and the $e\mu$

JHEP09(2020)049

	Events
$t\bar{t}\gamma$ $e\mu$	2391 ± 130
$tW\gamma$ $e\mu$	156 ± 15
Other $t\bar{t}\gamma/tW\gamma$	279 ± 15
h-fake	78 ± 40
e-fake	23 ± 12
Prompt γ bkg.	87 ± 40
Total	3014 ± 160
Data	3014

Table 1. Event yields before the profile likelihood fit of the signal and background processes to data after the full selection. All categories are estimated from MC simulation and include correction factors for detector effects as described in section 6. The combination of all $t\bar{t}\gamma$ and $tW\gamma$ categories is scaled to match the event yields in data. The quoted uncertainties correspond to the total statistical and systematic uncertainties (cf. section 6) added in quadrature.

invariant mass is required to be higher than 15 GeV. The event is required to have at least two jets and at least one of the jets must be b-tagged. In addition, all events must contain exactly one reconstructed photon fulfilling the condition that ΔR between the selected photon and any of the leptons is greater than 0.4.

The observed event yields after selection are listed in table 1 for the different signal and background categories described in section 3. The LO cross-section of the MC samples underestimates the expected number of signal events; therefore, for illustration purposes the combination of all $t\bar{t}\gamma$ and $tW\gamma$ categories is normalised to match the event yields in data. Correction factors for detector effects (described in section 6) are applied, when needed, to improve the description of the data by the simulation.

The modelling of signal and background processes is inspected through the comparison of distributions. A selection of these distributions showing a comparison between the MC simulation before the profile likelihood fit and data is presented in figure 2. The combination of all $t\bar{t}\gamma$ and $tW\gamma$ categories is normalised to match the event yields in data as done in table 1 to allow a comparison of the shapes of the kinematic variables. All systematic uncertainties that are introduced in section 6 are included in these distributions and their sum in quadrature, which assumes they are fully uncorrelated, is illustrated by the shaded error bands.

5 Analysis strategy

The inclusive and differential cross-sections are measured in the fiducial region described in section 5.1 and the same sources of background contributions and systematic uncertainties are considered. In the fiducial inclusive cross-section the S_{T} distribution is fitted and the post-fit background yields and systematic uncertainties are used to extract the signal cross-section, while no fit is performed for the determination of the differential cross-sections.

JHEP09(2020)049

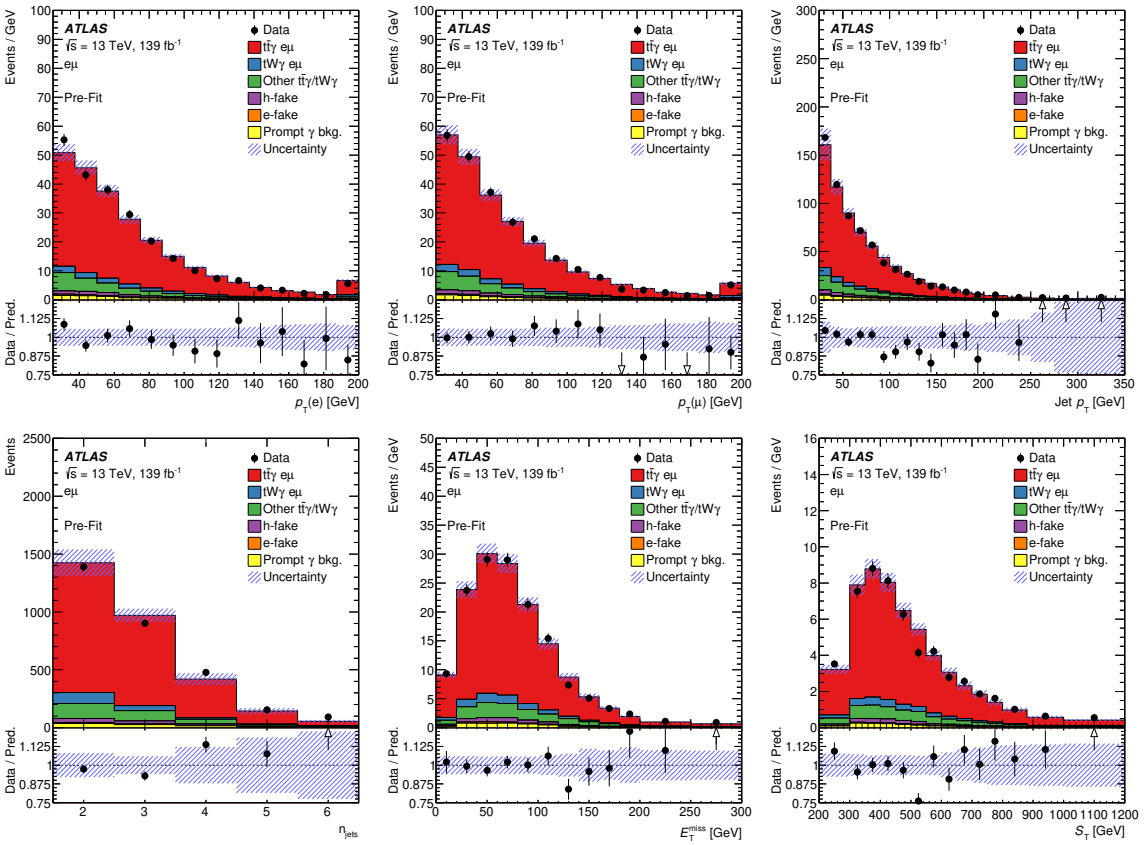

Figure 2. Distributions of the transverse momentum of the electron, the muon and all jets (top row), and the number of jets, $E_{\mathrm{T}}^{\mathrm{miss}}$ and S_{T} (bottom row) after event selection and before the profile likelihood fit. The combination of all $t\bar{t}\gamma$ and $tW\gamma$ categories is scaled to match the event yields in data. The shaded bands correspond to the statistical and systematic uncertainties (cf. section 6) added in quadrature. Overflow events are included in the last bin of each distribution. In the case of the S_{T} distribution, the underflow events are included in the first bin. The lower part of each plot shows the ratio of the data to the prediction.

5.1 Fiducial region definition

The cross-sections are reported at parton level in a fiducial region, defined by the kinematic properties of the signal process, in which all selected final-state objects are produced within the detector acceptance. This is done in a way that mimics the event selection as defined in the theoretical calculation. Objects at parton level are taken from the MC simulation history. Photons and leptons are selected as stable particles after final-state radiation. The leptons ($\ell = e, \mu$) must originate from W-boson decays and they are dressed with nearby photons within a cone of size of $\Delta R = 0.1$ around them and must have $p_{\mathrm{T}} > 25$ GeV and $|\eta| < 2.5$. Only events with exactly one electron and one muon are considered. Events with leptons originating from an intermediate τ-lepton in the top-quark decay chain are not considered. The b-jets at parton level in the calculation from refs. [10, 11] are jets clustered with the anti-k_t algorithm with a distance parameter of $R = 0.4$. Since showering and hadroni-

JHEP09(2020)049

sation effects are not considered in this calculation, the jets correspond to the b-quarks from the top-quark decay (with an additional parton in the cases where the NLO real emission leads to a parton close by a b-quark). To mimic this definition in the LO MC simulation, parton-level b-jets are defined as follows. The anti-k_t algorithm with a distance parameter $R = 0.4$ is applied to all partons that are radiated from the two b-quarks (including the b-quarks themselves) and from the two initial partons. The jets that include a b-quark from the decay of a top quark are selected as b-jets. The event is kept if there are two b-jets satisfying $p_{\mathrm{T}} > 25$ GeV and $|\eta| < 2.5$. Exactly one photon with $E_{\mathrm{T}} > 20$ GeV and $|\eta| < 2.37$ is required. Photons are required to be isolated from nearby jets by imposing a modified cone approach as described in ref. [58], as it is also done in the theory calculation in refs. [10, 11], to ensure soft and collinear safety. The event is dropped if any of the following requirements is not fulfilled: $\Delta R(\gamma, \ell) > 0.4$, $\Delta R(e, \mu) > 0.4$, $\Delta R(b, b) > 0.4$ or $\Delta R(\ell, b) > 0.4$.

5.2 Fiducial inclusive cross-section

The fiducial inclusive cross-section is extracted using a binned profile likelihood fit to the full S_{T} distribution. The distribution of S_{T} provides good separation between signal and background and was found to be less sensitive to systematic uncertainties than other distributions considered, such as the jet multiplicity or the p_{T} of individual jets. The expected signal and background distributions are modelled in the fit using template distributions taken from the simulated samples. The parameter of interest, the fiducial cross-section σ_{fid}, is related to the number of signal events in bin i of the S_{T} distribution as:

$$N_i^s = L \times \sigma_{\mathrm{fid}} \times C \times f_i^{S_{\mathrm{T}}}.$$

The term L is the integrated luminosity, $f_i^{S_{\mathrm{T}}}$ is the fraction of generated signal events falling into bin i of the S_{T} distribution after fiducial requirements are applied, and C is the correction factor for the signal efficiency ϵ and for migration into the fiducial region f_{out}, defined as follows:

$$f_{\mathrm{out}} = \frac{N_{\mathrm{reco}}^{\text{non-fid}}}{N_{\mathrm{reco}}}, \qquad \epsilon = \frac{N_{\mathrm{reco}}^{\mathrm{fid}}}{N_{\mathrm{MC}}^{\mathrm{fid}}} \qquad \Rightarrow C = \frac{\epsilon}{1 - f_{\mathrm{out}}} = \frac{N_{\mathrm{reco}}}{N_{\mathrm{MC}}^{\mathrm{fid}}},$$

where N_{reco} is the number of simulated signal events passing the event selection described in section 4, $N_{\mathrm{MC}}^{\mathrm{fid}}$ is the corresponding number of signal events generated in the fiducial region defined in section 5.1, and $N_{\mathrm{reco}}^{\mathrm{fid}}$ and $N_{\mathrm{reco}}^{\text{non-fid}}$ are the numbers of signal events that pass the event selection and are generated within and outside the fiducial region, respectively. The efficiency and outside migration are obtained from simulated $t\bar{t}\gamma$ and $tW\gamma$ events. The correction factor is estimated from the signal simulation to be $C = 0.462 \pm 0.002$ (statistical uncertainty only).

The likelihood function $\mathcal{L}$, based on Poisson statistics, is given by:

$$\mathcal{L} = \prod_i P\left(N_i^{\mathrm{obs}} | N_i^s(\vec{\theta}) + \sum_b N_i^b(\vec{\theta})\right) \times \prod_t G(0|\theta_t, 1),$$

where N_i^{obs}, N_i^s, and N_i^b are the observed number of events in data, the predicted number of signal events, and the estimated number of background events in bin i of the S_{T} distribution, respectively. The rates of those $t\bar{t}\gamma$ and $tW\gamma$ events not counted as part of the signal

JHEP09(2020)049

and categorised as *Other* $t\bar{t}\gamma/tW\gamma$ are scaled with the same parameter as the signal events in the fit, i.e. no independent production cross-section is assumed for these parts of the simulated $t\bar{t}\gamma/tW\gamma$ process. The vector $\vec{\theta}$, of components θ_t, represents the nuisance parameters that describe the sources of systematic uncertainties. Each nuisance parameter θ_t is constrained by a Gaussian distribution, $G(0|\theta_t, 1)$. The width of the Gaussian function corresponds to a change of ± 1 standard deviation of the corresponding quantity in the likelihood. For systematic uncertainties related to the finite number of simulated MC events, the Gaussian terms in the likelihood are replaced by Poisson terms. The cross-section is measured by profiling the nuisance parameters and minimising $-2\ln\mathcal{L}$ [59].

5.3 Absolute and normalised differential cross-sections

The measurements of the absolute and normalised differential cross-sections are performed as functions of the p_{T} and $|\eta|$ of the photon, and of angular variables between the photon and the leptons: ΔR between the photon and the closest lepton $\Delta R(\gamma,\ell)_{\mathrm{min}}$, as well as $\Delta\phi(\ell,\ell)$ and $|\Delta\eta(\ell,\ell)|$ between the two leptons. The kinematic properties of the photon are sensitive to the $t\gamma$ coupling. In particular, $\Delta R(\gamma,\ell)_{\mathrm{min}}$ is related to the angle between the top quark and the radiated photon, which could give insight into the structure of this coupling. The distributions of $\Delta\phi(\ell,\ell)$ and $|\Delta\eta(\ell,\ell)|$ are sensitive to the $t\bar{t}$ spin correlation. The corresponding distributions in data and SM simulations are compared in figure 3. The simulation describes reasonably well the data within the uncertainties although it favours smaller $\Delta R(\gamma,\ell)_{\mathrm{min}}$ and larger $\Delta\phi(\ell,\ell)$ values than the observed ones.

The data are corrected for detector resolution and acceptance effects to parton level in the fiducial phase space using an iterative matrix unfolding that uses Bayes' theorem [60] implemented in the RooUnfold package [61]. The differential cross-section is defined as:

$$\frac{\mathrm{d}\sigma}{\mathrm{d}X_k} = \frac{1}{L \times \Delta X_k \times \epsilon_k} \times \sum_j M_{jk}^{-1} \times (N_j^{\mathrm{obs}} - N_j^b) \times f_{e\mu,j} \times (1 - f_{\mathrm{out},j})\,.$$

The indices j and k represent the bin indices of the observable X at detector and parton levels, respectively. The variable N_j^{obs} is the number of observed events, and N_j^b is the number of estimated non-$t\bar{t}\gamma/tW\gamma$ background events (pre-fit) in bin j at detector level. The contribution from the *Other* $t\bar{t}\gamma/tW\gamma$ category is taken into account by correcting the remaining number of observed events by the signal fraction, $f_{e\mu,j}$, defined as the ratio of the number of selected $t\bar{t}\gamma$ and $tW\gamma$ $e\mu$ events to the total number of selected $t\bar{t}\gamma$ and $tW\gamma$ events, as determined from simulation. This avoids the dependence on the signal cross-section used for the normalisation. The efficiency ϵ_k is the fraction of signal events generated at parton level in bin k of the fiducial region that are reconstructed and selected at detector level. The total integrated luminosity is denoted by L, and ΔX_k represents the bin width. The migration matrix M_{kj} describes the detector response and expresses the probability for an event in bin k at parton level to be reconstructed in bin j at detector level, calculated from events passing both the fiducial-region selection and the event selection. The outside-migration fraction $f_{\mathrm{out},j}$ is the fraction of signal events generated outside the fiducial region but reconstructed and selected in bin j at detector level. The normalised

JHEP09(2020)049

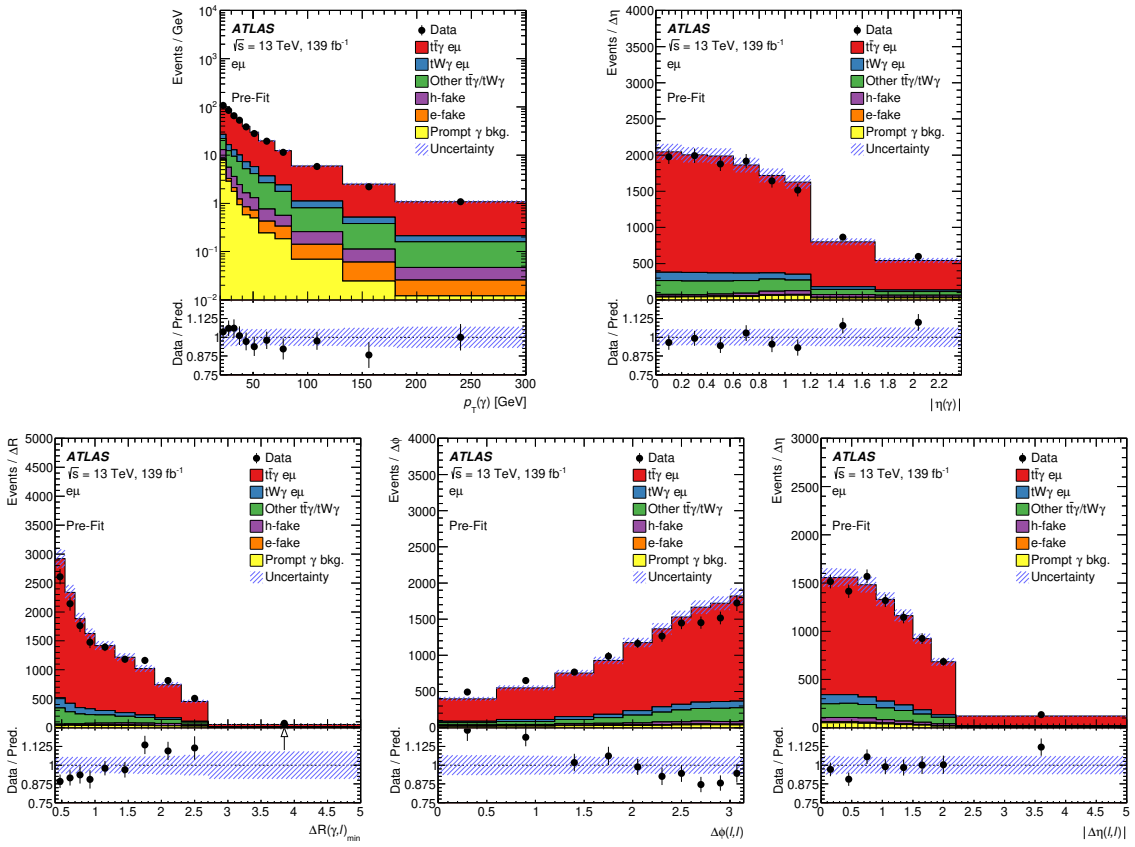

Figure 3. Distributions of the photon p_{T} and $|\eta|$ in the top row, and $\Delta R(\gamma,\ell)_{\mathrm{min}}$, $\Delta\phi(\ell,\ell)$ and $|\Delta\eta(\ell,\ell)|$ in the bottom row after event selection and before the profile likelihood fit. The combination of all $t\bar{t}\gamma$ and $tW\gamma$ categories is scaled to match the event yields in data. The shaded bands correspond to the statistical and systematic uncertainties (cf. section 6) added in quadrature. When overflow events are present, they are included in the last bin of the distribution. The lower part of each plot shows the ratio of the data to the prediction.

differential cross-section is derived by dividing the absolute result by the total cross-section, obtained by integrating over all bins of the observable.

The signal MC samples are used to determine ϵ_k, $f_{\mathrm{out},j}$, and M_{kj}. The unfolding method relies on the Bayesian probability formula, starting from a given prior of the parton-level distribution and iteratively updating it with the posterior distribution. The binning choices of the unfolded observables take into account the detector resolution and the expected statistical uncertainty. The bin width has to be larger than twice the resolution, and the statistical uncertainty is required to be around or below 10% across all bins, with the latter being the limiting factor in most of the cases. The resolution of the lepton and photon momenta is very high and, therefore, the fraction of events migrating from one bin to another is small. In all bins, the purity, defined as the fraction of reconstructed events that originate from the same bin at parton level, is larger than 80%, and it is above 90% for all observables except for the p_{T} of the photon. The number of iterations chosen is two, which provides good convergence of the unfolding distribution and a statistically stable result.

JHEP09(2020)049

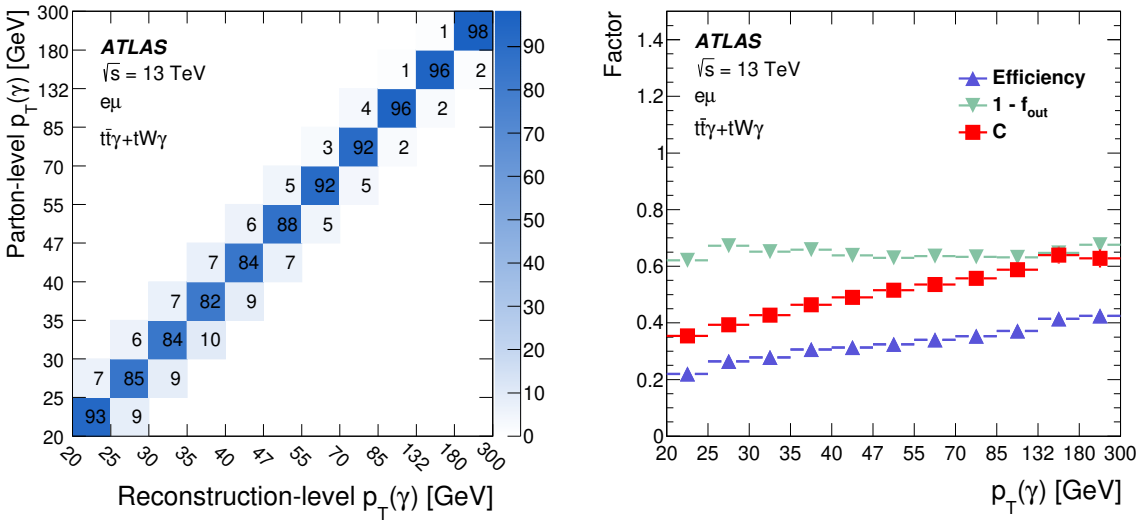

Figure 4. Left: migration matrix relating the photon p_{T} at the reconstruction and parton levels in the fiducial phase space, normalised by column and shown as percentages. Right: signal reconstruction and selection efficiency (ϵ), $(1 - f_{\mathrm{out}})$ fraction and resulting C correction factor as a function of the photon p_{T}.

For illustration purposes, the migration matrix is presented in the left panel of figure 4, while the right panel shows the efficiency, outside-migration fraction and the resulting C correction factor obtained for the distribution of the photon p_{T}. The performance of the unfolding procedure is tested for possible biases from the choice of input model. It was verified that when reweighting the shape of the signal simulation by up to 50% bin-by-bin with respect to the nominal shape, the unfolding procedure based on the nominal response matrix reproduces the altered shapes.

6 Systematic uncertainties

Various systematic uncertainties arising from detector effects are considered, along with theoretical uncertainties. Signal and background predictions are both subject to these uncertainties.

6.1 Experimental uncertainties

Experimental systematic uncertainties affect the normalisation and shape of the distributions of the simulated signal and background samples. These include reconstruction and identification efficiency uncertainties, as well as uncertainties in the energy and momentum scale and resolution for the reconstructed physics objects in the analysis, including leptons, photons, jets and $E_{\mathrm{T}}^{\mathrm{miss}}$. In addition, uncertainties in the flavour-tagging of jets, the jet vertex tagger (JVT) discriminant, the integrated luminosity value and the pile-up simulation are considered.

The photon identification and isolation efficiencies as well as the efficiencies of the lepton reconstruction, identification, isolation, and trigger in the MC samples are all corrected

JHEP09(2020)049

using scale factors to match the corresponding values in data. Similarly, corrections to the lepton and photon momentum scale and resolution are applied in simulation [46, 48]. All these corrections, which are p_{T} and η dependent, are varied within their uncertainties.

The jet energy scale (JES) uncertainty is derived using a combination of simulations, test-beam data and *in situ* measurements [52]. Additional contributions from jet-flavour composition, η-intercalibration, punch-through, single-particle response, calorimeter response to different jet flavours, and pile-up are taken into account, resulting in 30 uncorrelated JES uncertainty subcomponents, of which 29 are non-zero in a given event depending on the type of simulation used. The most relevant JES uncertainties are related to the pile-up correction (*JES pile-up correction*) and modelling aspects of the in situ calibration (*JES in situ calibration*). The jet energy resolution (JER) in simulation is smeared by the measured JER uncertainty [62] split into eight uncorrelated sources. The uncertainty associated with the JVT discriminant is obtained by varying the efficiency correction factors (labelled *jet vertex tagging* in the results, cf. figure 5).

The uncertainties related to the b-jet tagging calibration are determined separately for b-jets, c-jets and light-flavour jets [63–65]. For each jet category, the uncertainties are decomposed into several uncorrelated components. The corrections are varied by their measured uncertainties.

The uncertainties associated with energy scales and resolutions of photons, leptons and jets are propagated to the $E_{\mathrm{T}}^{\mathrm{miss}}$. Additional uncertainties originate from the modelling of its soft term [66].

The uncertainty in the combined 2015–2018 integrated luminosity is 1.7% [67], obtained using the LUCID-2 detector [68] for the primary luminosity measurements.

The uncertainty associated with the modelling of pile-up in the simulation is assessed by varying the pile-up reweighting in the simulation within its uncertainties.

6.2 Signal and background modelling uncertainties

The $t\bar{t}\gamma$ signal modelling uncertainties include the uncertainties owing to the choice of QCD scales, parton shower, amount of initial-state radiation (ISR), and PDF set. The effect of the QCD scale uncertainty is evaluated by varying the renormalisation and factorisation scales separately up and down by a factor of two from their nominal chosen values. The uncertainty from the parton shower and hadronisation ($t\bar{t}\gamma$ *PS model*) is estimated by comparing the $t\bar{t}\gamma$ nominal samples, produced with MadGraph5_aMC@NLO + Pythia 8, with an alternative sample interfaced to Herwig 7 [69, 70]. The ISR uncertainty ($t\bar{t}\gamma$ *ISR*) is studied by comparing the nominal MadGraph5_aMC@NLO + Pythia 8 sample with the results of varying the A14 tune parameter for radiation [23]. The PDF uncertainty ($t\bar{t}\gamma$ *PDF*) is evaluated using the standard deviation in each bin of the respective distribution formed by the set of 100 replicas of the NNPDF set [21].

For the $tW\gamma$ process the uncertainties due to the choice of renormalisation and factorisation scales are also estimated by varying them up and down separately by a factor of two relative to the nominal sample value. A systematic uncertainty from the parton shower and hadronisation model is considered by comparing Pythia 8 and Herwig 7 both interfaced

JHEP09(2020)049

to MadGraph5_aMC@NLO. The $tW\gamma$ modelling uncertainties are treated as uncorrelated with the $t\bar{t}\gamma$ signal modelling uncertainties.

The $tW\gamma$ process was generated in the five-flavour scheme at leading order in QCD and one of the two b-quarks is not included in the matrix-element generation step. This b-quark, expected to be produced in the initial state through the PDF, is only found in a fraction of the events at parton level in the MC simulation. The fractions of generated $tW\gamma$ events without a second b-quark were found to be around 30% and 50% for the MC samples interfaced with Herwig and Pythia, respectively. Therefore, an additional uncertainty associated with this possibly lost b-quark is assigned (*$tW\gamma$ parton definition*) as follows. Relative to the nominal $tW\gamma$ simulation, the parton-level event yields are doubled, assuming all b-jets are found, while the number of reconstructed events is kept constant. This leads to a variation of the correction factor C of 2.8%.

Several uncertainties in the modelling of $t\bar{t}$ processes, which give a dominant contribution to the h-fake and prompt γ background categories, are considered as shape-only uncertainties. The uncertainties associated with the parton shower and hadronisation are estimated by comparing the nominal simulation with alternative showering by Herwig 7. Uncertainties in the modelling of final-state radiation are estimated by evaluating the effects of varying four different parameters in the Powheg + Pythia 8 generator set-up described in the following. Uncertainties due to the renormalisation and factorisation scales are estimated by varying them up and down independently by a factor of two relative to the default scale choice. These scale variations are implemented with corresponding weights which are available as part of the nominal MC sample. Uncertainties due to the value of α_{S} used in the ISR parton shower modelling are estimated by comparing the nominal Powheg + Pythia 8 simulation with alternative samples that correspond to higher and lower radiation parameter settings in the A14 tune, controlled by the *var3c* parameter in Pythia 8. This parameter is varied within its uncertainties corresponding to variations of $\alpha_S(m_Z)$ between 0.115 and 0.140. An additional ISR uncertainty is obtained by comparing the nominal sample with an additional one where the h_{damp} parameter, which controls the p_{T} of the first additional emission, is varied by a factor of two as supported by measurements reported in ref. [71].

In addition to those background modelling uncertainties, global normalisation uncertainties of 50% are assigned to the following three categories: h-fake photons, e-fake photons and prompt γ background [9] (*h-fakes*, *e-fakes*, and *prompt γ normalisation*).

6.3 Treatment of the systematic uncertainties in the measurements

As stated in section 5, the impact of systematic uncertainties on the fiducial inclusive cross-section measurement is taken into account via nuisance parameters in the likelihood function. The nuisance parameters $\vec{\theta}$ are profiled in the maximum-likelihood fit. Variations of the nuisance parameters can affect the rate of events as well as the shape of the S_{T} distribution. In the case of signal modelling uncertainties, the rate uncertainty is composed of variations of the efficiency ϵ and the fraction f_{out}. All MC samples used to evaluate signal modelling uncertainties are scaled to the same number of events in the fiducial phase space, $N_{\mathrm{MC}}^{\mathrm{fid}}$. The only uncertainty that is not included as a nuisance parameter in the profile

JHEP09(2020)049

likelihood fit is the uncertainty from the $tW\gamma$ parton definition. This uncertainty does not affect the number of reconstructed events in the corresponding template in the profile likelihood fit. It comprises only an uncertainty in the number of generated events in the fiducial phase space. Thus, the $tW\gamma$ parton definition uncertainty is added in quadrature to the post-fit uncertainty of the profile likelihood fit.

To reduce the sensitivity to statistical fluctuations due to the limited number of events in the MC samples used in systematic variations, *smoothing* techniques are applied to the MC templates used to evaluate the signal and background modelling systematic uncertainties in the template fit. Additionally, the systematic uncertainties are symmetrised, taking the average of the up- and down-variation as the uncertainty. In the cases where both variations have the same sign or only one variation is available (e.g. the uncertainty from the parton shower and hadronisation signal modelling) the largest variation or the available one, respectively, is taken as both the up- and down-variations for the corresponding source. The ISR uncertainty suffers from statistical fluctuations in the available $t\bar{t}\gamma$ MC samples, so a more conservative approach is chosen for the symmetrisation. In this case, the largest of the two variations is taken and mirrored around the nominal prediction.

In the case of the differential cross-section measurements, each systematic uncertainty is determined individually in each bin of the measurement by varying the corresponding efficiency, resolution, and model parameter within its uncertainty. The same symmetrisation approach described for the fiducial inclusive cross-section is used for this measurement. For each variation, the measured differential cross-section is recalculated and the deviation from the nominal result per bin is taken as the systematic uncertainty. The overall uncertainty in the measurement is then derived by adding all contributions in quadrature, assuming the sources of systematic uncertainty to be fully uncorrelated.

Sources of systematic uncertainty relating only to the background prediction are evaluated by shifting the nominal distribution of the corresponding background process by its associated uncertainty. For the experimental uncertainties, the input is varied by the corresponding shift, which typically affects both the shape and normalisation of signal and background process distributions. The resulting distribution is unfolded and compared with the nominal unfolded distribution and the difference is assigned as an uncertainty. The systematic uncertainties due to signal modelling are evaluated by varying the signal corrections, i.e. the migration matrix M_{kj}, the efficiency ϵ_k and the fraction $f_{\text{out},j}$, by the corresponding model parameter uncertainty and calculating the difference between the resulting unfolded distributions and the nominal ones.

7 Fiducial inclusive cross-section measurement

The number of signal events is extracted using a profile likelihood fit to the S_{T} distribution and is translated into the signal cross-section in the fiducial phase space given by the kinematic boundaries of the signal as described in section 5.

The best-fit values of the nuisance parameters ranked highest in impact are shown in figure 5 along with their impact on the result. Rate and shape uncertainties from the $t\bar{t}\gamma$ PS model and $t\bar{t}\gamma$ ISR variations are treated as separate nuisance parameters.

JHEP09(2020)049

Category	Uncertainty
$t\bar{t}\gamma/tW\gamma$ modelling	3.8%
Background modelling	2.1%
Photons	1.9%
Luminosity	1.8%
Jets	1.6%
Pile-up	1.3%
Leptons	1.1%
Flavour-tagging	1.1%
MC statistics	0.4%
Soft term $E_{\mathrm{T}}^{\mathrm{miss}}$	0.2%
$tW\gamma$ parton definition	2.8%
Total syst.	6.3%

Table 2. Illustrative summary of the systematic uncertainties on the fiducial inclusive cross-section measurement grouped into different categories and their relative impact on the measurement (symmetrised). The categories '$t\bar{t}\gamma/tW\gamma$ modelling' and 'Background modelling' include all corresponding systematic uncertainties described in section 6.2. The '$tW\gamma$ parton definition' uncertainty is listed separately since it does not enter the profile likelihood fit directly as described in section 6.3. The category 'Photons' corresponds to the uncertainties related to photon identification and isolation as well as photon energy scale and resolution. 'Jets' includes the total uncertainty from the JES, JER and JVT discriminant, while the b-tagging-related uncertainties are given in a separate category ('Flavour-tagging'). The category 'Leptons' represents the uncertainties related to lepton identification, isolation and energy/momentum calibration.

This approach prevents pulls on the rate uncertainty due to differences in the shape of the S_{T} distribution between the data and simulation, in particular in the tail where the data overshoot the prediction and the fit compensates for this discrepancy by pulling the nuisance parameter of the $t\bar{t}\gamma$ PS model shape uncertainty. The impact of the individual nuisance parameters is evaluated as the difference between the reference best-fit value of the cross-section and the one obtained when fixing the corresponding nuisance parameter under scrutiny to its best-fit value and its $\pm$ one standard deviation ($\pm 1\sigma$). Table 2 shows the systematic uncertainties and their relative impact on the measurement of the fiducial inclusive cross-section. The effect of each category of uncertainties is calculated from the variance (σ^2) difference between the total uncertainty in the measured fiducial cross-section and the uncertainty from the fit with the corresponding nuisance parameters fixed to their fitted values. The uncertainties in the signal modelling, especially the rate uncertainties from the $t\bar{t}\gamma$ PS model and the ISR variation, have the largest impact on the result.

The distribution of the fitted S_{T} variable is shown in figure 6. The dashed band represents the post-fit uncertainties. The expected yields after the fit describe the data well.

JHEP09(2020)049

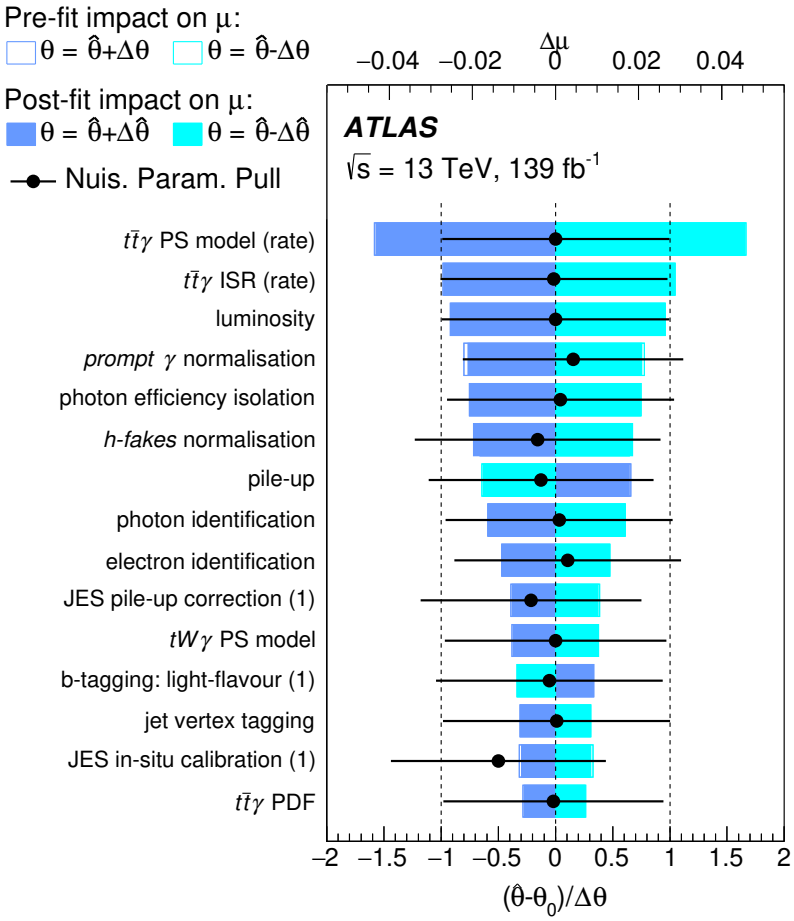

Figure 5. Ranking of the systematic uncertainties included in the profile likelihood fit used in the fiducial inclusive cross-section measurement. The blue and turquoise bands indicate the post-fit impact on the fit result, whereas the outlined blue and turquoise rectangles show the pre-fit impact. The difference between the two reflects the constraint of the nuisance parameter due to correlations in the fit. Most nuisance parameters are not or only marginally constrained. The impact is overlaid with the post-fit values of the nuisance parameters (pulls) shown by the black dots. The black lines represent the post-fit uncertainties normalised to the pre-fit uncertainties. For uncertainties parameterised with more than one nuisance parameter, the index (1) refers to the leading component.

Extrapolated to the fiducial phase space using the correction factor C, the fit result corresponds to a fiducial inclusive cross-section for the combined $t\bar{t}\gamma/tW\gamma$ process in the $e\mu$ channel of $\sigma_{\text{fid}} = 39.6 \pm 0.8\,(\text{stat})\,^{+2.6}_{-2.2}\,(\text{syst})\,\text{fb} = 39.6\,^{+2.7}_{-2.3}\,\text{fb}$. The measured cross-section is in good agreement with the dedicated theoretical calculation provided by the authors of refs. [10, 11], which predicts a value of $\sigma_{\text{fid}} = 38.50\,^{+0.56}_{-2.18}\,(\text{scale})\,^{+1.04}_{-1.18}\,(\text{PDF})\,\text{fb}$ for the chosen fiducial phase space using the CT14 PDF set [72]. The uncertainty in the theory prediction includes uncertainties owing to the scales and PDF. The PDF uncertainty is rescaled to the 68% CL. In the theoretical calculation, the renormalisation and factorisation scales are chosen as 1/4 of the total transverse momentum of the system, defined as the scalar sum of the p_{T} of the leptons, b-jets, photon and the total missing p_{T} from the neutrinos. The

JHEP09(2020)049

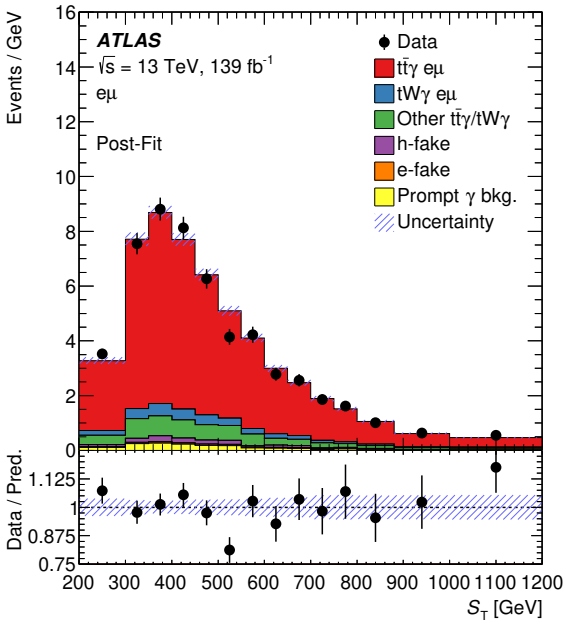

Figure 6. Post-fit distribution of the S_{T} variable. The uncertainty band represents the post-fit uncertainties. Underflow and overflow events are included in the first and last bins of the distribution, respectively. The lower part of the plot shows the ratio of the data to the prediction.

mass of the top quark is set to 173.2 GeV. The electroweak coupling in the calculation is derived from the Fermi constant G_μ and it is set to $\alpha_{G_\mu} \approx 1/132$, while it is 1/137 for the leading emission. Further details can be found in ref. [10].

8 Differential cross-section measurements

The absolute differential cross-sections are shown in figure 7 while the normalised measured differential cross-sections are presented in figure 8. The cross-sections are compared with the NLO calculation in the same fiducial phase space and with the combination of the $t\bar{t}\gamma$ and $tW\gamma$ LO MadGraph5_aMC@NLO simulations interfaced with Pythia 8 and Herwig 7, referred to as MG5_aMC+Pythia8 and MG5_aMC+Herwig7 in the following plots and tables. The calculated χ^2/ndf values for the absolute and normalised cross-sections and their corresponding p-values are summarised in tables 3 and 4, quantifying the probability of compatibility between data and each of the predictions. The χ^2 values are calculated as:

$$\chi^2 = \sum_{j,k} (\sigma_{j,\mathrm{data}} - \sigma_{j,\mathrm{pred.}}) \cdot C_{jk}^{-1} \cdot (\sigma_{k,\mathrm{data}} - \sigma_{k,\mathrm{pred.}}) \,,$$

where σ_{data} and $\sigma_{\mathrm{pred.}}$ are the unfolded and predicted differential cross-sections, C_{jk} is the covariance matrix of σ_{data}, calculated as the sum of the covariance matrix for the statistical uncertainty and the covariance matrices for the systematic uncertainties, and j and k are the binning indices of the distribution. The covariance matrix for each of the systematic uncertainties is estimated as $\sigma_j \times \sigma_k$, where σ_j and σ_k are the symmetrised

JHEP09(2020)049

Predictions	$p_{\mathrm{T}}(\gamma)$		$\lvert\eta(\gamma)\rvert$		$\Delta R(\gamma,\ell)_{\mathrm{min}}$		$\Delta\phi(\ell,\ell)$		$\lvert\Delta\eta(\ell,\ell)\rvert$	
	χ^2/ndf	p-value	χ^2/ndf	p-value	χ^2/ndf	p-value	χ^2/ndf	p-value	χ^2/ndf	p-value
Theory NLO	6.1/11	0.87	4.5/8	0.81	11.7/10	0.31	5.8/10	0.83	6.2/8	0.62

Table 3. χ^2/ndf and p-values between the measured absolute cross-sections and the NLO calculation.

Predictions	$p_{\mathrm{T}}(\gamma)$		$\lvert\eta(\gamma)\rvert$		$\Delta R(\gamma,\ell)_{\mathrm{min}}$		$\Delta\phi(\ell,\ell)$		$\lvert\Delta\eta(\ell,\ell)\rvert$	
	χ^2/ndf	p-value	χ^2/ndf	p-value	χ^2/ndf	p-value	χ^2/ndf	p-value	χ^2/ndf	p-value
$t\bar{t}\gamma$+$tW\gamma$ (MG5_aMC+Pythia8)	6.3/10	0.79	7.3/7	0.40	20.1/9	0.02	30.8/9	<0.01	6.5/7	0.48
$t\bar{t}\gamma$+$tW\gamma$ (MG5_aMC+Herwig7)	5.3/10	0.87	7.7/7	0.36	18.9/9	0.03	31.6/9	<0.01	6.8/7	0.45
Theory NLO	6.0/10	0.82	4.5/7	0.72	13.5/9	0.14	5.8/9	0.76	5.6/7	0.59

Table 4. χ^2/ndf and p-values between the measured normalised cross-sections and various predictions from the MC simulation and the NLO calculation.

uncertainties for bin j and bin k of the unfolded distribution. In the case of the normalised differential cross-sections, the last bin is removed from the χ^2 calculation and the number of degrees of freedom is reduced by one.

The shape of the measured differential distributions is generally well described by both the LO MC predictions from MadGraph5_aMC@NLO and the NLO theory prediction. The latter tends to describe the shape of the measured distribution slightly better. The shapes of $\Delta R(\gamma,\ell)_{\mathrm{min}}$ and $\Delta\phi(\ell,\ell)$ are not perfectly modelled by the MadGraph5_aMC@NLO simulation, while the NLO prediction provides a better description of these distributions.

The systematic uncertainties of the unfolded distributions are decomposed into signal modelling uncertainties, experimental uncertainties, and background modelling uncertainties. The breakdown of the categories of systematic uncertainties and the statistical one, which is the dominant source of uncertainty, is illustrated in figures 9 and 10 for the absolute and normalised differential cross-sections, respectively. The systematic uncertainty is dominated by the background and signal modelling.

9 Conclusions

Measurements of the fiducial inclusive production cross-section, as well as absolute and normalised differential production cross-sections, of the combined $t\bar{t}\gamma/tW\gamma$ process in the $e\mu$ decay channel are presented using pp collisions at a centre-of-mass energy of 13 TeV, corresponding to an integrated luminosity of 139 fb^{-1} recorded by the ATLAS detector at the LHC. For the estimation of efficiencies and acceptance corrections, a LO Monte Carlo simulation of the $2 \to 7$ process $pp \to e\nu\mu\nu bb\gamma$ was used for the $t\bar{t}\gamma$ part of the signal. The contribution from $tW\gamma$ was estimated from a combination of LO Monte Carlo simulations for the $2 \to 3$ process $pp \to tW\gamma$ and the $2 \to 6$ process $pp \to e\nu\mu\nu b\gamma$. The simulations include initial- and final-state radiation of the photon from all involved objects in the matrix element. The resonant top-quark production is taken into account in the

JHEP09(2020)049

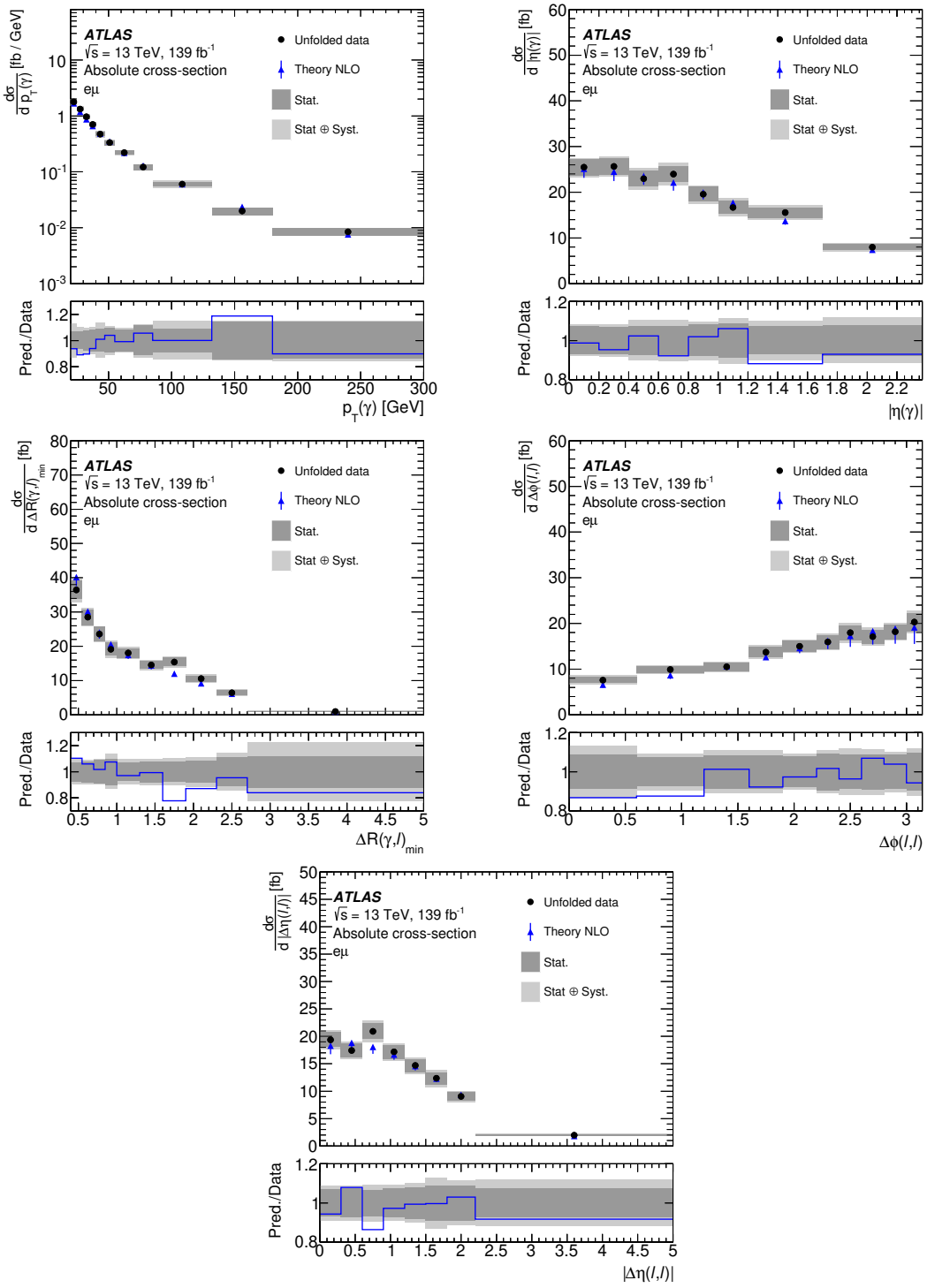

Figure 7. Absolute differential cross-section measured in the fiducial phase space as a function of the photon p_{T}, photon $|\eta|$, $\Delta R(\gamma,\ell)_{\mathrm{min}}$, $\Delta\phi(\ell,\ell)$, and $|\Delta\eta(\ell,\ell)|$ (from left to right and top to bottom). Data are compared with the NLO calculation provided by the authors of refs. [10, 11]. The uncertainty in the calculation corresponds to the total scale and PDF uncertainties. The PDF uncertainty is rescaled to the 68% CL. The lower part of each plot shows the ratio of the prediction to the data.

JHEP09(2020)049

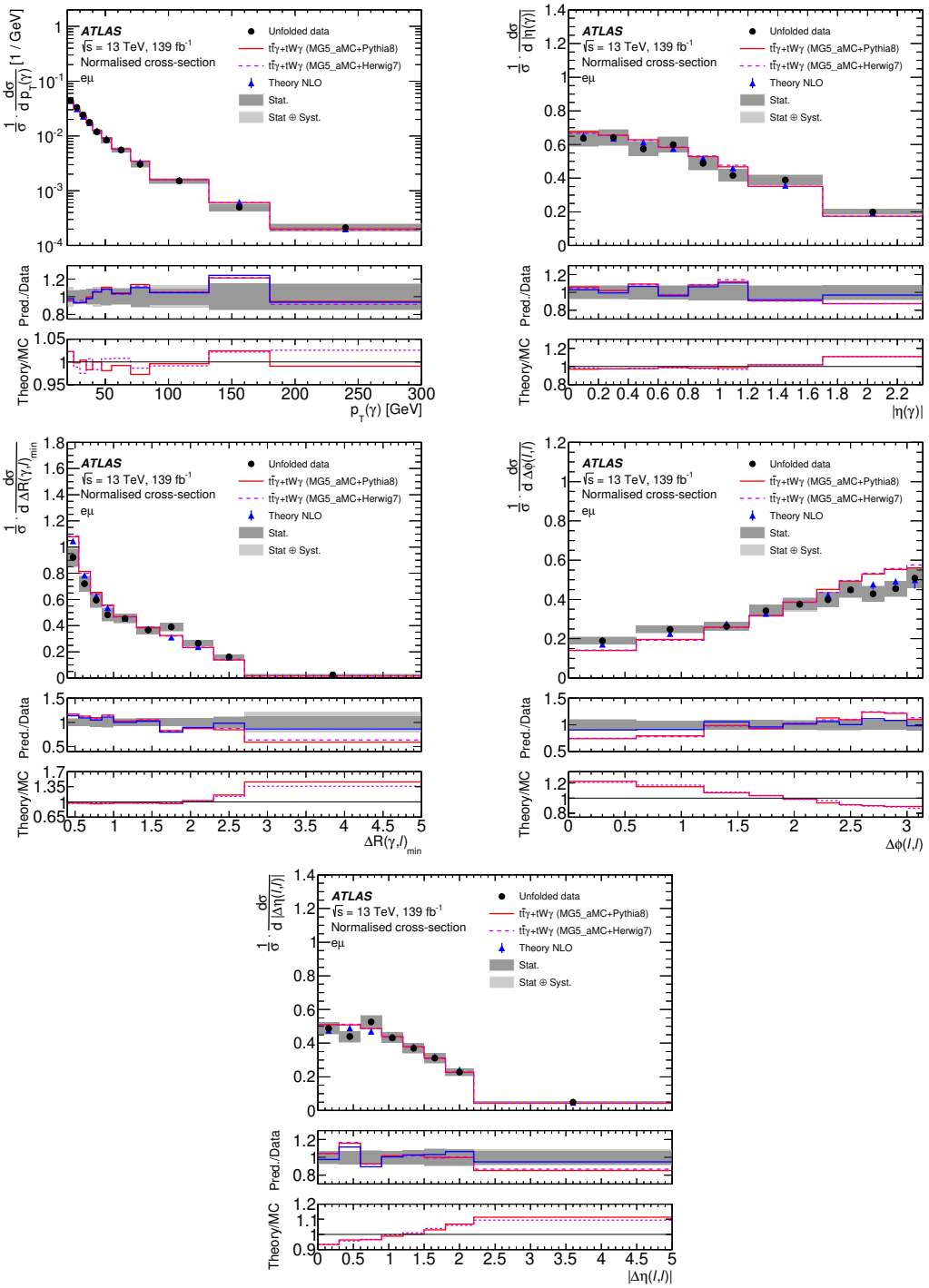

Figure 8. Normalised differential cross-section measured in the fiducial phase space as a function of the photon p_{T}, photon $|\eta|$, $\Delta R(\gamma,\ell)_{\mathrm{min}}$, $\Delta\phi(\ell,\ell)$, and $|\Delta\eta(\ell,\ell)|$ (from left to right and top to bottom). Data are compared with the NLO calculation provided by the authors of refs. [10, 11] and the MadGraph5_aMC@NLO simulation interfaced with Pythia 8 and Herwig 7. The uncertainty in the calculation corresponds to the total scale and PDF uncertainties. The PDF uncertainty is rescaled to the 68% CL. The lower parts of each plot show the ratio of the prediction to the data and the ratio of the NLO calculation to the MC simulations.

JHEP09(2020)049

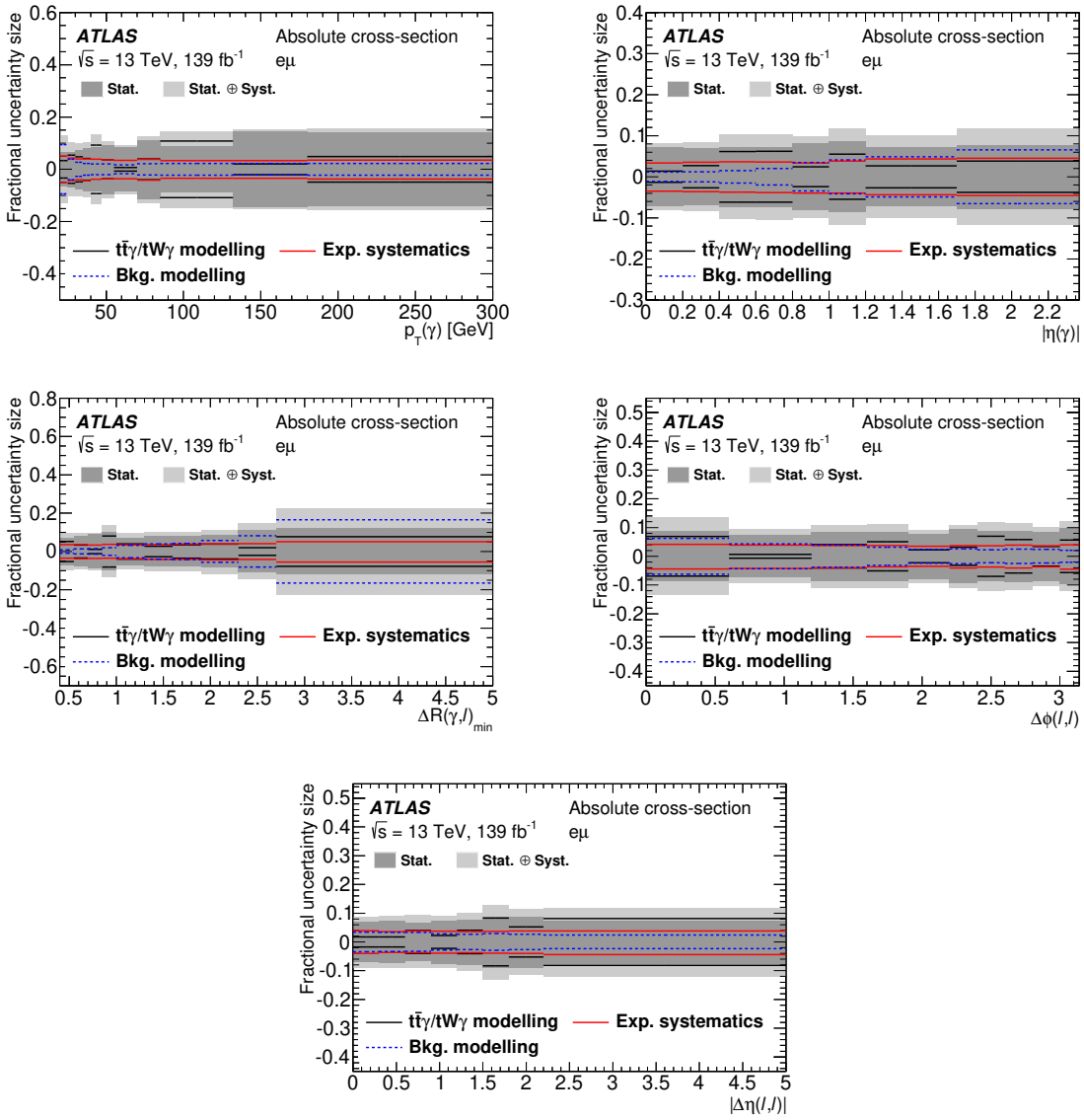

Figure 9. Contribution of each category of systematic uncertainties in each bin of the measurement of the absolute cross-sections as functions of the photon p_{T}, photon $|\eta|$, $\Delta R(\gamma,\ell)_{\mathrm{min}}$, $\Delta\phi(\ell,\ell)$ and $|\Delta\eta(\ell,\ell)|$.

simulation of $t\bar{t}\gamma$. Possible singly resonant production leading to the same final state is included in the simulation of the $tW\gamma$ process.

The results are compared with the prediction from the LO Monte Carlo simulations and also a dedicated NLO theory prediction which includes all off-shell contributions. The measured fiducial inclusive cross-section of $\sigma = 39.6\,^{+2.7}_{-2.3}\,\mathrm{fb}$ is found to be in good agreement with the predicted NLO cross-section. All considered differential distributions are also found to be well described by the NLO theory prediction.

JHEP09(2020)049

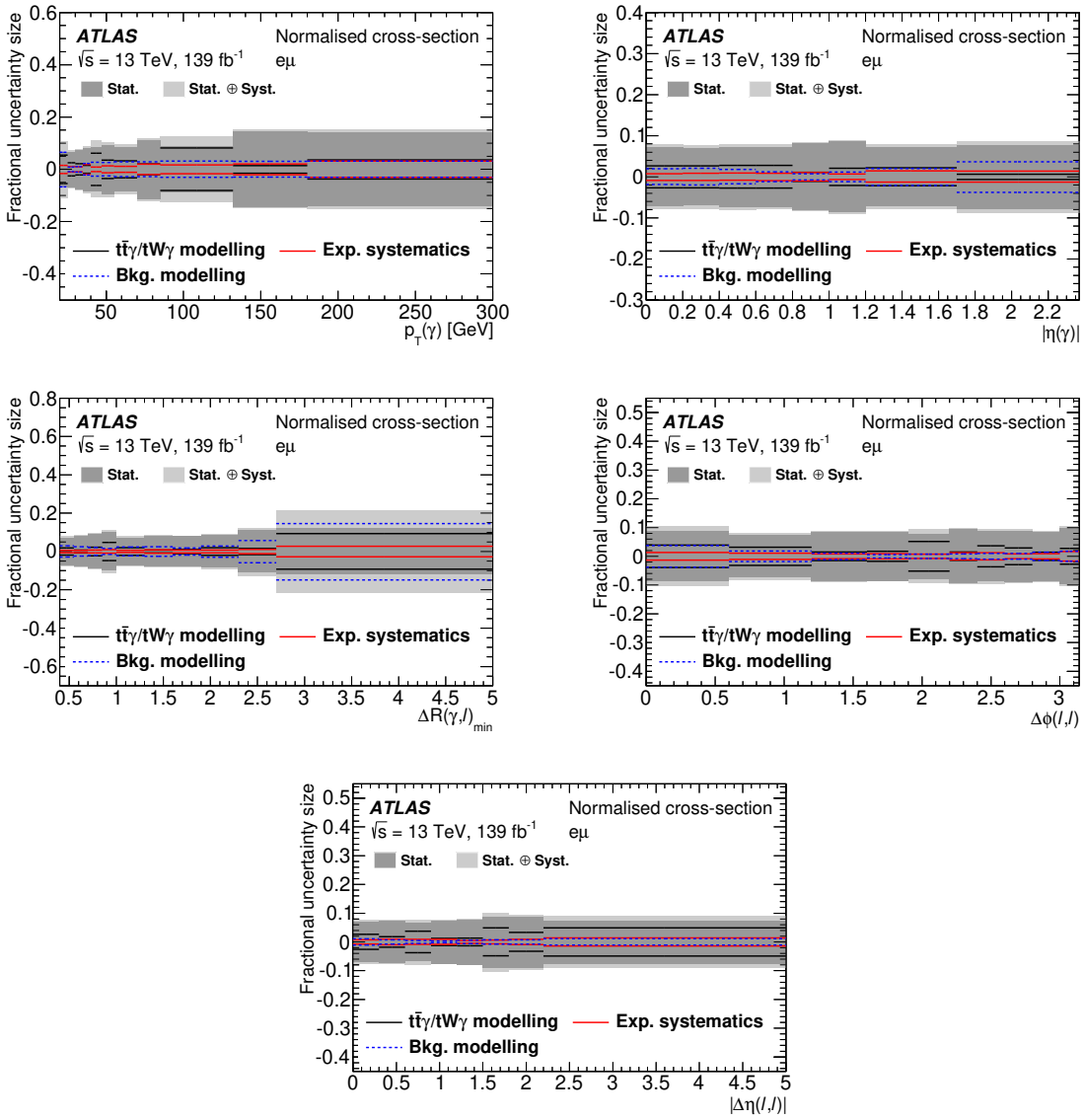

Figure 10. Contribution of each category of systematic uncertainties in each bin of the measurement of the normalised cross-sections as functions of the photon p_{T}, photon $|\eta|$, $\Delta R(\gamma,\ell)_{\mathrm{min}}$, $\Delta\phi(\ell,\ell)$ and $|\Delta\eta(\ell,\ell)|$ (from left to right and top to bottom).

Acknowledgments

We thank CERN for the very successful operation of the LHC, as well as the support staff from our institutions without whom ATLAS could not be operated efficiently.

We thank the authors, in particular M. Worek, for fruitful discussions and for providing dedicated theory predictions for our measurements.

We acknowledge the support of ANPCyT, Argentina; YerPhI, Armenia; ARC, Australia; BMWFW and FWF, Austria; ANAS, Azerbaijan; SSTC, Belarus; CNPq and FAPESP, Brazil; NSERC, NRC and CFI, Canada; CERN; CONICYT, Chile; CAS,

JHEP09(2020)049

MOST and NSFC, China; COLCIENCIAS, Colombia; MSMT CR, MPO CR and VSC CR, Czech Republic; DNRF and DNSRC, Denmark; IN2P3-CNRS and CEA-DRF/IRFU, France; SRNSFG, Georgia; BMBF, HGF and MPG, Germany; GSRT, Greece; RGC and Hong Kong SAR, China; ISF and Benoziyo Center, Israel; INFN, Italy; MEXT and JSPS, Japan; CNRST, Morocco; NWO, Netherlands; RCN, Norway; MNiSW and NCN, Poland; FCT, Portugal; MNE/IFA, Romania; MES of Russia and NRC KI, Russia Federation; JINR; MESTD, Serbia; MSSR, Slovakia; ARRS and MIZŠ, Slovenia; DST/NRF, South Africa; MINECO, Spain; SRC and Wallenberg Foundation, Sweden; SERI, SNSF and Cantons of Bern and Geneva, Switzerland; MOST, Taiwan; TAEK, Turkey; STFC, United Kingdom; DOE and NSF, United States of America. In addition, individual groups and members have received support from BCKDF, CANARIE, Compute Canada and CRC, Canada; ERC, ERDF, Horizon 2020, Marie Skłodowska-Curie Actions and COST, European Union; Investissements d'Avenir Labex, Investissements d'Avenir Idex and ANR, France; DFG and AvH Foundation, Germany; Herakleitos, Thales and Aristeia programmes co-financed by EU-ESF and the Greek NSRF, Greece; BSF-NSF and GIF, Israel; CERCA Programme Generalitat de Catalunya and PROMETEO Programme Generalitat Valenciana, Spain; Göran Gustafssons Stiftelse, Sweden; The Royal Society and Leverhulme Trust, United Kingdom.

The crucial computing support from all WLCG partners is acknowledged gratefully, in particular from CERN, the ATLAS Tier-1 facilities at TRIUMF (Canada), NDGF (Denmark, Norway, Sweden), CC-IN2P3 (France), KIT/GridKA (Germany), INFN-CNAF (Italy), NL-T1 (Netherlands), PIC (Spain), ASGC (Taiwan), RAL (U.K.) and BNL (U.S.A.), the Tier-2 facilities worldwide and large non-WLCG resource providers. Major contributors of computing resources are listed in ref. [73].

JHEP09(2020)049

References

[1] U. Baur, A. Juste, L.H. Orr and D. Rainwater, *Probing electroweak top quark couplings at hadron colliders*, *Phys. Rev. D* **71** (2005) 054013 [hep-ph/0412021] [INSPIRE].

[2] A.O. Bouzas and F. Larios, *Electromagnetic dipole moments of the top quark*, *Phys. Rev. D* **87** (2013) 074015 [arXiv:1212.6575] [INSPIRE].

[3] M. Schulze and Y. Soreq, *Pinning down electroweak dipole operators of the top quark*, *Eur. Phys. J. C* **76** (2016) 466 [arXiv:1603.08911] [INSPIRE].

[4] O. Bessidskaia Bylund, F. Maltoni, I. Tsinikos, E. Vryonidou and C. Zhang, *Probing top quark neutral couplings in the Standard Model effective field theory at NLO in QCD*, *JHEP* **05** (2016) 052 [arXiv:1601.08193] [INSPIRE].

[5] CDF collaboration, *Evidence for $t\bar{t}\gamma$ production and measurement of $\sigma_{t\bar{t}\gamma}/\sigma_{t\bar{t}}$*, *Phys. Rev. D* **84** (2011) 031104 [arXiv:1106.3970] [INSPIRE].

[6] ATLAS collaboration, *Observation of top-quark pair production in association with a photon and measurement of the $t\bar{t}\gamma$ production cross section in pp collisions at $\sqrt{s} = 7$ TeV using the ATLAS detector*, *Phys. Rev. D* **91** (2015) 072007 [arXiv:1502.00586] [INSPIRE].

[7] ATLAS collaboration, *Measurement of the $t\bar{t}\gamma$ production cross section in proton-proton collisions at $\sqrt{s} = 8$ TeV with the ATLAS detector*, *JHEP* **11** (2017) 086 [arXiv:1706.03046] [INSPIRE].

[8] CMS collaboration, *Measurement of the semileptonic $t\bar{t} + \gamma$ production cross section in pp collisions at $\sqrt{s} = 8$ TeV*, *JHEP* **10** (2017) 006 [arXiv:1706.08128] [INSPIRE].

[9] ATLAS collaboration, *Measurements of inclusive and differential fiducial cross-sections of $t\bar{t}\gamma$ production in leptonic final states at $\sqrt{s} = 13$ TeV in ATLAS*, *Eur. Phys. J. C* **79** (2019) 382 [arXiv:1812.01697] [INSPIRE].

[10] G. Bevilacqua, H.B. Hartanto, M. Kraus, T. Weber and M. Worek, *Hard photons in hadroproduction of top quarks with realistic final states*, *JHEP* **10** (2018) 158 [arXiv:1803.09916] [INSPIRE].

[11] G. Bevilacqua, H.B. Hartanto, M. Kraus, T. Weber and M. Worek, *Precise predictions for $t\bar{t}\gamma/t\bar{t}$ cross section ratios at the LHC*, *JHEP* **01** (2019) 188 [arXiv:1809.08562] [INSPIRE].

[12] ATLAS collaboration, *The ATLAS experiment at the CERN Large Hadron Collider*, 2008 *JINST* **3** S08003 [INSPIRE].

[13] ATLAS collaboration, *ATLAS insertable B-layer technical design report*, Tech. Rep. CERN-LHCC-2010-013, CERN, Geneva, Switzerland (2010) [ATLAS-TDR-19] [*Addendum* CERN-LHCC-2012-009] [*Addendum* ATLAS-TDR-19-ADD-1].

[14] ATLAS IBL collaboration, *Production and integration of the ATLAS insertable B-layer*, 2018 *JINST* **13** T05008 [arXiv:1803.00844] [INSPIRE].

[15] ATLAS collaboration, *Performance of the ATLAS trigger system in* 2015, *Eur. Phys. J. C* **77** (2017) 317 [arXiv:1611.09661] [INSPIRE].

[16] ATLAS collaboration, *The ATLAS simulation infrastructure*, *Eur. Phys. J. C* **70** (2010) 823 [arXiv:1005.4568] [INSPIRE].

[17] GEANT4 collaboration, *GEANT4 — a simulation toolkit*, *Nucl. Instrum. Meth. A* **506** (2003) 250 [INSPIRE].

[18] T. Sjöstrand, S. Mrenna and P.Z. Skands, *PYTHIA* 6.4 *physics and manual*, *JHEP* **05** (2006) 026 [hep-ph/0603175] [INSPIRE].

[19] T. Sjöstrand et al., *An introduction to PYTHIA* 8.2, *Comput. Phys. Commun.* **191** (2015) 159 [arXiv:1410.3012] [INSPIRE].

[20] ATLAS collaboration, *The PYTHIA* 8 *A3 tune description of ATLAS minimum bias and inelastic measurements incorporating the Donnachie-Landshoff diffractive model*, Tech. Rep. ATL-PHYS-PUB-2016-017, CERN, Geneva, Switzerland (2016).

[21] J. Pumplin, D.R. Stump, J. Huston, H.L. Lai, P.M. Nadolsky and W.K. Tung, *New generation of parton distributions with uncertainties from global QCD analysis*, *JHEP* **07** (2002) 012 [hep-ph/0201195] [INSPIRE].

[22] J. Alwall et al., *The automated computation of tree-level and next-to-leading order differential cross sections, and their matching to parton shower simulations*, *JHEP* **07** (2014) 079 [arXiv:1405.0301] [INSPIRE].

JHEP09(2020)049

[23] ATLAS collaboration, *ATLAS PYTHIA 8 tunes to 7 TeV datas*, Tech. Rep. ATL-PHYS-PUB-2014-021, CERN, Geneva, Switzerland (2014).

[24] D.J. Lange, *The EvtGen particle decay simulation package*, *Nucl. Instrum. Meth. A* **462** (2001) 152 [INSPIRE].

[25] T. Gleisberg et al., *Event generation with SHERPA 1.1*, *JHEP* **02** (2009) 007 [arXiv:0811.4622] [INSPIRE].

[26] S. Höche, F. Krauss, S. Schumann and F. Siegert, *QCD matrix elements and truncated showers*, *JHEP* **05** (2009) 053 [arXiv:0903.1219] [INSPIRE].

[27] T. Gleisberg and S. Höche, *Comix, a new matrix element generator*, *JHEP* **12** (2008) 039 [arXiv:0808.3674] [INSPIRE].

[28] S. Schumann and F. Krauss, *A parton shower algorithm based on Catani-Seymour dipole factorisation*, *JHEP* **03** (2008) 038 [arXiv:0709.1027] [INSPIRE].

[29] S. Höche, F. Krauss, M. Schönherr and F. Siegert, *A critical appraisal of NLO+PS matching methods*, *JHEP* **09** (2012) 049 [arXiv:1111.1220] [INSPIRE].

[30] S. Catani, F. Krauss, R. Kuhn and B.R. Webber, *QCD matrix elements + parton showers*, *JHEP* **11** (2001) 063 [hep-ph/0109231] [INSPIRE].

[31] S. Höche, F. Krauss, M. Schönherr and F. Siegert, *QCD matrix elements + parton showers: the NLO case*, *JHEP* **04** (2013) 027 [arXiv:1207.5030] [INSPIRE].

[32] F. Cascioli, P. Maierhöfer and S. Pozzorini, *Scattering amplitudes with open loops*, *Phys. Rev. Lett.* **108** (2012) 111601 [arXiv:1111.5206] [INSPIRE].

[33] A. Denner, S. Dittmaier and L. Hofer, *Collier: a fortran-based Complex One-Loop LIbrary in Extended Regularizations*, *Comput. Phys. Commun.* **212** (2017) 220 [arXiv:1604.06792] [INSPIRE].

[34] P. Nason, *A new method for combining NLO QCD with shower Monte Carlo algorithms*, *JHEP* **11** (2004) 040 [hep-ph/0409146] [INSPIRE].

[35] S. Frixione, P. Nason and C. Oleari, *Matching NLO QCD computations with parton shower simulations: the POWHEG method*, *JHEP* **11** (2007) 070 [arXiv:0709.2092] [INSPIRE].

[36] S. Alioli, P. Nason, C. Oleari and E. Re, *A general framework for implementing NLO calculations in shower Monte Carlo programs: the POWHEG BOX*, *JHEP* **06** (2010) 043 [arXiv:1002.2581] [INSPIRE].

[37] NNPDF collaboration, *Parton distributions for the LHC run II*, *JHEP* **04** (2015) 040 [arXiv:1410.8849] [INSPIRE].

[38] ATLAS collaboration, *Summary of ATLAS PYTHIA 8 tunes*, Tech. Rep. ATL-PHYS-PUB-2012-003, CERN, Geneva, Switzerland (2012).

[39] M. Czakon and A. Mitov, *Top++: a program for the calculation of the top-pair cross-section at hadron colliders*, *Comput. Phys. Commun.* **185** (2014) 2930 [arXiv:1112.5675] [INSPIRE].

[40] ATLAS collaboration, *Measurement of $W^{\pm}$ and Z-boson production cross sections in pp collisions at $\sqrt{s} = 13$ TeV with the ATLAS detector*, *Phys. Lett. B* **759** (2016) 601 [arXiv:1603.09222] [INSPIRE].

[41] J.M. Campbell and R. Ellis, *An update on vector boson pair production at hadron colliders*, *Phys. Rev. D* **60** (1999) 113006 [hep-ph/9905386] [INSPIRE].

JHEP09(2020)049

[42] LHC Higgs Cross Section Working Group collaboration, *Handbook of LHC Higgs cross sections: 4. Deciphering the nature of the Higgs sector*, arXiv:1610.07922 [INSPIRE].

[43] ATLAS collaboration, *Performance of electron and photon triggers in ATLAS during LHC run 2*, *Eur. Phys. J. C* **80** (2020) 47 [arXiv:1909.00761] [INSPIRE].

[44] ATLAS collaboration, *Performance of the ATLAS muon triggers in run 2*, arXiv:2004.13447 [INSPIRE].

[45] ATLAS collaboration, *Electron and photon performance measurements with the ATLAS detector using the 2015–2017 LHC proton-proton collision data*, 2019 *JINST* **14** P12006 [arXiv:1908.00005] [INSPIRE].

[46] ATLAS collaboration, *Muon reconstruction performance of the ATLAS detector in proton-proton collision data at* $\sqrt{s} = 13$ *TeV*, *Eur. Phys. J. C* **76** (2016) 292 [arXiv:1603.05598] [INSPIRE].

[47] ATLAS collaboration, *Measurement of the photon identification efficiencies with the ATLAS detector using LHC run 2 data collected in 2015 and 2016*, *Eur. Phys. J. C* **79** (2019) 205 [arXiv:1810.05087] [INSPIRE].

[48] ATLAS collaboration, *Electron and photon energy calibration with the ATLAS detector using 2015–2016 LHC proton-proton collision data*, 2019 *JINST* **14** P03017 [arXiv:1812.03848] [INSPIRE].

[49] M. Cacciari, G.P. Salam and G. Soyez, *The anti-*k_t *jet clustering algorithm*, *JHEP* **04** (2008) 063 [arXiv:0802.1189] [INSPIRE].

[50] M. Cacciari, G.P. Salam and G. Soyez, *FastJet user manual*, *Eur. Phys. J. C* **72** (2012) 1896 [arXiv:1111.6097] [INSPIRE].

[51] ATLAS collaboration, *Properties of jets and inputs to jet reconstruction and calibration with the ATLAS detector using proton-proton collisions at* $\sqrt{s} = 13$ *TeV*, Tech. Rep. ATL-PHYS-PUB-2015-036, CERN, Geneva, Switzerland (2015).

[52] ATLAS collaboration, *Jet energy scale measurements and their systematic uncertainties in proton-proton collisions at* $\sqrt{s} = 13$ *TeV with the ATLAS detector*, *Phys. Rev. D* **96** (2017) 072002 [arXiv:1703.09665] [INSPIRE].

[53] ATLAS collaboration, *Tagging and suppression of pileup jets with the ATLAS detector*, Tech. Rep. ATLAS-CONF-2014-018, CERN, Geneva, Switzerland (2014).

[54] ATLAS collaboration, *Optimisation and performance studies of the ATLAS b-tagging algorithms for the 2017–18 LHC run*, Tech. Rep. ATL-PHYS-PUB-2017-013, CERN, Geneva, Switzerland (2017).

[55] ATLAS collaboration, *Measurements of b-jet tagging efficiency with the ATLAS detector using* $t\bar{t}$ *events at* $\sqrt{s} = 13$ *TeV*, *JHEP* **08** (2018) 089 [arXiv:1805.01845] [INSPIRE].

[56] ATLAS collaboration, E_T^{miss} *performance in the ATLAS detector using 2015–2016 LHC pp collisions*, Tech. Rep. ATLAS-CONF-2018-023, CERN, Geneva, Switzerland (2018).

[57] ATLAS collaboration, *Performance of missing transverse momentum reconstruction with the ATLAS detector using proton-proton collisions at* $\sqrt{s} = 13$ *TeV*, *Eur. Phys. J. C* **78** (2018) 903 [arXiv:1802.08168] [INSPIRE].

[58] S. Frixione, *Isolated photons in perturbative QCD*, *Phys. Lett. B* **429** (1998) 369 [hep-ph/9801442] [INSPIRE].

JHEP09(2020)049

[59] G. Cowan, K. Cranmer, E. Gross and O. Vitells, *Asymptotic formulae for likelihood-based tests of new physics*, *Eur. Phys. J. C* **71** (2011) 1554 [*Erratum ibid.* **73** (2013) 2501] [arXiv:1007.1727] [INSPIRE].

[60] G. D'Agostini, *A multidimensional unfolding method based on Bayes' theorem*, *Nucl. Instrum. Meth. A* **362** (1995) 487 [INSPIRE].

[61] T. Adye, *Unfolding algorithms and tests using RooUnfold*, in *PHYSTAT* 2011, CERN-2011-006.313, CERN, Geneva, Switzerland (2011), pg. 313 [arXiv:1105.1160] [INSPIRE].

[62] ATLAS collaboration, *Jet calibration and systematic uncertainties for jets reconstructed in the ATLAS detector at* $\sqrt{s} = 13$ *TeV*, Tech. Rep. ATL-PHYS-PUB-2015-015, CERN, Geneva, Switzerland (2015).

[63] ATLAS collaboration, *Measurements of b-jet tagging efficiency with the ATLAS detector using* $t\bar{t}$ *events at* $\sqrt{s} = 13$ *TeV*, *JHEP* **08** (2018) 089 [arXiv:1805.01845] [INSPIRE].

[64] ATLAS collaboration, *Measurement of b-tagging efficiency of c-jets in* $t\bar{t}$ *events using a likelihood approach with the ATLAS detector*, Tech. Rep. ATLAS-CONF-2018-001, CERN, Geneva, Switzerland (2018).

[65] ATLAS collaboration, *Calibration of light-flavour b-jet mistagging rates using ATLAS proton-proton collision data at* $\sqrt{s} = 13$ *TeV*, Tech. Rep. ATLAS-CONF-2018-006, CERN, Geneva, Switzerland (2018).

[66] ATLAS collaboration, *Performance of missing transverse momentum reconstruction in ATLAS studied in proton-proton collisions recorded in* 2012 *at* 8 *TeV*, Tech. Rep. ATLAS-CONF-2013-082, CERN, Geneva, Switzerland (2013).

[67] ATLAS collaboration, *Luminosity determination in pp collisions at* $\sqrt{s} = 13$ *TeV using the ATLAS detector at the LHC*, Tech. Rep. ATLAS-CONF-2019-021, CERN, Geneva, Switzerland (2019).

[68] G. Avoni et al., *The new LUCID-2 detector for luminosity measurement and monitoring in ATLAS*, 2018 *JINST* **13** P07017 [INSPIRE].

[69] M. Bahr et al., *HERWIG++ physics and manual*, *Eur. Phys. J. C* **58** (2008) 639 [arXiv:0803.0883] [INSPIRE].

[70] J. Bellm et al., *HERWIG* 7.0/*HERWIG++* 3.0 *release note*, *Eur. Phys. J. C* **76** (2016) 196 [arXiv:1512.01178] [INSPIRE].

[71] ATLAS collaboration, *Improvements in* $t\bar{t}$ *modelling using NLO+PS Monte Carlo generators for run*2, Tech. Rep. ATL-PHYS-PUB-2018-009, CERN, Geneva, Switzerland (2018).

[72] S. Dulat et al., *New parton distribution functions from a global analysis of quantum chromodynamics*, *Phys. Rev. D* **93** (2016) 033006 [arXiv:1506.07443] [INSPIRE].

[73] ATLAS collaboration, *ATLAS computing acknowledgements*, Tech. Rep. ATL-SOFT-PUB-2020-001, CERN, Geneva, Switzerland (2020).

JHEP09(2020)049

The ATLAS collaboration

G. Aad [102], B. Abbott [128], D.C. Abbott [103], A. Abed Abud [36], K. Abeling [53], D.K. Abhayasinghe [94], S.H. Abidi [166], O.S. AbouZeid [40], N.L. Abraham [155], H. Abramowicz [160], H. Abreu [159], Y. Abulaiti [6], B.S. Acharya [67a,67b,n], B. Achkar [53], L. Adam [100], C. Adam Bourdarios [5], L. Adamczyk [84a], L. Adamek [166], J. Adelman [121], M. Adersberger [114], A. Adiguzel [12c], S. Adorni [54], T. Adye [143], A.A. Affolder [145], Y. Afik [159], C. Agapopoulou [65], M.N. Agaras [38], A. Aggarwal [119], C. Agheorghiesei [27c], J.A. Aguilar-Saavedra [139f,139a,ad], A. Ahmad [36], F. Ahmadov [80], W.S. Ahmed [104], X. Ai [18], G. Aielli [74a,74b], S. Akatsuka [86], M. Akbiyik [100], T.P.A. Åkesson [97], E. Akilli [54], A.V. Akimov [111], K. Al Khoury [65], G.L. Alberghi [23b,23a], J. Albert [175], M.J. Alconada Verzini [160], S. Alderweireldt [36], M. Aleksa [36], I.N. Aleksandrov [80], C. Alexa [27b], T. Alexopoulos [10], A. Alfonsi [120], F. Alfonsi [23b,23a], M. Alhroob [128], B. Ali [141], S. Ali [157], M. Aliev [165], G. Alimonti [69a], C. Allaire [36], B.M.M. Allbrooke [155], B.W. Allen [131], P.P. Allport [21], A. Aloisio [70a,70b], F. Alonso [89], C. Alpigiani [147], E. Alunno Camelia [74a,74b], M. Alvarez Estevez [99], M.G. Alviggi [70a,70b], Y. Amaral Coutinho [81b], A. Ambler [104], L. Ambroz [134], C. Amelung [26], D. Amidei [106], S.P. Amor Dos Santos [139a], S. Amoroso [46], C.S. Amrouche [54], F. An [79], C. Anastopoulos [148], N. Andari [144], T. Andeen [11], J.K. Anders [20], S.Y. Andrean [45a,45b], A. Andreazza [69a,69b], V. Andrei [61a], C.R. Anelli [175], S. Angelidakis [9], A. Angerami [39], A.V. Anisenkov [122b,122a], A. Annovi [72a], C. Antel [54], M.T. Anthony [148], E. Antipov [129], M. Antonelli [51], D.J.A. Antrim [170], F. Anulli [73a], M. Aoki [82], J.A. Aparisi Pozo [173], M.A. Aparo [155], L. Aperio Bella [46], N. Aranzabal Barrio [36], V. Araujo Ferraz [81a], R. Araujo Pereira [81b], C. Arcangeletti [51], A.T.H. Arce [49], F.A. Arduh [89], J-F. Arguin [110], S. Argyropoulos [52], J.-H. Arling [46], A.J. Armbruster [36], A. Armstrong [170], O. Arnaez [166], H. Arnold [120], Z.P. Arrubarrena Tame [114], G. Artoni [134], H. Asada [117], K. Asai [126], S. Asai [162], T. Asawatavonvanich [164], N. Asbah [59], E.M. Asimakopoulou [171], L. Asquith [155], J. Assahsah [35d], K. Assamagan [29], R. Astalos [28a], R.J. Atkin [33a], M. Atkinson [172], N.B. Atlay [19], H. Atmani [65], K. Augsten [141], V.A. Austrup [181], G. Avolio [36], M.K. Ayoub [15a], G. Azuelos [110,al], H. Bachacou [144], K. Bachas [161], M. Backes [134], F. Backman [45a,45b], P. Bagnaia [73a,73b], M. Bahmani [85], H. Bahrasemani [151], A.J. Bailey [173], V.R. Bailey [172], J.T. Baines [143], C. Bakalis [10], O.K. Baker [182], P.J. Bakker [120], E. Bakos [16], D. Bakshi Gupta [8], S. Balaji [156], R. Balasubramanian [120], E.M. Baldin [122b,122a], P. Balek [179], F. Balli [144], W.K. Balunas [134], J. Balz [100], E. Banas [85], M. Bandieramonte [138], A. Bandyopadhyay [24], Sw. Banerjee [180,i], L. Barak [160], W.M. Barbe [38], E.L. Barberio [105], D. Barberis [55b,55a], M. Barbero [102], G. Barbour [95], T. Barillari [115], M-S. Barisits [36], J. Barkeloo [131], T. Barklow [152], R. Barnea [159], B.M. Barnett [143], R.M. Barnett [18], Z. Barnovska-Blenessy [60a], A. Baroncelli [60a], G. Barone [29], A.J. Barr [134], L. Barranco Navarro [45a,45b], F. Barreiro [99], J. Barreiro Guimarães da Costa [15a], U. Barron [160], S. Barsov [137], F. Bartels [61a], R. Bartoldus [152], G. Bartolini [102], A.E. Barton [90], P. Bartos [28a], A. Basalaev [46], A. Basan [100], A. Bassalat [65,ai], M.J. Basso [166], R.L. Bates [57], S. Batlamous [35e], J.R. Batley [32], B. Batool [150], M. Battaglia [145], M. Bauce [73a,73b], F. Bauer [144], P. Bauer [24], H.S. Bawa [31], A. Bayirli [12c], J.B. Beacham [49], T. Beau [135], P.H. Beauchemin [169], F. Becherer [52], P. Bechtle [24], H.C. Beck [53], H.P. Beck [20,p], K. Becker [177], C. Becot [46], A. Beddall [12d], A.J. Beddall [12a], V.A. Bednyakov [80], M. Bedognetti [120], C.P. Bee [154], T.A. Beermann [181], M. Begalli [81b], M. Begel [29], A. Behera [154], J.K. Behr [46], F. Beisiegel [24], M. Belfkir [5], A.S. Bell [95], G. Bella [160], L. Bellagamba [23b], A. Bellerive [34], P. Bellos [9], K. Beloborodov [122b,122a], K. Belotskiy [112], N.L. Belyaev [112], D. Benchekroun [35a], N. Benekos [10], Y. Benhammou [160], D.P. Benjamin [6],

JHEP09(2020)049

M. Benoit [29], J.R. Bensinger [26], S. Bentvelsen [120], L. Beresford [134], M. Beretta [51], D. Berge [19], E. Bergeaas Kuutmann [171], N. Berger [5], B. Bergmann [141], L.J. Bergsten [26], J. Beringer [18], S. Berlendis [7], G. Bernardi [135], C. Bernius [152], F.U. Bernlochner [24], T. Berry [94], P. Berta [100], A. Berthold [48], I.A. Bertram [90], O. Bessidskaia Bylund [181], N. Besson [144], A. Bethani [101], S. Bethke [115], A. Betti [42], A.J. Bevan [93], J. Beyer [115], D.S. Bhattacharya [176], P. Bhattarai [26], V.S. Bhopatkar [6], R. Bi [138], R.M. Bianchi [138], O. Biebel [114], D. Biedermann [19], R. Bielski [36], K. Bierwagen [100], N.V. Biesuz [72a,72b], M. Biglietti [75a], T.R.V. Billoud [141], M. Bindi [53], A. Bingul [12d], C. Bini [73a,73b], S. Biondi [23b,23a], C.J. Birch-sykes [101], M. Birman [179], T. Bisanz [53], J.P. Biswal [3], D. Biswas [180,i], A. Bitadze [101], C. Bittrich [48], K. Bjørke [133], T. Blazek [28a], I. Bloch [46], C. Blocker [26], A. Blue [57], U. Blumenschein [93], G.J. Bobbink [120], V.S. Bobrovnikov [122b,122a], S.S. Bocchetta [97], D. Boerner [46], D. Bogavac [14], A.G. Bogdanchikov [122b,122a], C. Bohm [45a], V. Boisvert [94], P. Bokan [171,171,53], T. Bold [84a], A.E. Bolz [61b], M. Bomben [135], M. Bona [93], J.S. Bonilla [131], M. Boonekamp [144], C.D. Booth [94], A.G. Borbély [57], H.M. Borecka-Bielska [91], L.S. Borgna [95], A. Borisov [123], G. Borissov [90], D. Bortoletto [134], D. Boscherini [23b], M. Bosman [14], J.D. Bossio Sola [104], K. Bouaouda [35a], J. Boudreau [138], E.V. Bouhova-Thacker [90], D. Boumediene [38], A. Boveia [127], J. Boyd [36], D. Boye [33c], I.R. Boyko [80], A.J. Bozson [94], J. Bracinik [21], N. Brahimi [60d], G. Brandt [181], O. Brandt [32], F. Braren [46], B. Brau [103], J.E. Brau [131], W.D. Breaden Madden [57], K. Brendlinger [46], R. Brener [159], L. Brenner [36], R. Brenner [171], S. Bressler [179], B. Brickwedde [100], D.L. Briglin [21], D. Britton [57], D. Britzger [115], I. Brock [24], R. Brock [107], G. Brooijmans [39], W.K. Brooks [146d], E. Brost [29], P.A. Bruckman de Renstrom [85], B. Brüers [46], D. Bruncko [28b], A. Bruni [23b], G. Bruni [23b], M. Bruschi [23b], N. Bruscino [73a,73b], L. Bryngemark [152], T. Buanes [17], Q. Buat [154], P. Buchholz [150], A.G. Buckley [57], I.A. Budagov [80], M.K. Bugge [133], F. Bührer [52], O. Bulekov [112], B.A. Bullard [59], T.J. Burch [121], S. Burdin [91], C.D. Burgard [120], A.M. Burger [129], B. Burghgrave [8], J.T.P. Burr [46], C.D. Burton [11], J.C. Burzynski [103], V. Büscher [100], E. Buschmann [53], P.J. Bussey [57], J.M. Butler [25], C.M. Buttar [57], J.M. Butterworth [95], P. Butti [36], W. Buttinger [36], C.J. Buxo Vazquez [107], A. Buzatu [157], A.R. Buzykaev [122b,122a], G. Cabras [23b,23a], S. Cabrera Urbán [173], D. Caforio [56], H. Cai [138], V.M.M. Cairo [152], O. Cakir [4a], N. Calace [36], P. Calafiura [18], G. Calderini [135], P. Calfayan [66], G. Callea [57], L.P. Caloba [81b], A. Caltabiano [74a,74b], S. Calvente Lopez [99], D. Calvet [38], S. Calvet [38], T.P. Calvet [102], M. Calvetti [72a,72b], R. Camacho Toro [135], S. Camarda [36], D. Camarero Munoz [99], P. Camarri [74a,74b], M.T. Camerlingo [75a,75b], D. Cameron [133], C. Caminchar [36], S. Campana [36], M. Campanelli [95], A. Camplani [40], V. Canale [70a,70b], A. Canesse [104], M. Cano Bret [78], J. Cantero [129], T. Cao [160], Y. Cao [172], M.D.M. Capeans Garrido [36], M. Capua [41b,41a], R. Cardarelli [74a], F. Cardillo [148], G. Carducci [41b,41a], I. Carli [142], T. Carli [36], G. Carlino [70a], B.T. Carlson [138], E.M. Carlson [175,167a], L. Carminati [69a,69b], R.M.D. Carney [152], S. Caron [119], E. Carquin [146d], S. Carrá [46], G. Carratta [23b,23a], J.W.S. Carter [166], T.M. Carter [50], M.P. Casado [14,f], A.F. Casha [166], E.G. Castiglia [182], F.L. Castillo [173], L. Castillo Garcia [14], V. Castillo Gimenez [173], N.F. Castro [139a,139e], A. Catinaccio [36], J.R. Catmore [133], A. Cattai [36], V. Cavaliere [29], V. Cavasinni [72a,72b], E. Celebi [12b], F. Celli [134], K. Cerny [130], A.S. Cerqueira [81a], A. Cerri [155], L. Cerrito [74a,74b], F. Cerutti [18], A. Cervelli [23b,23a], S.A. Cetin [12b], Z. Chadi [35a], D. Chakraborty [121], J. Chan [180], W.S. Chan [120], W.Y. Chan [91], J.D. Chapman [32], B. Chargeishvili [158b], D.G. Charlton [21], T.P. Charman [93], M. Chatterjee [20], C.C. Chau [34], S. Che [127], S. Chekanov [6], S.V. Chekulaev [167a], G.A. Chelkov [80,ag], B. Chen [79], C. Chen [60a], C.H. Chen [79], H. Chen [15c], H. Chen [29], J. Chen [60a], J. Chen [39], J. Chen [26], S. Chen [136], S.J. Chen [15c], X. Chen [15b], Y. Chen [60a], Y-H. Chen [46], H.C. Cheng [63a],

JHEP09(2020)049

H.J. Cheng [15a], A. Cheplakov [80], E. Cheremushkina [123], R. Cherkaoui El Moursli [35e], E. Cheu [7], K. Cheung [64], T.J.A. Chevalérias [144], L. Chevalier [144], V. Chiarella [51], G. Chiarelli [72a], G. Chiodini [68a], A.S. Chisholm [21], A. Chitan [27b], I. Chiu [162], Y.H. Chiu [175], M.V. Chizhov [80], K. Choi [11], A.R. Chomont [73a,73b], Y.S. Chow [120], L.D. Christopher [33e], M.C. Chu [63a], X. Chu [15a,15d], J. Chudoba [140], J.J. Chwastowski [85], L. Chytka [130], D. Cieri [115], K.M. Ciesla [85], V. Cindro [92], I.A. Cioară [27b], A. Ciocio [18], F. Cirotto [70a,70b], Z.H. Citron [179,j], M. Citterio [69a], D.A. Ciubotaru [27b], B.M. Ciungu [166], A. Clark [54], M.R. Clark [39], P.J. Clark [50], S.E. Clawson [101], C. Clement [45a,45b], Y. Coadou [102], M. Cobal [67a,67c], A. Coccaro [55b], J. Cochran [79], R. Coelho Lopes De Sa [103], H. Cohen [160], A.E.C. Coimbra [36], B. Cole [39], A.P. Colijn [120], J. Collot [58], P. Conde Muiño [139a,139h], S.H. Connell [33c], I.A. Connelly [57], S. Constantinescu [27b], F. Conventi [70a,am], A.M. Cooper-Sarkar [134], F. Cormier [174], K.J.R. Cormier [166], L.D. Corpe [95], M. Corradi [73a,73b], E.E. Corrigan [97], F. Corriveau [104,ab], M.J. Costa [173], F. Costanza [5], D. Costanzo [148], G. Cowan [94], J.W. Cowley [32], J. Crane [101], K. Cranmer [125], R.A. Creager [136], S. Crépé-Renaudin [58], F. Crescioli [135], M. Cristinziani [24], V. Croft [169], G. Crosetti [41b,41a], A. Cueto [5], T. Cuhadar Donszelmann [170], H. Cui [15a,15d], A.R. Cukierman [152], W.R. Cunningham [57], S. Czekierda [85], P. Czodrowski [36], M.M. Czurylo [61b], M.J. Da Cunha Sargedas De Sousa [60b], J.V. Da Fonseca Pinto [81b], C. Da Via [101], W. Dabrowski [84a], F. Dachs [36], T. Dado [47], S. Dahbi [33e], T. Dai [106], C. Dallapiccola [103], M. Dam [40], G. D'amen [29], V. D'Amico [75a,75b], J. Damp [100], J.R. Dandoy [136], M.F. Daneri [30], M. Danninger [151], V. Dao [36], G. Darbo [55b], O. Dartsi [5], A. Dattagupta [131], T. Daubney [46], S. D'Auria [69a,69b], C. David [167b], T. Davidek [142], D.R. Davis [49], I. Dawson [148], K. De [8], R. De Asmundis [70a], M. De Beurs [120], S. De Castro [23b,23a], N. De Groot [119], P. de Jong [120], H. De la Torre [107], A. De Maria [15c], D. De Pedis [73a], A. De Salvo [73a], U. De Sanctis [74a,74b], M. De Santis [74a,74b], A. De Santo [155], J.B. De Vivie De Regie [65], D.V. Dedovich [80], A.M. Deiana [42], J. Del Peso [99], Y. Delabat Diaz [46], D. Delgove [65], F. Deliot [144], C.M. Delitzsch [7], M. Della Pietra [70a,70b], D. Della Volpe [54], A. Dell'Acqua [36], L. Dell'Asta [74a,74b], M. Delmastro [5], C. Delporte [65], P.A. Delsart [58], D.A. DeMarco [166], S. Demers [182], M. Demichev [80], G. Demontigny [110], S.P. Denisov [123], L. D'Eramo [121], D. Derendarz [85], J.E. Derkaoui [35d], F. Derue [135], P. Dervan [91], K. Desch [24], K. Dette [166], C. Deutsch [24], M.R. Devesa [30], P.O. Deviveiros [36], F.A. Di Bello [73a,73b], A. Di Ciaccio [74a,74b], L. Di Ciaccio [5], W.K. Di Clemente [136], C. Di Donato [70a,70b], A. Di Girolamo [36], G. Di Gregorio [72a,72b], B. Di Micco [75a,75b], R. Di Nardo [75a,75b], K.F. Di Petrillo [59], R. Di Sipio [166], C. Diaconu [102], F.A. Dias [120], T. Dias Do Vale [139a], M.A. Diaz [146a], F.G. Diaz Capriles [24], J. Dickinson [18], M. Didenko [165], E.B. Diehl [106], J. Dietrich [19], S. Díez Cornell [46], C. Diez Pardos [150], A. Dimitrievska [18], W. Ding [15b], J. Dingfelder [24], S.J. Dittmeier [61b], F. Dittus [36], F. Djama [102], T. Djobava [158b], J.I. Djuvsland [17], M.A.B. Do Vale [81c], M. Dobre [27b], D. Dodsworth [26], C. Doglioni [97], J. Dolejsi [142], Z. Dolezal [142], M. Donadelli [81d], B. Dong [60c], J. Donini [38], A. D'onofrio [15c], M. D'Onofrio [91], J. Dopke [143], A. Doria [70a], M.T. Dova [89], A.T. Doyle [57], E. Drechsler [151], E. Dreyer [151], T. Dreyer [53], A.S. Drobac [169], D. Du [60b], T.A. du Pree [120], Y. Duan [60d], F. Dubinin [111], M. Dubovsky [28a], A. Dubreuil [54], E. Duchovni [179], G. Duckeck [114], O.A. Ducu [36], D. Duda [115], A. Dudarev [36], A.C. Dudder [100], E.M. Duffield [18], M. D'uffizi [101], L. Duflot [65], M. Dührssen [36], C. Dülsen [181], M. Dumancic [179], A.E. Dumitriu [27b], M. Dunford [61a], A. Duperrin [102], H. Duran Yildiz [4a], M. Düren [56], A. Durglishvili [158b], D. Duschinger [48], B. Dutta [46], D. Duvnjak [1], G.I. Dyckes [136], M. Dyndal [36], S. Dysch [101], B.S. Dziedzic [85], M.G. Eggleston [49], T. Eifert [8], G. Eigen [17], K. Einsweiler [18], T. Ekelof [171], H. El Jarrari [35e], V. Ellajosyula [171], M. Ellert [171], F. Ellinghaus [181], A.A. Elliot [93], N. Ellis [36],

JHEP09(2020)049

J. Elmsheuser [29], M. Elsing [36], D. Emeliyanov [143], A. Emerman [39], Y. Enari [162], M.B. Epland [49], J. Erdmann [47], A. Ereditato [20], P.A. Erland [85], M. Errenst [181], M. Escalier [65], C. Escobar [173], O. Estrada Pastor [173], E. Etzion [160], G.E. Evans [139a,139b], H. Evans [66], M.O. Evans [155], A. Ezhilov [137], F. Fabbri [57], L. Fabbri [23b,23a], V. Fabiani [119], G. Facini [177], R.M. Fakhrutdinov [123], S. Falciano [73a], P.J. Falke [24], S. Falke [36], J. Faltova [142], Y. Fang [15a], Y. Fang [15a], G. Fanourakis [44], M. Fanti [69a,69b], M. Faraj [67a,67c], A. Farbin [8], A. Farilla [75a], E.M. Farina [71a,71b], T. Farooque [107], S.M. Farrington [50], P. Farthouat [36], F. Fassi [35e], P. Fassnacht [36], D. Fassouliotis [9], M. Faucci Giannelli [50], W.J. Fawcett [32], L. Fayard [65], O.L. Fedin [137,o], W. Fedorko [174], A. Fehr [20], M. Feickert [172], L. Feligioni [102], A. Fell [148], C. Feng [60b], M. Feng [49], M.J. Fenton [170], A.B. Fenyuk [123], S.W. Ferguson [43], J. Ferrando [46], A. Ferrante [172], A. Ferrari [171], P. Ferrari [120], R. Ferrari [71a], D.E. Ferreira de Lima [61b], A. Ferrer [173], D. Ferrere [54], C. Ferretti [106], F. Fiedler [100], A. Filipčič [92], F. Filthaut [119], K.D. Finelli [25], M.C.N. Fiolhais [139a,139c,a], L. Fiorini [173], F. Fischer [114], J. Fischer [100], W.C. Fisher [107], T. Fitschen [21], I. Fleck [150], P. Fleischmann [106], T. Flick [181], B.M. Flierl [114], L. Flores [136], L.R. Flores Castillo [63a], F.M. Follega [76a,76b], N. Fomin [17], J.H. Foo [166], G.T. Forcolin [76a,76b], B.C. Forland [66], A. Formica [144], F.A. Förster [14], A.C. Forti [101], E. Fortin [102], M.G. Foti [134], D. Fournier [65], H. Fox [90], P. Francavilla [72a,72b], S. Francescato [73a,73b], M. Franchini [23b,23a], S. Franchino [61a], D. Francis [36], L. Franco [5], L. Franconi [20], M. Franklin [59], G. Frattari [73a,73b], A.N. Fray [93], P.M. Freeman [21], B. Freund [110], W.S. Freund [81b], E.M. Freundlich [47], D.C. Frizzell [128], D. Froidevaux [36], J.A. Frost [134], M. Fujimoto [126], C. Fukunaga [163], E. Fullana Torregrosa [173], T. Fusayasu [116], J. Fuster [173], A. Gabrielli [23b,23a], A. Gabrielli [36], S. Gadatsch [54], P. Gadow [115], G. Gagliardi [55b,55a], L.G. Gagnon [110], G.E. Gallardo [134], E.J. Gallas [134], B.J. Gallop [143], R. Gamboa Goni [93], K.K. Gan [127], S. Ganguly [179], J. Gao [60a], Y. Gao [50], Y.S. Gao [31,l], F.M. Garay Walls [146a], C. García [173], J.E. García Navarro [173], J.A. García Pascual [15a], C. Garcia-Argos [52], M. Garcia-Sciveres [18], R.W. Gardner [37], N. Garelli [152], S. Gargiulo [52], C.A. Garner [166], V. Garonne [133], S.J. Gasiorowski [147], P. Gaspar [81b], A. Gaudiello [55b,55a], G. Gaudio [71a], P. Gauzzi [73a,73b], I.L. Gavrilenko [111], A. Gavrilyuk [124], C. Gay [174], G. Gaycken [46], E.N. Gazis [10], A.A. Geanta [27b], C.M. Gee [145], C.N.P. Gee [143], J. Geisen [97], M. Geisen [100], C. Gemme [55b], M.H. Genest [58], C. Geng [106], S. Gentile [73a,73b], S. George [94], T. Geralis [44], L.O. Gerlach [53], P. Gessinger-Befurt [100], G. Gessner [47], S. Ghasemi [150], M. Ghasemi Bostanabad [175], M. Ghneimat [150], A. Ghosh [65], A. Ghosh [78], B. Giacobbe [23b], S. Giagu [73a,73b], N. Giangiacomi [23b,23a], P. Giannetti [72a], A. Giannini [70a,70b], G. Giannini [14], S.M. Gibson [94], M. Gignac [145], D.T. Gil [84b], B.J. Gilbert [39], D. Gillberg [34], G. Gilles [181], N.E.K. Gillwald [46], D.M. Gingrich [3,al], M.P. Giordani [67a,67c], P.F. Giraud [144], G. Giugliarelli [67a,67c], D. Giugni [69a], F. Giuli [74a,74b], S. Gkaitatzis [161], I. Gkialas [9,g], E.L. Gkougkousis [14], P. Gkountoumis [10], L.K. Gladilin [113], C. Glasman [99], J. Glatzer [14], P.C.F. Glaysher [46], A. Glazov [46], G.R. Gledhill [131], I. Gnesi [41b,b], M. Goblirsch-Kolb [26], D. Godin [110], S. Goldfarb [105], T. Golling [54], D. Golubkov [123], A. Gomes [139a,139b], R. Goncalves Gama [53], R. Gonçalo [139a,139c], G. Gonella [131], L. Gonella [21], A. Gongadze [80], F. Gonnella [21], J.L. Gonski [39], S. González de la Hoz [173], S. Gonzalez Fernandez [14], R. Gonzalez Lopez [91], C. Gonzalez Renteria [18], R. Gonzalez Suarez [171], S. Gonzalez-Sevilla [54], G.R. Gonzalvo Rodriguez [173], L. Goossens [36], N.A. Gorasia [21], P.A. Gorbounov [124], H.A. Gordon [29], B. Gorini [36], E. Gorini [68a,68b], A. Gorišek [92], A.T. Goshaw [49], M.I. Gostkin [80], C.A. Gottardo [119], M. Gouighri [35b], A.G. Goussiou [147], N. Govender [33c], C. Goy [5], I. Grabowska-Bold [84a], E.C. Graham [91], J. Gramling [170], E. Gramstad [133], S. Grancagnolo [19], M. Grandi [155], V. Gratchev [137], P.M. Gravila [27f], F.G. Gravili [68a,68b], C. Gray [57], H.M. Gray [18], C. Grefe [24], K. Gregersen

JHEP09(2020)049

[97], I.M. Gregor [46], P. Grenier [152], K. Grevtsov [46], C. Grieco [14], N.A. Grieser [128], A.A. Grillo [145], K. Grimm [31,k], S. Grinstein [14,w], J.-F. Grivaz [65], S. Groh [100], E. Gross [179], J. Grosse-Knetter [53], Z.J. Grout [95], C. Grud [106], A. Grummer [118], J.C. Grundy [134], L. Guan [106], W. Guan [180], C. Gubbels [174], J. Guenther [36], A. Guerguichon [65], J.G.R. Guerrero Rojas [173], F. Guescini [115], D. Guest [170], R. Gugel [100], A. Guida [46], T. Guillemin [5], S. Guindon [36], J. Guo [60c], W. Guo [106], Y. Guo [60a], Z. Guo [102], R. Gupta [46], S. Gurbuz [12c], G. Gustavino [128], M. Guth [52], P. Gutierrez [128], C. Gutschow [95], C. Guyot [144], C. Gwenlan [134], C.B. Gwilliam [91], E.S. Haaland [133], A. Haas [125], C. Haber [18], H.K. Hadavand [8], A. Hadef [60a], M. Haleem [176], J. Haley [129], J.J. Hall [148], G. Halladjian [107], G.D. Hallewell [102], K. Hamano [175], H. Hamdaoui [35e], M. Hamer [24], G.N. Hamity [50], K. Han [60a,v], L. Han [15c], L. Han [60a], S. Han [18], Y.F. Han [166], K. Hanagaki [82,t], M. Hance [145], D.M. Handl [114], M.D. Hank [37], R. Hankache [135], E. Hansen [97], J.B. Hansen [40], J.D. Hansen [40], M.C. Hansen [24], P.H. Hansen [40], E.C. Hanson [101], K. Hara [168], T. Harenberg [181], S. Harkusha [108], P.F. Harrison [177], N.M. Hartman [152], N.M. Hartmann [114], Y. Hasegawa [149], A. Hasib [50], S. Hassani [144], S. Haug [20], R. Hauser [107], L.B. Havener [39], M. Havranek [141], C.M. Hawkes [21], R.J. Hawkings [36], S. Hayashida [117], D. Hayden [107], C. Hayes [106], R.L. Hayes [174], C.P. Hays [134], J.M. Hays [93], H.S. Hayward [91], S.J. Haywood [143], F. He [60a], Y. He [164], M.P. Heath [50], V. Hedberg [97], S. Heer [24], A.L. Heggelund [133], C. Heidegger [52], K.K. Heidegger [52], W.D. Heidorn [79], J. Heilman [34], S. Heim [46], T. Heim [18], B. Heinemann [46,aj], J.J. Heinrich [131], L. Heinrich [36], J. Hejbal [140], L. Helary [46], A. Held [125], S. Hellesund [133], C.M. Helling [145], S. Hellman [45a,45b], C. Helsens [36], R.C.W. Henderson [90], Y. Heng [180], L. Henkelmann [32], A.M. Henriques Correia [36], H. Herde [26], Y. Hernández Jiménez [33e], H. Herr [100], M.G. Herrmann [114], T. Herrmann [48], G. Herten [52], R. Hertenberger [114], L. Hervas [36], T.C. Herwig [136], G.G. Hesketh [95], N.P. Hessey [167a], H. Hibi [83], S. Higashino [82], E. Higón-Rodriguez [173], K. Hildebrand [37], J.C. Hill [32], K.K. Hill [29], K.H. Hiller [46], S.J. Hillier [21], M. Hils [48], I. Hinchliffe [18], F. Hinterkeuser [24], M. Hirose [132], S. Hirose [168], D. Hirschbuehl [181], B. Hiti [92], O. Hladik [140], J. Hobbs [154], N. Hod [179], M.C. Hodgkinson [148], A. Hoecker [36], D. Hohn [52], D. Hohov [65], T. Holm [24], T.R. Holmes [37], M. Holzbock [115], L.B.A.H. Hommels [32], T.M. Hong [138], J.C. Honig [52], A. Hönle [115], B.H. Hooberman [172], W.H. Hopkins [6], Y. Horii [117], P. Horn [48], L.A. Horyn [37], S. Hou [157], A. Hoummada [35a], J. Howarth [57], J. Hoya [89], M. Hrabovsky [130], J. Hrdinka [77], J. Hrivnac [65], A. Hrynevich [109], T. Hryn'ova [5], P.J. Hsu [64], S.-C. Hsu [147], Q. Hu [29], S. Hu [60c], Y.F. Hu [15a,15d,an], D.P. Huang [95], X. Huang [15c], Y. Huang [60a], Y. Huang [15a], Z. Hubacek [141], F. Hubaut [102], M. Huebner [24], F. Huegging [24], T.B. Huffman [134], M. Huhtinen [36], R. Hulsken [58], R.F.H. Hunter [34], P. Huo [154], N. Huseynov [80,ac], J. Huston [107], J. Huth [59], R. Hyneman [152], S. Hyrych [28a], G. Iacobucci [54], G. Iakovidis [29], I. Ibragimov [150], L. Iconomidou-Fayard [65], P. Iengo [36], R. Ignazzi [40], O. Igonkina [120,y,*], R. Iguchi [162], T. Iizawa [54], Y. Ikegami [82], M. Ikeno [82], N. Ilic [119,166,ab], F. Iltzsche [48], H. Imam [35a], G. Introzzi [71a,71b], M. Iodice [75a], K. Iordanidou [167a], V. Ippolito [73a,73b], M.F. Isacson [171], M. Ishino [162], W. Islam [129], C. Issever [19,46], S. Istin [159], J.M. Iturbe Ponce [63a], R. Iuppa [76a,76b], A. Ivina [179], J.M. Izen [43], V. Izzo [70a], P. Jacka [140], P. Jackson [1], R.M. Jacobs [46], B.P. Jaeger [151], V. Jain [2], G. Jäkel [181], K.B. Jakobi [100], K. Jakobs [52], T. Jakoubek [179], J. Jamieson [57], K.W. Janas [84a], R. Jansky [54], M. Janus [53], P.A. Janus [84a], G. Jarlskog [97], A.E. Jaspan [91], N. Javadov [80,ac], T. Javůrek [36], M. Javurkova [103], F. Jeanneau [144], L. Jeanty [131], J. Jejelava [158a], P. Jenni [52,c], N. Jeong [46], S. Jézéquel [5], H. Ji [180], J. Jia [154], Z. Jia [15c], H. Jiang [79], Y. Jiang [60a], Z. Jiang [152], S. Jiggins [52], F.A. Jimenez Morales [38], J. Jimenez Pena [115], S. Jin [15c], A. Jinaru [27b], O. Jinnouchi [164], H. Jivan [33e],

JHEP09(2020)049

P. Johansson [148], K.A. Johns [7], C.A. Johnson [66], E. Jones [177], R.W.L. Jones [90], S.D. Jones [155], T.J. Jones [91], J. Jongmanns [61a], J. Jovicevic [36], X. Ju [18], J.J. Junggeburth [115], A. Juste Rozas [14,w], A. Kaczmarska [85], M. Kado [73a,73b], H. Kagan [127], M. Kagan [152], A. Kahn [39], C. Kahra [100], T. Kaji [178], E. Kajomovitz [159], C.W. Kalderon [29], A. Kaluza [100], A. Kamenshchikov [123], M. Kaneda [162], N.J. Kang [145], S. Kang [79], Y. Kano [117], J. Kanzaki [82], L.S. Kaplan [180], D. Kar [33e], K. Karava [134], M.J. Kareem [167b], I. Karkanias [161], S.N. Karpov [80], Z.M. Karpova [80], V. Kartvelishvili [90], A.N. Karyukhin [123], E. Kasimi [161], A. Kastanas [45a,45b], C. Kato [60d], J. Katzy [46], K. Kawade [149], K. Kawagoe [88], T. Kawaguchi [117], T. Kawamoto [144], G. Kawamura [53], E.F. Kay [175], S. Kazakos [14], V.F. Kazanin [122b,122a], J.M. Keaveney [33a], R. Keeler [175], J.S. Keller [34], E. Kellermann [97], D. Kelsey [155], J.J. Kempster [21], J. Kendrick [21], K.E. Kennedy [39], O. Kepka [140], S. Kersten [181], B.P. Kerševan [92], S. Ketabchi Haghighat [166], M. Khader [172], F. Khalil-Zada [13], M. Khandoga [144], A. Khanov [129], A.G. Kharlamov [122b,122a], T. Kharlamova [122b,122a], E.E. Khoda [174], A. Khodinov [165], T.J. Khoo [54], G. Khoriauli [176], E. Khramov [80], J. Khubua [158b], S. Kido [83], M. Kiehn [36], E. Kim [164], Y.K. Kim [37], N. Kimura [95], A. Kirchhoff [53], D. Kirchmeier [48], J. Kirk [143], A.E. Kiryunin [115], T. Kishimoto [162], D.P. Kisliuk [166], V. Kitali [46], C. Kitsaki [10], O. Kivernyk [24], T. Klapdor-Kleingrothaus [52], M. Klassen [61a], C. Klein [34], M.H. Klein [106], M. Klein [91], U. Klein [91], K. Kleinknecht [100], P. Klimek [121], A. Klimentov [29], T. Klingl [24], T. Klioutchnikova [36], F.F. Klitzner [114], P. Kluit [120], S. Kluth [115], E. Kneringer [77], E.B.F.G. Knoops [102], A. Knue [52], D. Kobayashi [88], M. Kobel [48], M. Kocian [152], T. Kodama [162], P. Kodys [142], D.M. Koeck [155], P.T. Koenig [24], T. Koffas [34], N.M. Köhler [36], M. Kolb [144], I. Koletsou [5], T. Komarek [130], T. Kondo [82], K. Köneke [52], A.X.Y. Kong [1], A.C. König [119], T. Kono [126], V. Konstantinides [95], N. Konstantinidis [95], B. Konya [97], R. Kopeliansky [66], S. Koperny [84a], K. Korcyl [85], K. Kordas [161], G. Koren [160], A. Korn [95], I. Korolkov [14], E.V. Korolkova [148], N. Korotkova [113], O. Kortner [115], S. Kortner [115], V.V. Kostyukhin [148,165], A. Kotsokechagia [65], A. Kotwal [49], A. Koulouris [10], A. Kourkoumeli-Charalampidi [71a,71b], C. Kourkoumelis [9], E. Kourlitis [6], V. Kouskoura [29], R. Kowalewski [175], W. Kozanecki [101], A.S. Kozhin [123], V.A. Kramarenko [113], G. Kramberger [92], D. Krasnopevtsev [60a], M.W. Krasny [135], A. Krasznahorkay [36], D. Krauss [115], J.A. Kremer [100], J. Kretzschmar [91], P. Krieger [166], F. Krieter [114], A. Krishnan [61b], M. Krivos [142], K. Krizka [18], K. Kroeninger [47], H. Kroha [115], J. Kroll [140], J. Kroll [136], K.S. Krowpman [107], U. Kruchonak [80], H. Krüger [24], N. Krumnack [79], M.C. Kruse [49], J.A. Krzysiak [85], A. Kubota [164], O. Kuchinskaia [165], S. Kuday [4b], J.T. Kuechler [46], S. Kuehn [36], T. Kuhl [46], V. Kukhtin [80], Y. Kulchitsky [108,ae], S. Kuleshov [146b], Y.P. Kulinich [172], M. Kuna [58], A. Kupco [140], T. Kupfer [47], O. Kuprash [52], H. Kurashige [83], L.L. Kurchaninov [167a], Y.A. Kurochkin [108], A. Kurova [112], M.G. Kurth [15a,15d], E.S. Kuwertz [36], M. Kuze [164], A.K. Kvam [147], J. Kvita [130], T. Kwan [104], F. La Ruffa [41b,41a], C. Lacasta [173], F. Lacava [73a,73b], D.P.J. Lack [101], H. Lacker [19], D. Lacour [135], E. Ladygin [80], R. Lafaye [5], B. Laforge [135], T. Lagouri [146c], S. Lai [53], I.K. Lakomiec [84a], J.E. Lambert [128], S. Lammers [66], W. Lampl [7], C. Lampoudis [161], E. Lançon [29], U. Landgraf [52], M.P.J. Landon [93], M.C. Lanfermann [54], V.S. Lang [52], J.C. Lange [53], R.J. Langenberg [103], A.J. Lankford [170], F. Lanni [29], K. Lantzsch [24], A. Lanza [71a], A. Lapertosa [55b,55a], J.F. Laporte [144], T. Lari [69a], F. Lasagni Manghi [23b,23a], M. Lassnig [36], V. Latonova [140], T.S. Lau [63a], A. Laudrain [100], A. Laurier [34], M. Lavorgna [70a,70b], S.D. Lawlor [94], M. Lazzaroni [69a,69b], B. Le [101], E. Le Guirriec [102], A. Lebedev [79], M. LeBlanc [7], T. LeCompte [6], F. Ledroit-Guillon [58], A.C.A. Lee [95], C.A. Lee [29], G.R. Lee [17], L. Lee [59], S.C. Lee [157], S. Lee [79], B. Lefebvre [167a], H.P. Lefebvre [94], M. Lefebvre [175], C. Leggett [18], K. Lehmann [151], N. Lehmann [20], G. Lehmann Miotto [36], W.A. Leight [46],

JHEP09(2020)049

A. Leisos [161,u], M.A.L. Leite [81d], C.E. Leitgeb [114], R. Leitner [142], D. Lellouch [179,*], K.J.C. Leney [42], T. Lenz [24], S. Leone [72a], C. Leonidopoulos [50], A. Leopold [135], C. Leroy [110], R. Les [107], C.G. Lester [32], M. Levchenko [137], J. Levêque [5], D. Levin [106], L.J. Levinson [179], D.J. Lewis [21], B. Li [15b], B. Li [106], C-Q. Li [60c,60d], F. Li [60c], H. Li [60a], H. Li [60b], J. Li [60c], K. Li [147], L. Li [60c], M. Li [15a,15d], Q. Li [15a,15d], Q.Y. Li [60a], S. Li [60d,60c], X. Li [46], Y. Li [46], Z. Li [60b], Z. Li [134], Z. Li [104], Z. Liang [15a], M. Liberatore [46], B. Liberti [74a], A. Liblong [166], K. Lie [63c], S. Lim [29], C.Y. Lin [32], K. Lin [107], R.A. Linck [66], R.E. Lindley [7], J.H. Lindon [21], A. Linss [46], A.L. Lionti [54], E. Lipeles [136], A. Lipniacka [17], T.M. Liss [172,ak], A. Lister [174], J.D. Little [8], B. Liu [79], B.L. Liu [151], H.B. Liu [29], J.B. Liu [60a], J.K.K. Liu [37], K. Liu [60d], M. Liu [60a], M.Y. Liu [60a], P. Liu [15a], X. Liu [60a], Y. Liu [46], Y. Liu [15a,15d], Y.L. Liu [106], Y.W. Liu [60a], M. Livan [71a,71b], A. Lleres [58], J. Llorente Merino [151], S.L. Lloyd [93], C.Y. Lo [63b], E.M. Lobodzinska [46], P. Loch [7], S. Loffredo [74a,74b], T. Lohse [19], K. Lohwasser [148], M. Lokajicek [140], J.D. Long [172], R.E. Long [90], I. Longarini [73a,73b], L. Longo [36], K.A. Looper [127], I. Lopez Paz [101], A. Lopez Solis [148], J. Lorenz [114], N. Lorenzo Martinez [5], A.M. Lory [114], P.J. Lösel [114], A. Lösle [52], X. Lou [45a,45b], X. Lou [15a], A. Lounis [65], J. Love [6], P.A. Love [90], J.J. Lozano Bahilo [173], M. Lu [60a], Y.J. Lu [64], H.J. Lubatti [147], C. Luci [73a,73b], F.L. Lucio Alves [15c], A. Lucotte [58], F. Luehring [66], I. Luise [135], L. Luminari [73a], B. Lund-Jensen [153], M.S. Lutz [160], D. Lynn [29], H. Lyons [91], R. Lysak [140], E. Lytken [97], F. Lyu [15a], V. Lyubushkin [80], T. Lyubushkina [80], H. Ma [29], L.L. Ma [60b], Y. Ma [95], D.M. Mac Donell [175], G. Maccarrone [51], A. Macchiolo [115], C.M. Macdonald [148], J.C. Macdonald [148], J. Machado Miguens [136], D. Madaffari [173], R. Madar [38], W.F. Mader [48], M. Madugoda Ralalage Don [129], N. Madysa [48], J. Maeda [83], T. Maeno [29], M. Maerker [48], V. Magerl [52], N. Magini [79], J. Magro [67a,67c,q], D.J. Mahon [39], C. Maidantchik [81b], T. Maier [114], A. Maio [139a,139b,139d], K. Maj [84a], O. Majersky [28a], S. Majewski [131], Y. Makida [82], N. Makovec [65], B. Malaescu [135], Pa. Malecki [85], V.P. Maleev [137], F. Malek [58], D. Malito [41b,41a], U. Mallik [78], D. Malon [6], C. Malone [32], S. Maltezos [10], S. Malyukov [80], J. Mamuzic [173], G. Mancini [70a,70b], I. Mandić [92], L. Manhaes de Andrade Filho [81a], I.M. Maniatis [161], J. Manjarres Ramos [48], K.H. Mankinen [97], A. Mann [114], A. Manousos [77], B. Mansoulie [144], I. Manthos [161], S. Manzoni [120], A. Marantis [161], G. Marceca [30], L. Marchese [134], G. Marchiori [135], M. Marcisovsky [140], L. Marcoccia [74a,74b], C. Marcon [97], M. Marjanovic [128], Z. Marshall [18], M.U.F. Martensson [171], S. Marti-Garcia [173], C.B. Martin [127], T.A. Martin [177], V.J. Martin [50], B. Martin dit Latour [17], L. Martinelli [75a,75b], M. Martinez [14,w], P. Martinez Agullo [173], V.I. Martinez Outschoorn [103], S. Martin-Haugh [143], V.S. Martoiu [27b], A.C. Martyniuk [95], A. Marzin [36], S.R. Maschek [115], L. Masetti [100], T. Mashimo [162], R. Mashinistov [111], J. Masik [101], A.L. Maslennikov [122b,122a], L. Massa [23b,23a], P. Massarotti [70a,70b], P. Mastrandrea [72a,72b], A. Mastroberardino [41b,41a], T. Masubuchi [162], D. Matakias [29], A. Matic [114], N. Matsuzawa [162], P. Mättig [24], J. Maurer [27b], B. Maček [92], D.A. Maximov [122b,122a], R. Mazini [157], I. Maznas [161], S.M. Mazza [145], J.P. Mc Gowan [104], S.P. Mc Kee [106], T.G. McCarthy [115], W.P. McCormack [18], E.F. McDonald [105], A.E. Mcdougall [120], J.A. Mcfayden [18], G. Mchedlidze [158b], M.A. McKay [42], K.D. McLean [175], S.J. McMahon [143], P.C. McNamara [105], C.J. McNicol [177], R.A. McPherson [175,ab], J.E. Mdhluli [33e], Z.A. Meadows [103], S. Meehan [36], T. Megy [38], S. Mehlhase [114], A. Mehta [91], B. Meirose [43], D. Melini [159], B.R. Mellado Garcia [33e], J.D. Mellenthin [53], M. Melo [28a], F. Meloni [46], A. Melzer [24], E.D. Mendes Gouveia [139a,139e], A.M. Mendes Jacques Da Costa [21], L. Meng [36], X.T. Meng [106], S. Menke [115], E. Meoni [41b,41a], S. Mergelmeyer [19], S.A.M. Merkt [138], C. Merlassino [134], P. Mermod [54], L. Merola [70a,70b], C. Meroni [69a], G. Merz [106], O. Meshkov [113,111], J.K.R. Meshreki [150], J. Metcalfe [6],

JHEP09(2020)049

A.S. Mete [6], C. Meyer [66], J-P. Meyer [144], M. Michetti [19], R.P. Middleton [143], L. Mijović [50], G. Mikenberg [179], M. Mikestikova [140], M. Mikuž [92], H. Mildner [148], A. Milic [166], C.D. Milke [42], D.W. Miller [37], A. Milov [179], D.A. Milstead [45a,45b], R.A. Mina [152], A.A. Minaenko [123], I.A. Minashvili [158b], A.I. Mincer [125], B. Mindur [84a], M. Mineev [80], Y. Minegishi [162], Y. Mino [86], L.M. Mir [14], M. Mironova [134], K.P. Mistry [136], T. Mitani [178], J. Mitrevski [114], V.A. Mitsou [173], M. Mittal [60c], O. Miu [166], A. Miucci [20], P.S. Miyagawa [93], A. Mizukami [82], J.U. Mjörnmark [97], T. Mkrtchyan [61a], M. Mlynarikova [142], T. Moa [45a,45b], S. Mobius [53], K. Mochizuki [110], P. Mogg [114], S. Mohapatra [39], R. Moles-Valls [24], K. Mönig [46], E. Monnier [102], A. Montalbano [151], J. Montejo Berlingen [36], M. Montella [95], F. Monticelli [89], S. Monzani [69a], N. Morange [65], A.L. Moreira De Carvalho [139a], D. Moreno [22a], M. Moreno Llácer [173], C. Moreno Martinez [14], P. Morettini [55b], M. Morgenstern [159], S. Morgenstern [48], D. Mori [151], M. Morii [59], M. Morinaga [178], V. Morisbak [133], A.K. Morley [36], G. Mornacchi [36], A.P. Morris [95], L. Morvaj [154], P. Moschovakos [36], B. Moser [120], M. Mosidze [158b], T. Moskalets [144], P. Moskvitina [119], J. Moss [31,m], E.J.W. Moyse [103], S. Muanza [102], J. Mueller [138], R.S.P. Mueller [114], D. Muenstermann [90], G.A. Mullier [97], D.P. Mungo [69a,69b], J.L. Munoz Martinez [14], F.J. Munoz Sanchez [101], P. Murin [28b], W.J. Murray [177,143], A. Murrone [69a,69b], J.M. Muse [128], M. Muškinja [18], C. Mwewa [33a], A.G. Myagkov [123,ag], A.A. Myers [138], G. Myers [66], J. Myers [131], M. Myska [141], B.P. Nachman [18], O. Nackenhorst [47], A.Nag Nag [48], K. Nagai [134], K. Nagano [82], Y. Nagasaka [62], J.L. Nagle [29], E. Nagy [102], A.M. Nairz [36], Y. Nakahama [117], K. Nakamura [82], T. Nakamura [162], H. Nanjo [132], F. Napolitano [61a], R.F. Naranjo Garcia [46], R. Narayan [42], I. Naryshkin [137], M. Naseri [34], T. Naumann [46], G. Navarro [22a], P.Y. Nechaeva [111], F. Nechansky [46], T.J. Neep [21], A. Negri [71a,71b], M. Negrini [23b], C. Nellist [119], C. Nelson [104], M.E. Nelson [45a,45b], S. Nemecek [140], M. Nessi [36,e], M.S. Neubauer [172], F. Neuhaus [100], M. Neumann [181], R. Newhouse [174], P.R. Newman [21], C.W. Ng [138], Y.S. Ng [19], Y.W.Y. Ng [170], B. Ngair [35e], H.D.N. Nguyen [102], T. Nguyen Manh [110], E. Nibigira [38], R.B. Nickerson [134], R. Nicolaidou [144], D.S. Nielsen [40], J. Nielsen [145], M. Niemeyer [53], N. Nikiforou [11], V. Nikolaenko [123,ag], I. Nikolic-Audit [135], K. Nikolopoulos [21], P. Nilsson [29], H.R. Nindhito [54], A. Nisati [73a], N. Nishu [60c], R. Nisius [115], I. Nitsche [47], T. Nitta [178], T. Nobe [162], D.L. Noel [32], Y. Noguchi [86], I. Nomidis [135], M.A. Nomura [29], M. Nordberg [36], J. Novak [92], T. Novak [92], O. Novgorodova [48], R. Novotny [141], L. Nozka [130], K. Ntekas [170], E. Nurse [95], F.G. Oakham [34,al], H. Oberlack [115], J. Ocariz [135], A. Ochi [83], I. Ochoa [39], J.P. Ochoa-Ricoux [146a], K. O'Connor [26], S. Oda [88], S. Odaka [82], S. Oerdek [53], A. Ogrodnik [84a], A. Oh [101], C.C. Ohm [153], H. Oide [164], M.L. Ojeda [166], H. Okawa [168], Y. Okazaki [86], M.W. O'Keefe [91], Y. Okumura [162], A. Olariu [27b], L.F. Oleiro Seabra [139a], S.A. Olivares Pino [146a], D. Oliveira Damazio [29], J.L. Oliver [1], M.J.R. Olsson [170], A. Olszewski [85], J. Olszowska [85], Ö.O. Öncel [24], D.C. O'Neil [151], A.P. O'neill [134], A. Onofre [139a,139e], P.U.E. Onyisi [11], H. Oppen [133], R.G. Oreamuno Madriz [121], M.J. Oreglia [37], G.E. Orellana [89], D. Orestano [75a,75b], N. Orlando [14], R.S. Orr [166], V. O'Shea [57], R. Ospanov [60a], G. Otero y Garzon [30], H. Otono [88], P.S. Ott [61a], G.J. Ottino [18], M. Ouchrif [35d], J. Ouellette [29], F. Ould-Saada [133], A. Ouraou [144], Q. Ouyang [15a], M. Owen [57], R.E. Owen [143], V.E. Ozcan [12c], N. Ozturk [8], J. Pacalt [130], H.A. Pacey [32], K. Pachal [49], A. Pacheco Pages [14], C. Padilla Aranda [14], S. Pagan Griso [18], G. Palacino [66], S. Palazzo [50], S. Palestini [36], M. Palka [84b], P. Palni [84a], C.E. Pandini [54], J.G. Panduro Vazquez [94], P. Pani [46], G. Panizzo [67a,67c], L. Paolozzi [54], C. Papadatos [110], K. Papageorgiou [9,g], S. Parajuli [42], A. Paramonov [6], C. Paraskevopoulos [10], D. Paredes Hernandez [63b], S.R. Paredes Saenz [134], B. Parida [179], T.H. Park [166], A.J. Parker [31], M.A. Parker [32], F. Parodi [55b,55a], E.W. Parrish [121], J.A. Parsons [39], U. Parzefall [52], L. Pascual Dominguez

JHEP09(2020)049

[135], V.R. Pascuzzi [18], J.M.P. Pasner [145], F. Pasquali [120], E. Pasqualucci [73a], S. Passaggio [55b], F. Pastore [94], P. Pasuwan [45a,45b], S. Pataraia [100], J.R. Pater [101], A. Pathak [180,i], J. Patton [91], T. Pauly [36], J. Pearkes [152], B. Pearson [115], M. Pedersen [133], L. Pedraza Diaz [119], R. Pedro [139a], T. Peiffer [53], S.V. Peleganchuk [122b,122a], O. Penc [140], H. Peng [60a], B.S. Peralva [81a], M.M. Perego [65], A.P. Pereira Peixoto [139a], L. Pereira Sanchez [45a,45b], D.V. Perepelitsa [29], E. Perez Codina [167a], F. Peri [19], L. Perini [69a,69b], H. Pernegger [36], S. Perrella [36], A. Perrevoort [120], K. Peters [46], R.F.Y. Peters [101], B.A. Petersen [36], T.C. Petersen [40], E. Petit [102], V. Petousis [141], A. Petridis [1], C. Petridou [161], P. Petroff [65], F. Petrucci [75a,75b], M. Pettee [182], N.E. Pettersson [103], K. Petukhova [142], A. Peyaud [144], R. Pezoa [146d], L. Pezzotti [71a,71b], T. Pham [105], P.W. Phillips [143], M.W. Phipps [172], G. Piacquadio [154], E. Pianori [18], A. Picazio [103], R.H. Pickles [101], R. Piegaia [30], D. Pietreanu [27b], J.E. Pilcher [37], A.D. Pilkington [101], M. Pinamonti [67a,67c], J.L. Pinfold [3], C. Pitman Donaldson [95], M. Pitt [160], L. Pizzimento [74a,74b], A. Pizzini [120], M.-A. Pleier [29], V. Plesanovs [52], V. Pleskot [142], E. Plotnikova [80], P. Podberezko [122b,122a], R. Poettgen [97], R. Poggi [54], L. Poggioli [135], I. Pogrebnyak [107], D. Pohl [24], I. Pokharel [53], G. Polesello [71a], A. Poley [151,167a], A. Policicchio [73a,73b], R. Polifka [142], A. Polini [23b], C.S. Pollard [46], V. Polychronakos [29], D. Ponomarenko [112], L. Pontecorvo [36], S. Popa [27a], G.A. Popeneciu [27d], L. Portales [5], D.M. Portillo Quintero [58], S. Pospisil [141], K. Potamianos [46], I.N. Potrap [80], C.J. Potter [32], H. Potti [11], T. Poulsen [97], J. Poveda [173], T.D. Powell [148], G. Pownall [46], M.E. Pozo Astigarraga [36], A. Prades Ibanez [173], P. Pralavorio [102], M.M. Prapa [44], S. Prell [79], D. Price [101], M. Primavera [68a], M.L. Proffitt [147], N. Proklova [112], K. Prokofiev [63c], F. Prokoshin [80], S. Protopopescu [29], J. Proudfoot [6], M. Przybycien [84a], D. Pudzha [137], A. Puri [172], P. Puzo [65], D. Pyatiizbyantseva [112], J. Qian [106], Y. Qin [101], A. Quadt [53], M. Queitsch-Maitland [36], M. Racko [28a], F. Ragusa [69a,69b], G. Rahal [98], J.A. Raine [54], S. Rajagopalan [29], A. Ramirez Morales [93], K. Ran [15a,15d], D.M. Rauch [46], F. Rauscher [114], S. Rave [100], B. Ravina [57], I. Ravinovich [179], J.H. Rawling [101], M. Raymond [36], A.L. Read [133], N.P. Readioff [148], M. Reale [68a,68b], D.M. Rebuzzi [71a,71b], G. Redlinger [29], K. Reeves [43], D. Reikher [160], A. Reiss [100], A. Rej [150], C. Rembser [36], A. Renardi [46], M. Renda [27b], M.B. Rendel [115], A.G. Rennie [57], S. Resconi [69a], E.D. Resseguie [18], S. Rettie [95], B. Reynolds [127], E. Reynolds [21], O.L. Rezanova [122b,122a], P. Reznicek [142], E. Ricci [76a,76b], R. Richter [115], S. Richter [46], E. Richter-Was [84b], M. Ridel [135], P. Rieck [115], O. Rifki [46], M. Rijssenbeek [154], A. Rimoldi [71a,71b], M. Rimoldi [46], L. Rinaldi [23b], T.T. Rinn [172], G. Ripellino [153], I. Riu [14], P. Rivadeneira [46], J.C. Rivera Vergara [175], F. Rizatdinova [129], E. Rizvi [93], C. Rizzi [36], S.H. Robertson [104,ab], M. Robin [46], D. Robinson [32], C.M. Robles Gajardo [146d], M. Robles Manzano [100], A. Robson [57], A. Rocchi [74a,74b], E. Rocco [100], C. Roda [72a,72b], S. Rodriguez Bosca [173], A. Rodriguez Rodriguez [52], A.M. Rodríguez Vera [167b], S. Roe [36], J. Roggel [181], O. Røhne [133], R. Röhrig [115], R.A. Rojas [146d], B. Roland [52], C.P.A. Roland [66], J. Roloff [29], A. Romaniouk [112], M. Romano [23b,23a], N. Rompotis [91], M. Ronzani [125], L. Roos [135], S. Rosati [73a], G. Rosin [103], B.J. Rosser [136], E. Rossi [46], E. Rossi [75a,75b], E. Rossi [70a,70b], L.P. Rossi [55b], L. Rossini [46], R. Rosten [14], M. Rotaru [27b], B. Rottler [52], D. Rousseau [65], G. Rovelli [71a,71b], A. Roy [11], D. Roy [33e], A. Rozanov [102], Y. Rozen [159], X. Ruan [33e], T.A. Ruggeri [1], F. Rühr [52], A. Ruiz-Martinez [173], A. Rummler [36], Z. Rurikova [52], N.A. Rusakovich [80], H.L. Russell [104], L. Rustige [38,47], J.P. Rutherfoord [7], E.M. Rüttinger [148], M. Rybar [39], G. Rybkin [65], E.B. Rye [133], A. Ryzhov [123], J.A. Sabater Iglesias [46], P. Sabatini [53], L. Sabetta [73a,73b], S. Sacerdoti [65], H.F-W. Sadrozinski [145], R. Sadykov [80], F. Safai Tehrani [73a], B. Safarzadeh Samani [155], M. Safdari [152], P. Saha [121], S. Saha [104], M. Sahinsoy [115], A. Sahu [181], M. Saimpert [36], M. Saito [162], T. Saito [162], H. Sakamoto [162], D. Salamani [54],

JHEP09(2020)049

G. Salamanna [75a,75b], A. Salnikov [152], J. Salt [173], A. Salvador Salas [14], D. Salvatore [41b,41a], F. Salvatore [155], A. Salvucci [63a,63b,63c], A. Salzburger [36], J. Samarati [36], D. Sammel [52], D. Sampsonidis [161], D. Sampsonidou [161], J. Sánchez [173], A. Sanchez Pineda [67a,36,67c], H. Sandaker [133], C.O. Sander [46], I.G. Sanderswood [90], M. Sandhoff [181], C. Sandoval [22b], D.P.C. Sankey [143], M. Sannino [55b,55a], Y. Sano [117], A. Sansoni [51], C. Santoni [38], H. Santos [139a,139b], S.N. Santpur [18], A. Santra [173], K.A. Saoucha [148], A. Sapronov [80], J.G. Saraiva [139a,139d], O. Sasaki [82], K. Sato [168], F. Sauerburger [52], E. Sauvan [5], P. Savard [166,al], R. Sawada [162], C. Sawyer [143], L. Sawyer [96,af], I. Sayago Galvan [173], C. Sbarra [23b], A. Sbrizzi [67a,67c], T. Scanlon [95], J. Schaarschmidt [147], P. Schacht [115], D. Schaefer [37], L. Schaefer [136], S. Schaepe [36], U. Schäfer [100], A.C. Schaffer [65], D. Schaile [114], R.D. Schamberger [154], E. Schanet [114], C. Scharf [19], N. Scharmberg [101], V.A. Schegelsky [137], D. Scheirich [142], F. Schenck [19], M. Schernau [170], C. Schiavi [55b,55a], L.K. Schildgen [24], Z.M. Schillaci [26], E.J. Schioppa [68a,68b], M. Schioppa [41b,41a], K.E. Schleicher [52], S. Schlenker [36], K.R. Schmidt-Sommerfeld [115], K. Schmieden [36], C. Schmitt [100], S. Schmitt [46], L. Schoeffel [144], A. Schoening [61b], P.G. Scholer [52], E. Schopf [134], M. Schott [100], J.F.P. Schouwenberg [119], J. Schovancova [36], S. Schramm [54], F. Schroeder [181], A. Schulte [100], H-C. Schultz-Coulon [61a], M. Schumacher [52], B.A. Schumm [145], Ph. Schune [144], A. Schwartzman [152], T.A. Schwarz [106], Ph. Schwemling [144], R. Schwienhorst [107], A. Sciandra [145], G. Sciolla [26], M. Scornajenghi [41b,41a], F. Scuri [72a], F. Scutti [105], L.M. Scyboz [115], C.D. Sebastiani [91], P. Seema [19], S.C. Seidel [118], A. Seiden [145], B.D. Seidlitz [29], T. Seiss [37], C. Seitz [46], J.M. Seixas [81b], G. Sekhniaidze [70a], S.J. Sekula [42], N. Semprini-Cesari [23b,23a], S. Sen [49], C. Serfon [29], L. Serin [65], L. Serkin [67a,67b], M. Sessa [60a], H. Severini [128], S. Sevova [152], F. Sforza [55b,55a], A. Sfyrla [54], E. Shabalina [53], J.D. Shahinian [145], N.W. Shaikh [45a,45b], D. Shaked Renous [179], L.Y. Shan [15a], M. Shapiro [18], A. Sharma [134], A.S. Sharma [1], P.B. Shatalov [124], K. Shaw [155], S.M. Shaw [101], M. Shehade [179], Y. Shen [128], A.D. Sherman [25], P. Sherwood [95], L. Shi [95], C.O. Shimmin [182], Y. Shimogama [178], M. Shimojima [116], J.D. Shinner [94], I.P.J. Shipsey [134], S. Shirabe [164], M. Shiyakova [80,z], J. Shlomi [179], A. Shmeleva [111], M.J. Shochet [37], J. Shojaii [105], D.R. Shope [153], S. Shrestha [127], E.M. Shrif [33e], M.J. Shroff [175], E. Shulga [179], P. Sicho [140], A.M. Sickles [172], E. Sideras Haddad [33e], O. Sidiropoulou [36], A. Sidoti [23b,23a], F. Siegert [48], Dj. Sijacki [16], M.Jr. Silva [180], M.V. Silva Oliveira [36], S.B. Silverstein [45a], S. Simion [65], R. Simoniello [100], C.J. Simpson-allsop [21], S. Simsek [12b], P. Sinervo [166], V. Sinetckii [113], S. Singh [151], M. Sioli [23b,23a], I. Siral [131], S.Yu. Sivoklokov [113], J. Sjölin [45a,45b], A. Skaf [53], E. Skorda [97], P. Skubic [128], M. Slawinska [85], K. Sliwa [169], R. Slovak [142], V. Smakhtin [179], B.H. Smart [143], J. Smiesko [28b], N. Smirnov [112], S.Yu. Smirnov [112], Y. Smirnov [112], L.N. Smirnova [113,r], O. Smirnova [97], E.A. Smith [37], H.A. Smith [134], M. Smizanska [90], K. Smolek [141], A. Smykiewicz [85], A.A. Snesarev [111], H.L. Snoek [120], I.M. Snyder [131], S. Snyder [29], R. Sobie [175,ab], A. Soffer [160], A. Søgaard [50], F. Sohns [53], C.A. Solans Sanchez [36], E.Yu. Soldatov [112], U. Soldevila [173], A.A. Solodkov [123], A. Soloshenko [80], O.V. Solovyanov [123], V. Solovyev [137], P. Sommer [148], H. Son [169], A. Sonay [14], W. Song [143], W.Y. Song [167b], A. Sopczak [141], A.L. Sopio [95], F. Sopkova [28b], S. Sottocornola [71a,71b], R. Soualah [67a,67c], A.M. Soukharev [122b,122a], D. South [46], S. Spagnolo [68a,68b], M. Spalla [115], M. Spangenberg [177], F. Spanò [94], D. Sperlich [52], T.M. Spieker [61a], G. Spigo [36], M. Spina [155], D.P. Spiteri [57], M. Spousta [142], A. Stabile [69a,69b], B.L. Stamas [121], R. Stamen [61a], M. Stamenkovic [120], A. Stampekis [21], E. Stanecka [85], B. Stanislaus [134], M.M. Stanitzki [46], M. Stankaityte [134], B. Stapf [120], E.A. Starchenko [123], G.H. Stark [145], J. Stark [58], P. Staroba [140], P. Starovoitov [61a], S. Stärz [104], R. Staszewski [85], G. Stavropoulos [44], M. Stegler [46], P. Steinberg [29], A.L. Steinhebel [131], B. Stelzer [151,167a], H.J. Stelzer [138],

JHEP09(2020)049

O. Stelzer-Chilton [167a], H. Stenzel [56], T.J. Stevenson [155], G.A. Stewart [36], M.C. Stockton [36], G. Stoicea [27b], M. Stolarski [139a], S. Stonjek [115], A. Straessner [48], J. Strandberg [153], S. Strandberg [45a,45b], M. Strauss [128], T. Strebler [102], P. Strizenec [28b], R. Ströhmer [176], D.M. Strom [131], R. Stroynowski [42], A. Strubig [50], S.A. Stucci [29], B. Stugu [17], J. Stupak [128], N.A. Styles [46], D. Su [152], W. Su [60c,147], X. Su [60a], V.V. Sulin [111], M.J. Sullivan [91], D.M.S. Sultan [54], S. Sultansoy [4c], T. Sumida [86], S. Sun [106], X. Sun [101], C.J.E. Suster [156], M.R. Sutton [155], S. Suzuki [82], M. Svatos [140], M. Swiatlowski [167a], S.P. Swift [2], T. Swirski [176], A. Sydorenko [100], I. Sykora [28a], M. Sykora [142], T. Sykora [142], D. Ta [100], K. Tackmann [46,x], J. Taenzer [160], A. Taffard [170], R. Tafirout [167a], E. Tagiev [123], R. Takashima [87], K. Takeda [83], T. Takeshita [149], E.P. Takeva [50], Y. Takubo [82], M. Talby [102], A.A. Talyshev [122b,122a], K.C. Tam [63b], N.M. Tamir [160], J. Tanaka [162], R. Tanaka [65], S. Tapia Araya [172], S. Tapprogge [100], A. Tarek Abouelfadl Mohamed [107], S. Tarem [159], K. Tariq [60b], G. Tarna [27b,d], G.F. Tartarelli [69a], P. Tas [142], M. Tasevsky [140], E. Tassi [41b,41a], A. Tavares Delgado [139a], Y. Tayalati [35e], A.J. Taylor [50], G.N. Taylor [105], W. Taylor [167b], H. Teagle [91], A.S. Tee [90], R. Teixeira De Lima [152], P. Teixeira-Dias [94], H. Ten Kate [36], J.J. Teoh [120], K. Terashi [162], J. Terron [99], S. Terzo [14], M. Testa [51], R.J. Teuscher [166,ab], S.J. Thais [182], N. Themistokleous [50], T. Theveneaux-Pelzer [46], F. Thiele [40], D.W. Thomas [94], J.O. Thomas [42], J.P. Thomas [21], E.A. Thompson [46], P.D. Thompson [21], E. Thomson [136], E.J. Thorpe [93], R.E. Ticse Torres [53], V.O. Tikhomirov [111,ah], Yu.A. Tikhonov [122b,122a], S. Timoshenko [112], P. Tipton [182], S. Tisserant [102], K. Todome [23b,23a], S. Todorova-Nova [142], S. Todt [48], J. Tojo [88], S. Tokár [28a], K. Tokushuku [82], E. Tolley [127], R. Tombs [32], K.G. Tomiwa [33e], M. Tomoto [82,117], L. Tompkins [152], P. Tornambe [103], E. Torrence [131], H. Torres [48], E. Torró Pastor [173], M. Toscani [30], C. Tosciri [134], J. Toth [102,aa], D.R. Tovey [148], A. Traeet [17], C.J. Treado [125], T. Trefzger [176], F. Tresoldi [155], A. Tricoli [29], I.M. Trigger [167a], S. Trincaz-Duvoid [135], D.A. Trischuk [174], W. Trischuk [166], B. Trocmé [58], A. Trofymov [65], C. Troncon [69a], F. Trovato [155], L. Truong [33c], M. Trzebinski [85], A. Trzupek [85], F. Tsai [46], J.C-L. Tseng [134], P.V. Tsiareshka [108,ae], A. Tsirigotis [161,u], V. Tsiskaridze [154], E.G. Tskhadadze [158a], M. Tsopoulou [161], I.I. Tsukerman [124], V. Tsulaia [18], S. Tsuno [82], D. Tsybychev [154], Y. Tu [63b], A. Tudorache [27b], V. Tudorache [27b], T.T. Tulbure [27a], A.N. Tuna [59], S. Turchikhin [80], D. Turgeman [179], I. Turk Cakir [4b,s], R.J. Turner [21], R. Turra [69a], P.M. Tuts [39], S. Tzamarias [161], E. Tzovara [100], K. Uchida [162], F. Ukegawa [168], G. Unal [36], M. Unal [11], A. Undrus [29], G. Unel [170], F.C. Ungaro [105], Y. Unno [82], K. Uno [162], J. Urban [28b], P. Urquijo [105], G. Usai [8], Z. Uysal [12d], V. Vacek [141], B. Vachon [104], K.O.H. Vadla [133], T. Vafeiadis [36], A. Vaidya [95], C. Valderanis [114], E. Valdes Santurio [45a,45b], M. Valente [54], S. Valentinetti [23b,23a], A. Valero [173], L. Valéry [46], R.A. Vallance [21], A. Vallier [36], J.A. Valls Ferrer [173], T.R. Van Daalen [14], P. Van Gemmeren [6], S. Van Stroud [95], I. Van Vulpen [120], M. Vanadia [74a,74b], W. Vandelli [36], M. Vandenbroucke [144], E.R. Vandewall [129], A. Vaniachine [165], D. Vannicola [73a,73b], R. Vari [73a], E.W. Varnes [7], C. Varni [55b,55a], T. Varol [157], D. Varouchas [65], K.E. Varvell [156], M.E. Vasile [27b], G.A. Vasquez [175], F. Vazeille [38], D. Vazquez Furelos [14], T. Vazquez Schroeder [36], J. Veatch [53], V. Vecchio [101], M.J. Veen [120], L.M. Veloce [166], F. Veloso [139a,139c], S. Veneziano [73a], A. Ventura [68a,68b], A. Verbytskyi [115], V. Vercesi [71a], M. Verducci [72a,72b], C.M. Vergel Infante [79], C. Vergis [24], W. Verkerke [120], A.T. Vermeulen [120], J.C. Vermeulen [120], C. Vernieri [152], P.J. Verschuuren [94], M.C. Vetterli [151,al], N. Viaux Maira [146d], T. Vickey [148], O.E. Vickey Boeriu [148], G.H.A. Viehhauser [134], L. Vigani [61b], M. Villa [23b,23a], M. Villaplana Perez [3], E.M. Villhauer [50], E. Vilucchi [51], M.G. Vincter [34], G.S. Virdee [21], A. Vishwakarma [50], C. Vittori [23b,23a], I. Vivarelli [155], M. Vogel [181], P. Vokac [141], S.E. von Buddenbrock [33e], E. Von Toerne [24], V. Vorobel [142],

JHEP09(2020)049

K. Vorobev [112], M. Vos [173], J.H. Vossebeld [91], M. Vozak [101], N. Vranjes [16], M. Vranjes Milosavljevic [16], V. Vrba [141], M. Vreeswijk [120], N.K. Vu [102], R. Vuillermet [36], I. Vukotic [37], S. Wada [168], P. Wagner [24], W. Wagner [181], J. Wagner-Kuhr [114], S. Wahdan [181], H. Wahlberg [89], R. Wakasa [168], V.M. Walbrecht [115], J. Walder [143], R. Walker [114], S.D. Walker [94], W. Walkowiak [150], V. Wallangen [45a,45b], A.M. Wang [59], A.Z. Wang [180], C. Wang [60a], C. Wang [60c], F. Wang [180], H. Wang [18], H. Wang [3], J. Wang [63a], P. Wang [42], Q. Wang [128], R.-J. Wang [100], R. Wang [60a], R. Wang [6], S.M. Wang [157], W.T. Wang [60a], W. Wang [15c], W.X. Wang [60a], Y. Wang [60a], Z. Wang [106], C. Wanotayaroj [46], A. Warburton [104], C.P. Ward [32], R.J. Ward [21], N. Warrack [57], A.T. Watson [21], M.F. Watson [21], G. Watts [147], B.M. Waugh [95], A.F. Webb [11], C. Weber [29], M.S. Weber [20], S.A. Weber [34], S.M. Weber [61a], A.R. Weidberg [134], J. Weingarten [47], M. Weirich [100], C. Weiser [52], P.S. Wells [36], T. Wenaus [29], B. Wendland [47], T. Wengler [36], S. Wenig [36], N. Wermes [24], M. Wessels [61a], T.D. Weston [20], K. Whalen [131], A.M. Wharton [90], A.S. White [106], A. White [8], M.J. White [1], D. Whiteson [170], B.W. Whitmore [90], W. Wiedenmann [180], C. Wiel [48], M. Wielers [143], N. Wieseotte [100], C. Wiglesworth [40], L.A.M. Wiik-Fuchs [52], H.G. Wilkens [36], L.J. Wilkins [94], H.H. Williams [136], S. Williams [32], S. Willocq [103], P.J. Windischhofer [134], I. Wingerter-Seez [5], E. Winkels [155], F. Winklmeier [131], B.T. Winter [52], M. Wittgen [152], M. Wobisch [96], A. Wolf [100], R. Wölker [134], J. Wollrath [52], M.W. Wolter [85], H. Wolters [139a,139c], V.W.S. Wong [174], N.L. Woods [145], S.D. Worm [46], B.K. Wosiek [85], K.W. Woźniak [85], K. Wraight [57], S.L. Wu [180], X. Wu [54], Y. Wu [60a], J. Wuerzinger [134], T.R. Wyatt [101], B.M. Wynne [50], S. Xella [40], L. Xia [177], J. Xiang [63c], X. Xiao [106], X. Xie [60a], I. Xiotidis [155], D. Xu [15a], H. Xu [60a], H. Xu [60a], L. Xu [29], T. Xu [144], W. Xu [106], Y. Xu [15b], Z. Xu [60b], Z. Xu [152], B. Yabsley [156], S. Yacoob [33a], D.P. Yallup [95], N. Yamaguchi [88], Y. Yamaguchi [164], A. Yamamoto [82], M. Yamatani [162], T. Yamazaki [162], Y. Yamazaki [83], J. Yan [60c], Z. Yan [25], H.J. Yang [60c,60d], H.T. Yang [18], S. Yang [60a], T. Yang [63c], X. Yang [60b,58], Y. Yang [162], Z. Yang [60a], W-M. Yao [18], Y.C. Yap [46], E. Yatsenko [60c], H. Ye [15c], J. Ye [42], S. Ye [29], I. Yeletskikh [80], M.R. Yexley [90], E. Yigitbasi [25], P. Yin [39], K. Yorita [178], K. Yoshihara [79], C.J.S. Young [36], C. Young [152], J. Yu [79], R. Yuan [60b,h], X. Yue [61a], M. Zaazoua [35e], B. Zabinski [85], G. Zacharis [10], E. Zaffaroni [54], J. Zahreddine [135], A.M. Zaitsev [123,ag], T. Zakareishvili [158b], N. Zakharchuk [34], S. Zambito [36], D. Zanzi [36], S.V. Zeißner [47], C. Zeitnitz [181], G. Zemaityte [134], J.C. Zeng [172], O. Zenin [123], T. Ženiš [28a], D. Zerwas [65], M. Zgubič [134], B. Zhang [15c], D.F. Zhang [15b], G. Zhang [15b], J. Zhang [6], Kaili. Zhang [15a], L. Zhang [15c], L. Zhang [60a], M. Zhang [172], R. Zhang [180], S. Zhang [106], X. Zhang [60c], X. Zhang [60b], Y. Zhang [15a,15d], Z. Zhang [63a], Z. Zhang [65], P. Zhao [49], Z. Zhao [60a], A. Zhemchugov [80], Z. Zheng [106], D. Zhong [172], B. Zhou [106], C. Zhou [180], H. Zhou [7], M.S. Zhou [15a,15d], M. Zhou [154], N. Zhou [60c], Y. Zhou [7], C.G. Zhu [60b], C. Zhu [15a,15d], H.L. Zhu [60a], H. Zhu [15a], J. Zhu [106], Y. Zhu [60a], X. Zhuang [15a], K. Zhukov [111], V. Zhulanov [122b,122a], D. Zieminska [66], N.I. Zimine [80], S. Zimmermann [52], Z. Zinonos [115], M. Ziolkowski [150], L. Živković [16], G. Zobernig [180], A. Zoccoli [23b,23a], K. Zoch [53], T.G. Zorbas [148], R. Zou [37] and L. Zwalinski [36]

[1] *Department of Physics, University of Adelaide, Adelaide; Australia*

[2] *Physics Department, SUNY Albany, Albany NY; United States of America*

[3] *Department of Physics, University of Alberta, Edmonton AB; Canada*

[4] [(a)] *Department of Physics, Ankara University, Ankara;* [(b)] *Istanbul Aydin University, Application and Research Center for Advanced Studies, Istanbul;* [(c)] *Division of Physics, TOBB University of Economics and Technology, Ankara; Turkey*

[5] *LAPP, Université Grenoble Alpes, Université Savoie Mont Blanc, CNRS/IN2P3, Annecy; France*

JHEP09(2020)049

[6] High Energy Physics Division, Argonne National Laboratory, Argonne IL; United States of America
[7] Department of Physics, University of Arizona, Tucson AZ; United States of America
[8] Department of Physics, University of Texas at Arlington, Arlington TX; United States of America
[9] Physics Department, National and Kapodistrian University of Athens, Athens; Greece
[10] Physics Department, National Technical University of Athens, Zografou; Greece
[11] Department of Physics, University of Texas at Austin, Austin TX; United States of America
[12] [(a)] Bahcesehir University, Faculty of Engineering and Natural Sciences, Istanbul; [(b)] Istanbul Bilgi University, Faculty of Engineering and Natural Sciences, Istanbul; [(c)] Department of Physics, Bogazici University, Istanbul; [(d)] Department of Physics Engineering, Gaziantep University, Gaziantep; Turkey
[13] Institute of Physics, Azerbaijan Academy of Sciences, Baku; Azerbaijan
[14] Institut de Física d'Altes Energies (IFAE), Barcelona Institute of Science and Technology, Barcelona; Spain
[15] [(a)] Institute of High Energy Physics, Chinese Academy of Sciences, Beijing; [(b)] Physics Department, Tsinghua University, Beijing; [(c)] Department of Physics, Nanjing University, Nanjing; [(d)] University of Chinese Academy of Science (UCAS), Beijing; China
[16] Institute of Physics, University of Belgrade, Belgrade; Serbia
[17] Department for Physics and Technology, University of Bergen, Bergen; Norway
[18] Physics Division, Lawrence Berkeley National Laboratory and University of California, Berkeley CA; United States of America
[19] Institut für Physik, Humboldt Universität zu Berlin, Berlin; Germany
[20] Albert Einstein Center for Fundamental Physics and Laboratory for High Energy Physics, University of Bern, Bern; Switzerland
[21] School of Physics and Astronomy, University of Birmingham, Birmingham; United Kingdom
[22] [(a)] Facultad de Ciencias y Centro de Investigaciónes, Universidad Antonio Nariño, Bogotá; [(b)] Departamento de Física, Universidad Nacional de Colombia, Bogotá, Colombia; Colombia
[23] [(a)] INFN Bologna and Universita' di Bologna, Dipartimento di Fisica; [(b)] INFN Sezione di Bologna; Italy
[24] Physikalisches Institut, Universität Bonn, Bonn; Germany
[25] Department of Physics, Boston University, Boston MA; United States of America
[26] Department of Physics, Brandeis University, Waltham MA; United States of America
[27] [(a)] Transilvania University of Brasov, Brasov; [(b)] Horia Hulubei National Institute of Physics and Nuclear Engineering, Bucharest; [(c)] Department of Physics, Alexandru Ioan Cuza University of Iasi, Iasi; [(d)] National Institute for Research and Development of Isotopic and Molecular Technologies, Physics Department, Cluj-Napoca; [(e)] University Politehnica Bucharest, Bucharest; [(f)] West University in Timisoara, Timisoara; Romania
[28] [(a)] Faculty of Mathematics, Physics and Informatics, Comenius University, Bratislava; [(b)] Department of Subnuclear Physics, Institute of Experimental Physics of the Slovak Academy of Sciences, Kosice; Slovak Republic
[29] Physics Department, Brookhaven National Laboratory, Upton NY; United States of America
[30] Departamento de Física, Universidad de Buenos Aires, Buenos Aires; Argentina
[31] California State University, CA; United States of America
[32] Cavendish Laboratory, University of Cambridge, Cambridge; United Kingdom
[33] [(a)] Department of Physics, University of Cape Town, Cape Town; [(b)] iThemba Labs, Western Cape; [(c)] Department of Mechanical Engineering Science, University of Johannesburg, Johannesburg; [(d)] University of South Africa, Department of Physics, Pretoria; [(e)] School of Physics, University of the Witwatersrand, Johannesburg; South Africa
[34] Department of Physics, Carleton University, Ottawa ON; Canada
[35] [(a)] Faculté des Sciences Ain Chock, Réseau Universitaire de Physique des Hautes Energies — Université Hassan II, Casablanca; [(b)] Faculté des Sciences, Université Ibn-Tofail, Kénitra; [(c)] Faculté des Sciences Semlalia, Université Cadi Ayyad, LPHEA-Marrakech; [(d)] Faculté des Sciences, Université Mohamed Premier and LPTPM, Oujda; [(e)] Faculté des sciences, Université Mohammed V, Rabat; Morocco

JHEP09(2020)049

[36] CERN, Geneva; Switzerland
[37] Enrico Fermi Institute, University of Chicago, Chicago IL; United States of America
[38] LPC, Université Clermont Auvergne, CNRS/IN2P3, Clermont-Ferrand; France
[39] Nevis Laboratory, Columbia University, Irvington NY; United States of America
[40] Niels Bohr Institute, University of Copenhagen, Copenhagen; Denmark
[41] [(a)] Dipartimento di Fisica, Università della Calabria, Rende;[(b)] INFN Gruppo Collegato di Cosenza, Laboratori Nazionali di Frascati; Italy
[42] Physics Department, Southern Methodist University, Dallas TX; United States of America
[43] Physics Department, University of Texas at Dallas, Richardson TX; United States of America
[44] National Centre for Scientific Research "Demokritos", Agia Paraskevi; Greece
[45] [(a)] Department of Physics, Stockholm University;[(b)] Oskar Klein Centre, Stockholm; Sweden
[46] Deutsches Elektronen-Synchrotron DESY, Hamburg and Zeuthen; Germany
[47] Lehrstuhl für Experimentelle Physik IV, Technische Universität Dortmund, Dortmund; Germany
[48] Institut für Kern- und Teilchenphysik, Technische Universität Dresden, Dresden; Germany
[49] Department of Physics, Duke University, Durham NC; United States of America
[50] SUPA — School of Physics and Astronomy, University of Edinburgh, Edinburgh; United Kingdom
[51] INFN e Laboratori Nazionali di Frascati, Frascati; Italy
[52] Physikalisches Institut, Albert-Ludwigs-Universität Freiburg, Freiburg; Germany
[53] II. Physikalisches Institut, Georg-August-Universität Göttingen, Göttingen; Germany
[54] Département de Physique Nucléaire et Corpusculaire, Université de Genève, Genève; Switzerland
[55] [(a)] Dipartimento di Fisica, Università di Genova, Genova;[(b)] INFN Sezione di Genova; Italy
[56] II. Physikalisches Institut, Justus-Liebig-Universität Giessen, Giessen; Germany
[57] SUPA — School of Physics and Astronomy, University of Glasgow, Glasgow; United Kingdom
[58] LPSC, Université Grenoble Alpes, CNRS/IN2P3, Grenoble INP, Grenoble; France
[59] Laboratory for Particle Physics and Cosmology, Harvard University, Cambridge MA; United States of America
[60] [(a)] Department of Modern Physics and State Key Laboratory of Particle Detection and Electronics, University of Science and Technology of China, Hefei;[(b)] Institute of Frontier and Interdisciplinary Science and Key Laboratory of Particle Physics and Particle Irradiation (MOE), Shandong University, Qingdao;[(c)] School of Physics and Astronomy, Shanghai Jiao Tong University, KLPPAC-MoE, SKLPPC, Shanghai;[(d)] Tsung-Dao Lee Institute, Shanghai; China
[61] [(a)] Kirchhoff-Institut für Physik, Ruprecht-Karls-Universität Heidelberg, Heidelberg;[(b)] Physikalisches Institut, Ruprecht-Karls-Universität Heidelberg, Heidelberg; Germany
[62] Faculty of Applied Information Science, Hiroshima Institute of Technology, Hiroshima; Japan
[63] [(a)] Department of Physics, Chinese University of Hong Kong, Shatin, N.T., Hong Kong;[(b)] Department of Physics, University of Hong Kong, Hong Kong;[(c)] Department of Physics and Institute for Advanced Study, Hong Kong University of Science and Technology, Clear Water Bay, Kowloon, Hong Kong; China
[64] Department of Physics, National Tsing Hua University, Hsinchu; Taiwan
[65] IJCLab, Université Paris-Saclay, CNRS/IN2P3, 91405, Orsay; France
[66] Department of Physics, Indiana University, Bloomington IN; United States of America
[67] [(a)] INFN Gruppo Collegato di Udine, Sezione di Trieste, Udine;[(b)] ICTP, Trieste;[(c)] Dipartimento Politecnico di Ingegneria e Architettura, Università di Udine, Udine; Italy
[68] [(a)] INFN Sezione di Lecce;[(b)] Dipartimento di Matematica e Fisica, Università del Salento, Lecce; Italy
[69] [(a)] INFN Sezione di Milano;[(b)] Dipartimento di Fisica, Università di Milano, Milano; Italy
[70] [(a)] INFN Sezione di Napoli;[(b)] Dipartimento di Fisica, Università di Napoli, Napoli; Italy
[71] [(a)] INFN Sezione di Pavia;[(b)] Dipartimento di Fisica, Università di Pavia, Pavia; Italy
[72] [(a)] INFN Sezione di Pisa;[(b)] Dipartimento di Fisica E. Fermi, Università di Pisa, Pisa; Italy
[73] [(a)] INFN Sezione di Roma;[(b)] Dipartimento di Fisica, Sapienza Università di Roma, Roma; Italy
[74] [(a)] INFN Sezione di Roma Tor Vergata;[(b)] Dipartimento di Fisica, Università di Roma Tor Vergata, Roma; Italy

JHEP09(2020)049

[75] [(a)] INFN Sezione di Roma Tre;[(b)] Dipartimento di Matematica e Fisica, Università Roma Tre, Roma; Italy
[76] [(a)] INFN-TIFPA;[(b)] Università degli Studi di Trento, Trento; Italy
[77] Institut für Astro- und Teilchenphysik, Leopold-Franzens-Universität, Innsbruck; Austria
[78] University of Iowa, Iowa City IA; United States of America
[79] Department of Physics and Astronomy, Iowa State University, Ames IA; United States of America
[80] Joint Institute for Nuclear Research, Dubna; Russia
[81] [(a)] Departamento de Engenharia Elétrica, Universidade Federal de Juiz de Fora (UFJF), Juiz de Fora;[(b)] Universidade Federal do Rio De Janeiro COPPE/EE/IF, Rio de Janeiro;[(c)] Universidade Federal de São João del Rei (UFSJ), São João del Rei;[(d)] Instituto de Física, Universidade de São Paulo, São Paulo; Brazil
[82] KEK, High Energy Accelerator Research Organization, Tsukuba; Japan
[83] Graduate School of Science, Kobe University, Kobe; Japan
[84] [(a)] AGH University of Science and Technology, Faculty of Physics and Applied Computer Science, Krakow;[(b)] Marian Smoluchowski Institute of Physics, Jagiellonian University, Krakow; Poland
[85] Institute of Nuclear Physics Polish Academy of Sciences, Krakow; Poland
[86] Faculty of Science, Kyoto University, Kyoto; Japan
[87] Kyoto University of Education, Kyoto; Japan
[88] Research Center for Advanced Particle Physics and Department of Physics, Kyushu University, Fukuoka ; Japan
[89] Instituto de Física La Plata, Universidad Nacional de La Plata and CONICET, La Plata; Argentina
[90] Physics Department, Lancaster University, Lancaster; United Kingdom
[91] Oliver Lodge Laboratory, University of Liverpool, Liverpool; United Kingdom
[92] Department of Experimental Particle Physics, Jožef Stefan Institute and Department of Physics, University of Ljubljana, Ljubljana; Slovenia
[93] School of Physics and Astronomy, Queen Mary University of London, London; United Kingdom
[94] Department of Physics, Royal Holloway University of London, Egham; United Kingdom
[95] Department of Physics and Astronomy, University College London, London; United Kingdom
[96] Louisiana Tech University, Ruston LA; United States of America
[97] Fysiska institutionen, Lunds universitet, Lund; Sweden
[98] Centre de Calcul de l'Institut National de Physique Nucléaire et de Physique des Particules (IN2P3), Villeurbanne; France
[99] Departamento de Física Teorica C-15 and CIAFF, Universidad Autónoma de Madrid, Madrid; Spain
[100] Institut für Physik, Universität Mainz, Mainz; Germany
[101] School of Physics and Astronomy, University of Manchester, Manchester; United Kingdom
[102] CPPM, Aix-Marseille Université, CNRS/IN2P3, Marseille; France
[103] Department of Physics, University of Massachusetts, Amherst MA; United States of America
[104] Department of Physics, McGill University, Montreal QC; Canada
[105] School of Physics, University of Melbourne, Victoria; Australia
[106] Department of Physics, University of Michigan, Ann Arbor MI; United States of America
[107] Department of Physics and Astronomy, Michigan State University, East Lansing MI; United States of America
[108] B.I. Stepanov Institute of Physics, National Academy of Sciences of Belarus, Minsk; Belarus
[109] Research Institute for Nuclear Problems of Byelorussian State University, Minsk; Belarus
[110] Group of Particle Physics, University of Montreal, Montreal QC; Canada
[111] P.N. Lebedev Physical Institute of the Russian Academy of Sciences, Moscow; Russia
[112] National Research Nuclear University MEPhI, Moscow; Russia
[113] D.V. Skobeltsyn Institute of Nuclear Physics, M.V. Lomonosov Moscow State University, Moscow; Russia
[114] Fakultät für Physik, Ludwig-Maximilians-Universität München, München; Germany
[115] Max-Planck-Institut für Physik (Werner-Heisenberg-Institut), München; Germany

JHEP09(2020)049

[116] Nagasaki Institute of Applied Science, Nagasaki; Japan
[117] Graduate School of Science and Kobayashi-Maskawa Institute, Nagoya University, Nagoya; Japan
[118] Department of Physics and Astronomy, University of New Mexico, Albuquerque NM; United States of America
[119] Institute for Mathematics, Astrophysics and Particle Physics, Radboud University Nijmegen/Nikhef, Nijmegen; Netherlands
[120] Nikhef National Institute for Subatomic Physics and University of Amsterdam, Amsterdam; Netherlands
[121] Department of Physics, Northern Illinois University, DeKalb IL; United States of America
[122] [(a)] Budker Institute of Nuclear Physics and NSU, SB RAS, Novosibirsk;[(b)] Novosibirsk State University Novosibirsk; Russia
[123] Institute for High Energy Physics of the National Research Centre Kurchatov Institute, Protvino; Russia
[124] Institute for Theoretical and Experimental Physics named by A.I. Alikhanov of National Research Centre "Kurchatov Institute", Moscow; Russia
[125] Department of Physics, New York University, New York NY; United States of America
[126] Ochanomizu University, Otsuka, Bunkyo-ku, Tokyo; Japan
[127] Ohio State University, Columbus OH; United States of America
[128] Homer L. Dodge Department of Physics and Astronomy, University of Oklahoma, Norman OK; United States of America
[129] Department of Physics, Oklahoma State University, Stillwater OK; United States of America
[130] Palacký University, RCPTM, Joint Laboratory of Optics, Olomouc; Czech Republic
[131] Institute for Fundamental Science, University of Oregon, Eugene, OR; United States of America
[132] Graduate School of Science, Osaka University, Osaka; Japan
[133] Department of Physics, University of Oslo, Oslo; Norway
[134] Department of Physics, Oxford University, Oxford; United Kingdom
[135] LPNHE, Sorbonne Université, Université de Paris, CNRS/IN2P3, Paris; France
[136] Department of Physics, University of Pennsylvania, Philadelphia PA; United States of America
[137] Konstantinov Nuclear Physics Institute of National Research Centre "Kurchatov Institute", PNPI, St. Petersburg; Russia
[138] Department of Physics and Astronomy, University of Pittsburgh, Pittsburgh PA; United States of America
[139] [(a)] Laboratório de Instrumentação e Física Experimental de Partículas — LIP, Lisboa;[(b)] Departamento de Física, Faculdade de Ciências, Universidade de Lisboa, Lisboa;[(c)] Departamento de Física, Universidade de Coimbra, Coimbra;[(d)] Centro de Física Nuclear da Universidade de Lisboa, Lisboa;[(e)] Departamento de Física, Universidade do Minho, Braga;[(f)] Departamento de Física Teórica y del Cosmos, Universidad de Granada, Granada (Spain);[(g)] Dep Física and CEFITEC of Faculdade de Ciências e Tecnologia, Universidade Nova de Lisboa, Caparica;[(h)] Instituto Superior Técnico, Universidade de Lisboa, Lisboa; Portugal
[140] Institute of Physics of the Czech Academy of Sciences, Prague; Czech Republic
[141] Czech Technical University in Prague, Prague; Czech Republic
[142] Charles University, Faculty of Mathematics and Physics, Prague; Czech Republic
[143] Particle Physics Department, Rutherford Appleton Laboratory, Didcot; United Kingdom
[144] IRFU, CEA, Université Paris-Saclay, Gif-sur-Yvette; France
[145] Santa Cruz Institute for Particle Physics, University of California Santa Cruz, Santa Cruz CA; United States of America
[146] [(a)] Departamento de Física, Pontificia Universidad Católica de Chile, Santiago;[(b)] Universidad Andres Bello, Department of Physics, Santiago;[(c)] Instituto de Alta Investigación, Universidad de Tarapacá;[(d)] Departamento de Física, Universidad Técnica Federico Santa María, Valparaíso; Chile
[147] Department of Physics, University of Washington, Seattle WA; United States of America
[148] Department of Physics and Astronomy, University of Sheffield, Sheffield; United Kingdom
[149] Department of Physics, Shinshu University, Nagano; Japan

JHEP09(2020)049

[150] Department Physik, Universität Siegen, Siegen; Germany
[151] Department of Physics, Simon Fraser University, Burnaby BC; Canada
[152] SLAC National Accelerator Laboratory, Stanford CA; United States of America
[153] Physics Department, Royal Institute of Technology, Stockholm; Sweden
[154] Departments of Physics and Astronomy, Stony Brook University, Stony Brook NY; United States of America
[155] Department of Physics and Astronomy, University of Sussex, Brighton; United Kingdom
[156] School of Physics, University of Sydney, Sydney; Australia
[157] Institute of Physics, Academia Sinica, Taipei; Taiwan
[158] [(a)] E. Andronikashvili Institute of Physics, Iv. Javakhishvili Tbilisi State University, Tbilisi;[(b)] High Energy Physics Institute, Tbilisi State University, Tbilisi; Georgia
[159] Department of Physics, Technion, Israel Institute of Technology, Haifa; Israel
[160] Raymond and Beverly Sackler School of Physics and Astronomy, Tel Aviv University, Tel Aviv; Israel
[161] Department of Physics, Aristotle University of Thessaloniki, Thessaloniki; Greece
[162] International Center for Elementary Particle Physics and Department of Physics, University of Tokyo, Tokyo; Japan
[163] Graduate School of Science and Technology, Tokyo Metropolitan University, Tokyo; Japan
[164] Department of Physics, Tokyo Institute of Technology, Tokyo; Japan
[165] Tomsk State University, Tomsk; Russia
[166] Department of Physics, University of Toronto, Toronto ON; Canada
[167] [(a)] TRIUMF, Vancouver BC;[(b)] Department of Physics and Astronomy, York University, Toronto ON; Canada
[168] Division of Physics and Tomonaga Center for the History of the Universe, Faculty of Pure and Applied Sciences, University of Tsukuba, Tsukuba; Japan
[169] Department of Physics and Astronomy, Tufts University, Medford MA; United States of America
[170] Department of Physics and Astronomy, University of California Irvine, Irvine CA; United States of America
[171] Department of Physics and Astronomy, University of Uppsala, Uppsala; Sweden
[172] Department of Physics, University of Illinois, Urbana IL; United States of America
[173] Instituto de Física Corpuscular (IFIC), Centro Mixto Universidad de Valencia — CSIC, Valencia; Spain
[174] Department of Physics, University of British Columbia, Vancouver BC; Canada
[175] Department of Physics and Astronomy, University of Victoria, Victoria BC; Canada
[176] Fakultät für Physik und Astronomie, Julius-Maximilians-Universität Würzburg, Würzburg; Germany
[177] Department of Physics, University of Warwick, Coventry; United Kingdom
[178] Waseda University, Tokyo; Japan
[179] Department of Particle Physics, Weizmann Institute of Science, Rehovot; Israel
[180] Department of Physics, University of Wisconsin, Madison WI; United States of America
[181] Fakultät für Mathematik und Naturwissenschaften, Fachgruppe Physik, Bergische Universität Wuppertal, Wuppertal; Germany
[182] Department of Physics, Yale University, New Haven CT; United States of America

[a] Also at Borough of Manhattan Community College, City University of New York, New York NY; United States of America
[b] Also at Centro Studi e Ricerche Enrico Fermi; Italy
[c] Also at CERN, Geneva; Switzerland
[d] Also at CPPM, Aix-Marseille Université, CNRS/IN2P3, Marseille; France
[e] Also at Département de Physique Nucléaire et Corpusculaire, Université de Genève, Genève; Switzerland
[f] Also at Departament de Fisica de la Universitat Autonoma de Barcelona, Barcelona; Spain

JHEP09(2020)049

[g] Also at Department of Financial and Management Engineering, University of the Aegean, Chios; Greece
[h] Also at Department of Physics and Astronomy, Michigan State University, East Lansing MI; United States of America
[i] Also at Department of Physics and Astronomy, University of Louisville, Louisville, KY; United States of America
[j] Also at Department of Physics, Ben Gurion University of the Negev, Beer Sheva; Israel
[k] Also at Department of Physics, California State University, East Bay; United States of America
[l] Also at Department of Physics, California State University, Fresno; United States of America
[m] Also at Department of Physics, California State University, Sacramento; United States of America
[n] Also at Department of Physics, King's College London, London; United Kingdom
[o] Also at Department of Physics, St. Petersburg State Polytechnical University, St. Petersburg; Russia
[p] Also at Department of Physics, University of Fribourg, Fribourg; Switzerland
[q] Also at Dipartimento di Matematica, Informatica e Fisica, Università di Udine, Udine; Italy
[r] Also at Faculty of Physics, M.V. Lomonosov Moscow State University, Moscow; Russia
[s] Also at Giresun University, Faculty of Engineering, Giresun; Turkey
[t] Also at Graduate School of Science, Osaka University, Osaka; Japan
[u] Also at Hellenic Open University, Patras; Greece
[v] Also at IJCLab, Université Paris-Saclay, CNRS/IN2P3, 91405, Orsay; France
[w] Also at Institucio Catalana de Recerca i Estudis Avancats, ICREA, Barcelona; Spain
[x] Also at Institut für Experimentalphysik, Universität Hamburg, Hamburg; Germany
[y] Also at Institute for Mathematics, Astrophysics and Particle Physics, Radboud University Nijmegen/Nikhef, Nijmegen; Netherlands
[z] Also at Institute for Nuclear Research and Nuclear Energy (INRNE) of the Bulgarian Academy of Sciences, Sofia; Bulgaria
[aa] Also at Institute for Particle and Nuclear Physics, Wigner Research Centre for Physics, Budapest; Hungary
[ab] Also at Institute of Particle Physics (IPP), Vancouver; Canada
[ac] Also at Institute of Physics, Azerbaijan Academy of Sciences, Baku; Azerbaijan
[ad] Also at Instituto de Fisica Teorica, IFT-UAM/CSIC, Madrid; Spain
[ae] Also at Joint Institute for Nuclear Research, Dubna; Russia
[af] Also at Louisiana Tech University, Ruston LA; United States of America
[ag] Also at Moscow Institute of Physics and Technology State University, Dolgoprudny; Russia
[ah] Also at National Research Nuclear University MEPhI, Moscow; Russia
[ai] Also at Physics Department, An-Najah National University, Nablus; Palestine
[aj] Also at Physikalisches Institut, Albert-Ludwigs-Universität Freiburg, Freiburg; Germany
[ak] Also at The City College of New York, New York NY; United States of America
[al] Also at TRIUMF, Vancouver BC; Canada
[am] Also at Universita di Napoli Parthenope, Napoli; Italy
[an] Also at University of Chinese Academy of Sciences (UCAS), Beijing; China
[*] Deceased

JHEP09(2020)049